ANA PAULA
GOULART ARAUJO

Taxonomic review of the terrestrial planarian genus *Issoca* Froehlich, 1955 (Platyhelminthes, Tricladida, Geoplaninae) and related species

Revisão taxonômica do gênero de planárias terrestres *Issoca* Froehlich, 1955 (Platyhelminthes, Tricladida, Geoplaninae) e espécies afins

Single Volume

SÃO PAULO
2021

ANA PAULA
GOULART ARAUJO

Taxonomic review of the terrestrial planarian genus *Issoca* Froehlich, 1955 (Platyhelminthes, Tricladida, Geoplaninae) and related species

Revisão taxonômica do gênero de planárias terrestres *Issoca* Froehlich, 1955 (Platyhelminthes, Tricladida, Geoplaninae) e espécies afins

---

Single Volume

Original Version

Dissertation submitted to the Graduate Program of the Museu de Zoologia da Universidade de São Paulo in partial fulfillment of the requirements for the degree of Master of Science (Systematics, Animal Taxonomy and Biodiversity).

Advisor: Prof. Dr. Fernando Carbayo Baz

SÃO PAULO

2021

Serviço de Biblioteca e Documentação
Museu de Zoologia da Universidade de São Paulo

Cataloging in Publication

Araujo, Ana Paula Goulart
Taxonomic review of the terrestrial planarian genus Issoca Froehlich, 1955 (Platyhelminthes, Tricladida, Geoplaninae) and related species. = Revisão Taxonômica do gênero de planárias terrestres Issoca Froehlich, 1955 (Platyhelminthes, Tricladida, Geoplaninae / Ana Paula Goulart Araujo; orientador Fernando Carbayo Baz. São Paulo, 2021.
115p.

Dissertação apresentada ao Programa de Pós Graduação do Museu de Zoologia da Universidade de São Paulo em cumprimento parcial dos requisitos para o grau de Mestre em Ciências (Sistemática, Taxonomia Animal e Biodiversidade) .
Versão original
Volume único

1. Planaria terrestre – revisão taxonômica. 2. Platyhelminthes - Geoplaninae. I. Carbayo Baz, Fernando orient. II. Título.

CRB 8/ 3805

ARAUJO, Ana Paula Goulart

Taxonomic review of the terrestrial planarian genus *Issoca* Froehlich, 1955 (Platyhelminthes, Tricladida, Geoplaninae) and related species)

Revisão taxonômica do gênero de planárias terrestres *Issoca* Froehlich, 1955 (Platyhelminthes, Tricladida, Geoplaninae) e espécies afins

Dissertation submitted to the Graduate Program of the Museu de Zoologia da Universidade de São Paulo in partial fulfillment of the requirements for the degree of Master of Science (Systematics, Animal Taxonomy and Biodiversity).

Date approved: _____/_____/_____

COMMITTEE MEMBERS

Prof. Dr.	Institution:
Decision:	Signature:
Prof. Dr.	Institution:
Decision:	Signature:
Prof. Dr.	Institution:
Decision:	Signature:

Dedicado, genuinamente, aos meus pais, Alice e João, alicerces de quem me tornei, que me criaram e educaram com amor incondicional.

À minha irmã, Ana Luisa, que, com sua sensibilidade e bondade, sempre esteve ao meu lado.

Aos amigos Ana Laura Almeida, Beatriz Santos Souza e Marcos Santos Silva, pessoas incríveis as quais tenho a honra de conhecer.

Ao meu tio e padrinho Clemente e em memória à minha tia e madrinha Matilde, que tanto me ajudaram de diversas maneiras.

AGRADECIMENTOS / ACKNOWLEDGMENTS

Agradeço aos meus pais, Alice de Matos Goulart Araujo e João Vieira de Araujo, pela educação, amor e respeito incondicional dedicados a mim ao longo de toda minha vida e por sempre me incentivarem, apoiarem e mostrarem que a Educação é o melhor caminho a ser trilhado.

Ao meu orientador, Fernando Carbayo, pelas oportunidades que me foram concedidas ao longo da minha formação acadêmica, por todo conhecimento sobre planárias terrestres que me foi transmitido, por sua paciência comigo, por respeitar meu tempo e por sua dedicação e comprometimento com este trabalho.

Ao Prof. Dr. Marcos Ryotaro Hara por, em diversas ocasiões, se dispor a sanar dúvidas e dar dicas sobre conceitos de sistemática filogenética. Além disso, por ter me proporcionado momentos de descontração e conversas agradáveis sobre assuntos variados.

À Marta Riutort e à Marta Álvarez-Presas (Universitat Barcelona, Espanha) por terem me recebido em seu laboratório e me ensinado técnicas e conceitos sobre filogenia molecular.

Às amigas do curso de Lic. em Ciências da Natureza, Paula Camacho Buceli, Samira Barbosa da Silva, Jéssica Alves da Silva, Ana Laura Almeida dos Santos, Beatriz Santos de Souza, Luiza Coatti, Bianca Lujan Pereira, Karine Gobetti de Oliveira, Bianca Hyon Joo Lee, Marina Costa Rodrigues e Caroline Lopes dos Santos por me apoiarem, me escutarem, me acolherem, me proporcionarem momentos incríveis e por me fazerem sorrir mesmo em momentos de dificuldades. Obrigada por serem mulheres fortes.

À minha irmã Ana Luisa Goulart Araujo que, apesar das dificuldades, me ajudou muito, sempre me transmitiu segurança e exemplo de força e perseverança.

À Matilde e Clemente, minha madrinha e padrinho, por me ajudarem em diversos momentos e de diversas formas.

Ao meu companheiro Caio Felipe Carneiro Bergamasco por estar ao meu lado desde o início desse trabalho me apoiando, me incentivando e me ajudando a configurar programas utilizados nesse trabalho.

Aos colegas e amigos de laboratório e de trabalho de campo, Domingo Lago Barcia, Maytê Suguimoto, Thaís de Oliveira dos Santos, Júlio Francisco Hisada Pedroni, Amanda Cseh, Karine Gobetti de Oliveira e Ítalo Silva de Oliveira Souza.

Agradeço aos colegas Amanda Cseh, Marcos Santos Silva, Ítalo Silva de Oliveira Souza, Lucas Beltrami e Geison Castro da Silveira, pela preparação histológica do material biológico estudado nesse trabalho. Agradeço especialmente à Ana Cristina Machado Vasconcelos que, além de preparar lâminas histológicas, dedicou parte do seu tempo para me ensinar este procedimento.

Agradeço aos técnicos do laboratório de biologia molecular do Instituto de Biociências da USP Beatriz Vieira Freire, Manuel Junior e Sabrina Baroni, por sempre estarem à disposição em auxiliar no trabalho de bancada para extração de DNA. Agradeço também à Ana Laura Almeida dos Santos e à Bianca Lujan Pereira por me ajudarem nesse mesmo trabalho de bancada e, além disso, me proporcionarem momentos que transcenderam a relação acadêmica.

À CAPES pela concessão da bolsa de mestrado (Proc. 88882.378121/2019-01). / This study was financed in part by the Coordenação de Aperfeiçoamento de Pessoal de Nível Superior - Brasil (CAPES) - Finance Code 001.

À FAPESP, pelo auxílio de pesquisa (Proc. 2019/12357-7) concedido ao orientador. / São Paulo Research Foundation (FAPESP, Process # 2019/12357-7) provided financial support to FC.

E, por fim, agradeço especialmente e imensamente aos meus grandes amigos Ana Laura Almeida dos Santos, Beatriz Santos de

Souza e Marcos Santos Silva por sempre estarem ao meu lado e não medirem esforços para me ajudarem em todas as dificuldades desde a minha primeira iniciação científica até a finalização desse trabalho.

RESUMO

A sistemática dos gêneros de planárias terrestres Neotropicais *Luteostriata*, *Winsoria*, *Issoca* e *Supramontana* (Platyhelminthes, Tricladida, Geoplaninae) -abreviado LWIS- é fraca, uma vez que os gêneros são diagnosticados por características bastante semelhantes, apenas variando nos detalhes. A sistemática de LWIS é revisada por meio de uma abordagem morfológica e molecular. Quatro espécies de *Issoca* são redescritas pelo estudo dos espécimes-tipo e/ou material adicional preparado em lâminas histológicas ou por microtomografia computadorizada. A filogenética molecular recuperou (a) LWIS e todas as 13 espécies estudadas como monofiléticas, (b) *Issoca rezendei* como irmã do LWIS restante, (c) *Issoca* e *Luteostriata* polifiléticas e (d) *Winsoria* e *Supramonana* aninhadas cada uma dentro do respectivo clado heterogêneo com respeito à composição das espécies. Apesar do baixo suporte estatístico para alguns clados, a filogenia é congruente com a morfologia das espécies. Morfologicamente, *Issoca rezendei* se diferencia das outras espécies de LWIS e um rediagnóstico do gênero é proposto. Os membros restantes do LWIS são colocados em *Supramontana*, que também é rediagnosticado, e *Luteostriata* e *Winsoria* são considerados sinomias juniores. Finalmente, quatro novas espécies de *Supramontana* são descritas.

Palavras-chave: Taxonomia. Filogenia molecular. *Supramontana*, *Luteostriata*. *Winsoria*.

ABSTRACT

The systematics of the Neotropical land planarian genera *Luteostriata*, *Winsoria*, *Issoca* and *Supramontana* (Platyhelminthes, Tricladida, Geoplaninae) -abbreviated LWIS- is weak since the genera are diagnosed by rather similar features, only varying in the details. The systematics of LWIS is revised through a morphological and molecular approach. Four species of *Issoca* are redescribed by studying the type specimens and/or additional material prepared on histological slides or through micro-computed tomography. The molecular phylogenetics retrieved (a) LWIS and all 13 species studied as monophyletic, (b) *Issoca rezendei* as sister to the remaining LWIS, (c) *Issoca* and *Luteostriata* polyphyletic and (d) *Winsoria* and *Supramontana* nested each within the respective heterogenous clade with respect to the species composition. Despite the low statistical support for some clades, the phylogeny is congruent with the morphology of the species. Morphologically, *Issoca rezendei* stands apart from the other species of LWIS and a rediagnosis of the genus is proposed. The remaining LWIS members are placed into *Supramontana*, which is also rediagnosed, and *Luteostriata* and *Winsoria* are considered junior synomyms. Finally, four new species of *Supramontana* are described.

Keywords: Taxonomy. Molecular phylogeny. *Supramontana*, *Luteostriata*. *Winsoria*.

LIST OF FIGURES

LIST OF TABLES

CONTENTS

1. INTRODUCTION

Molecular information (DNA) may constitute a powerful tool to test morphology-based hypotheses of species (Winsor, 1998; Tautz *et al*., 2003). The systematics of land flatworms, land planarians or Geoplanidae (Platyhelminthes, Tricladida) represents a good example of this, even more because of the scarcity of morphological traits they pose. These soft-bodies organisms are poor in morphological attributes with taxonomic value and these attributes can be affected by artifacts caused during fixation (Negrete *et al*., 2015).

Early descriptions of land planarians were exclusively based on the external appearance (e.g. Darwin, 1844). Innovation of histological techniques provided new insights into the internal morphology (e.g. Graff, 1899). Current standards in taxonomic descriptions require a detailed account of sensory organs, muscular systems, and anatomy and histology of the pharynx and, principally, the copulatory apparatus.

The history of the *Issoca* and close relatives, i. e., the genera *Supramontana*, *Issoca*, and *Winsoria* (Geoplaninae), hereafter abbreviated LWIS, illustrates how molecular phylogenetics can help uncover natural groups. Currently LWIS includes 19 species, which are distributed across Southeast and South Brazil and North Argentina.

There are 10 species in the genus *Issoca* Froehlich, 1955. This genus was proposed for *Geoplana rezendei* Schirch, 1929, a species originally only known from its external appearance. Froehlich studied in detail the internal morphology of the species and characterized it mainly as having a sucker-like glandulo-muscular organ in the ventral side of the cephalic region, the retractor muscle being derived from the ventral subcutaneous longitudinal muscle (Froehlich, 1955). In the

same paper, *Choeradoplana spatulata* Graff, 1899 (up to date only known from its external aspect only) was transferred to *Issoca* since the cephalic region is spoon-shaped and in other memebrs of the genus, and *I. jandaia* Froehlich, 1955 and *I. piranga* Froehlich, 1955 were also described. Carbayo & Leal-Zanchet (2003) studied further details of *I. rezendei* and complemented the diagnosis of the genus mainly by adding the presence of a sub-neural transverse parenchymal muscle layer interspersed with muscle fibres of the retractor muscle (Carbayo & Leal-Zanchet, 2003). This feature was not observed in *I. assanga* Araujo & Carbayo, 2018, and it was interpreted as evidence of the polyphyletic status of the genus (Araujo & Carbayo, 2018).

Comprising two species, the genus *Supramontana* Carbayo & Leal-Zanchet, 2003 resembles *Issoca* in the morphology, and differs from it in that the cephalic extremity is not spoon-shaped but rounded, the retractor muscle bundles are dispersed in bundles running towards the body margins (*vs.* towards margins of body the direction of the margins and to the dorsal body surface), a glandular component associated with the retractor is absent (*vs.* present), the subneural parenchymatic muscle is dorsal to the retractor muscle (*vs.* interspersed), and the ventral longitudinal cutaneous muscle is partially sunken into the parenchyma (*vs*. not sunken).

Many Geoplaninae species resemble each other in the general shape of the copulatory organs. It was the regular study of the cephalic region that helped recognize homogeneous groups of species, such as several species of *Notogynaphallia* Ogren & Kawakatsu, 1990. The main features of this genus are the absence of a penis papilla and the proflex condition of the female genital canal (i.e., this canal is oriented forwards). Currently with 10 species, *Luteostriata* Carbayo, 2010 was erected for species with these traits but also having a cephalic retractor muscle. Accordingly, some species of *Notogynaphallia* were transferred to *Luteostriata*. The genus differs

from *Issoca* and *Supramontana* mainly in that the cephalic region is not spoon-shaped; the glandular ventral surface of the cephalic musculo-glandular organ is U-shaped; the retractor muscle is lens-shaped in cross section; the sub-neural mesenchymal muscle layer is not intermingled with retractor, and cellular bodies of rhabditogen cells lie between the retractor muscle and the epidermis in the cephalic region.

Independent tests of morphology-based systematics entered the Geoplaninae group in 2013. A molecular phylogeny of Geoplaninae demonstrated the close relationship of the genera *Luteostriata*, *Issoca* and *Supramontana*, constituting a monophyletic group, the so-called clade LIS (Carbayo *et al*., 2013). That study also revealed that *Issoca*, and *Luteostriata* are polyphyletic, and that *Supramontana* was nested within a clade with *Issoca* members (Carbayo et a., 2013).

Among the target genera of this study, only *Winsoria* Negrete *et al*., 2019 was proposed by means of an integration of morphology and DNA phylogenetics (see Negrete *et al*., 2019). This monotypic genus was retrieved as sister to one species of a polyphyletic *Issoca*, whereas *Luteostriata* was also recovered as polyphyletic. In turn, *Supramontana* was nested within a group with species of *Luteostriata*.

Despite the non-monophyletic condition of these genera, no taxonomic initiatives were taken to review the systematics of the group. This is the main purpose of the present paper, which we tackle with both morphological and molecular approaches. The paper also includes the redescription of four species of *Issoca* and descriptions of four species.

2. MATERIAL AND METHODS

2.1. Acquisition of molecular data

One specimen of genera *Issoca* and 16 specimens of *Supramontana* were selected for molecular studies. Genomic DNA extractions were performed with the ammonia acetate protocol. Preserving alcohol was removed from the tissue by either pressing it gently on absorbent paper or in a vacuum pump for 5 minutes, or in the hothouse (37º C) for 15 minutes. Then, 300 µl of lysis solution and 5 µl of Proteinase-K (20mg / ml) were added and mixed by vortexing and incubate overnight at 55º C. Then the samples were cooled to room temperature and subsequently 300µl of ammonia acetate were added and the samples were vortexed and incubated on ice or on a cold shelf (in the freezer) for 30 minutes. The samples were centrifuged for 10 minutes (13,000 rpm at 4ºC). The supernatant of each sample was transferred to a new tube to which 600µl of absolute isopropanol (cold) were added and the tube was inverted gently 10 times and left for 1 hour at -20º C (freezer). The samples were centrifuged for 10 minutes (13,000 rpm at 4ºC) and the supernatant discarded. Following 600µl of 70% ethanol (cold) were added and after a 10-minute centrifugation (13,000 rpm at 4ºC) the ethanol was discarded carefully. Subsequently, the tubes were inverted on absorbent paper and then the pellet was dried in a vacuum pump for 30 minutes.

The polymerase chain reaction (PCR) was used to amplify partial sequences of the mitochondrial region of Cytochrome Oxidase I (COI) gene and the nuclear gene (28S rDNA). Amplifications were performed in a 20 µL volume containing 1 µL of DNA, 4 µL of 5× Phusion Buffer GC (Thermo Scientific) 1.5 mM Tris–HCl (pH 8.4), 50 mM KCl, 1 µL of l M dNTPs, 1.0–3.0 mM MgCl2 , 1 µL of l M of each primer, and 0.2 µL of Phusion High-Fidelity DNA Polymerase (Thermo Scientific). General PCR conditions included initial denaturation for 3

min at 98 °C, 35 cycles of denaturation for 10 s at 98 °C, annealing for 30 s at specific temperatures (see below), extension for 1 min at 72 °C, and a final extension for 5 min at 72 °C. Amplifications and sequencing were performed with the primers in Table 2. The PCR products were purified using ExoSap purification (ExoSap-it, GE Healthcare). Products were subsequently cycle sequenced directly using the corresponding PCR primers and ABI Big-Dye Sequence Terminator (v. 3.1), with a standard cycle sequencing profile (96° C/30 s; 35 cycles of 96° C/10 s, 50° C/10 s, 60° C/4 min; and 4° C/∞). Reaction products were cleaned with ethanol precipitation, and sequenced on an ABI Prism Genetic Analyzer (3131XL) automated sequencer (Applied Biosystems/ThermoFisher) facility installed in Departamento de Botânica do Instituto de Biociências da Universidade de São Paulo.

2.2. Sequence analysis and phylogenetic analyses

Alignment. Sequencer reads were assembled using the Consed/ Phred/Phrap package (Ewing & Green 1998; Ewing *et al*., 1998; Gordon, Abajian & Green, 1998; Gordon, Desmarais & Green, 2001). We compiled 62 COI and 54 28S sequences from the GenBank (https://www.ncbi.nlm.nih.gov/genbank/), including 16 representatives of the target group (i.e., members of *Issoca, Supramontana, Luteostriata, and Winsoria*), and diverse representatives of Geoplaninae, of which *Gusana* and *Polycladus* were used as outgroup (Table 1). Before submitting the data to phylogenetic analysis, we aligned the sequences with MAFFT (Katoh *et al*., 2002) using the G-INS-i iterative refinement method with 1000 cycles, and visualized and edited the sequences in BioEdit (Hall, 1999). Aligned sequences of COI was checked for stop codons using the DNA-to-protein translation online resource by Bikandi *et al*. (2004, http://insilico.ehu.es) using the Echinoderm mitochondrial and the standard genetic code, respectively. Phylogenetic analyses were conducted using maximum likelihood (ML) and inference Bayesian

(IB) for a set of concatenated data. PartitionFinder2 ver. 2.1.1 software (Lanfear *et al*., 2016) was used to discover the partitions and the evolutionary model which best fit the nucleotide dataset under the Akaike Information Criterion corrected (AICc) (Hurvich and Tsai, 1989). Maximum likelihood analyses were performed on XSEDE (CIPRES Gateway to Science (Miller *et al*., 2010) with the program RAxML v. 8.2.12 (Stamatakis, 2016) using the GTR+Γ model for the concatenated dataset. Bayesian inference analyses were performed with the program MR. BAYES v. 3.1.2 (Ronquist & Huelsenbeck 2003). Here, we considered the GTR+I+Γ model for the concatenated dataset.

2.3. Specimen acquisition, preparation and identification

The specimens were either collected in the field or loaned from collections. Specimens collected were searched in areas covered with Atlantic Forest in the states of Espírito Santo, Rio de Janeiro, São Paulo and Paraná, Brazil. The specimens were photographed, killed in boiling water and subsequently fixed in 10% formalin with the exception of a small body piece that was cut off and kept frozen in absolute ethanol. After 1-4 week in formalin, different regions of the body of the specimens underwent histological processing: dehydration in alcoholic series, dealcoholization in clove oil, inclusion in Paraplast (c), serial sectioning at 5-7 microns in thickness with retracting rotary microtome (Microm HM315 R), rehydration and staining with Mallory's trichrome as modified by Cason (1950). Histological glass slides were examined and photographed with an Olympus BX51TF stereomicroscope. Photomicrographs were taken with the digital camera Olympus DP72 digital camera attached to the microscope. Drawings of the copulatory apparatus were made with the aid of a camera lucida attached to the microscope Olympus BX41TF and BX51TF. The images were edited with the software GIMP (GNU Image Manipulation Program 2.8.16; The GIMP team www.gimp.org, 1995-2016) to enhance contrast and brightness and

sharpness. Unless nothing is stated, figures are oriented so that the anterior end of the body is to the left. Specimens from MNRJ and MZUSP collections were preserved in ethanol or processed material on histological slides. Each syntype from *Issoca rezendei* (deposited in the MNRJ) was given an additional label to distinguish it from the remaining type specimens. The length of the copulatory apparatus was measured as that delimited by the common muscle coat. Different size ratios of the copulatory apparatus were measured on diagrammatic reconstructions of the new and known species. The material was deposited at the Museu de Zoologia da Universidade de São Paulo (MZUSP), São Paulo, SP, Brazil.

2.4. Microcomputed tomography

The syntype MNRJ 8927 of *Issoca rezendei* was obtained on loan from the Museu Nacional do Rio de Janeiro, Brazil. The specimens were preserved in 100% ethanol. The external aspect of the syntypes was studied with a stereomicroscope. Additionally, the anatomy of the copulatory apparatus of the largest specimen was studied through virtual two-dimensional sections obtained from microcomputed tomography (mCT) following this procedures: submersion in a solution of 0.3% phosphotungstic acid (PTA) and 3% dimethyl sulfoxide (DMSO) in 95% hydrated ethanol for approximately 6 weeks to let PTA penetration into the body (Fernández *et al*., 2014; Silva & Carbayo, 2020). One day before scanning, the specimen was rinsed in 95% hydrated ethanol and transferred to a vial with 95% ethanol for mCT data acquisition. The region of the copulatory apparatus was scanned in General Electric V-Tomex equipment (housed in the Laboratório de Paleontologia e Microtomografia, Museum of Zoology of the Universidade de São Paulo) under the basic settings ranging from 23-75kV, and 174-340A. See details in Appendix. The visualization, editing and manipulation of the 3D images was done with the program myVGL (https://www.volumegraphics.com/en/products/myvgl.html) of free

use. The contrast of grey-scale virtual sections was enhanced with GIMP (GNU Image Manipulation Program 2.8.10).

2.5. Abbreviations used in the figures

(af) annular-shaped fold of male atrium
(cb) cerebral ganglion
(cl) subepithelial circular layer
(co) common glandular ovovitelline duct
(db) double diagonal cutaneous muscles
(dc) parenchymal layer of decussate fibres
(de) dorsal epidermis
(di) diagonal parenchymal muscle
(dv) dorso-ventral parenchymal muscle
(e) eye
(ej) ejaculatory duct
(ep) esophagus
(f) fold
(fa) female atrium
(fd) female genital canal
(g) gonopore
(gl) glands
(gs) ventral glandular surface of the cephalic region
(i) intestine
(ln) normal longitudinal cutaneous muscles
(m) muscle
(ma) male genital atrium
(mo) mouth
(o) ovary
(ov) ovovitelline duct
(p) pharynx
(po) pharyngeal pouch
(pp) penis papilla
(pv) prostatic vesicle
(r) cephalic retractor muscle
(s) sensory pits
(sb) subintestinal transverse muscles
(sd) sperm duct
(sg) shell glands
(sh) sheath
(sn) subneural transverse muscles
(sp) supraintestinal transverse muscles
(t) testis
(ve) ventral epidermis
(vi) vitellaria
(vn) ventral nerve plate

3. RESULTS

3.1. Molecular results

We obtained new sequences of the COI fragment of 17 specimens and 28S new sequences of 17 specimens (Tab. 1, marked with an asterisk). Among the new species here described, we failed to sequence DNA fragments of *S. 4* sp. n. (see below). The final data matrices consisted of 678 base pairs (bp) and 79 terminals for COI and 1003 bp and 75 terminals for 28S. All individuals were represented by both gene fragments, except for *Winsoria bipatria*, which is represented by sequences of COI only.

In the ML tree with the concatenated genes the group LWIS (*Luteostriata*, *Winsoria*, *Issoca*, and *Supramontana*) is highly supported as monophyletic and is nested within a large clade with all species of the East Andes (Fig. 2). All LWIS species are also highly supported as monophyletic. The remaining interrelationships of the LWIS vary in the support, ranging between low and very low. In these unstable relationships, *Issoca rezendei* is sister to the remaining LWIS members; *Issoca* and *Luteostriata* are polyphyletic (*Winsoria* and *Supramontana* are each represented by one species), and the three new species (a fourth new species lacks molecular data) are nested in different clades.

In the IB tree with the concatenated genes LWIS was also retrieved a clade with maximum PP (Fig. S1, Appendix) and all species are monophyletic, either with PP = 0.98 (*S. irritata*) or PP= 1.0 (remaining LWIS species). The PP of the remaining interrelationships are low, including two deep polytomies. Besides *I. rezendei* as sister to the other LWIS members, both ML and IB trees retrieved the following clades: (W. *bipatria*, *S. 3*), (((*L.* muelleri, *L. ernesti*), *L. graffi*), *S. 1* sp. n.), and (*L. abundans*, *L. ceciliae*). The phylogenetic relationships

between *Luteostriata*, *Supramontana*, *Winsoria* and the remaining species of *Issoca* are unclear.

3.2. Morphological results. Taxonomic section

Family **Geoplanidae** Stimpson, 1857

Subfamily **Geoplaninae** Stimpson, 1857

Genus ***Issoca*** Froehlich, 1955

3.2.1. *Issoca rezendei* (Schirch, 1929)

Synonymy

Geoplana rezendei Schirch, 1929 sp. n., p. 31-32, 36, pl. III. Type locality: Teresópolis, Rio de Janeiro, Brazil.

Issoca rezendei: Froehlich, 1955a, comb. nov., p. 228-234, pls. VIII-IX. Ubatuba, Vila Atlântica and Itanhaém (São Paulo state); Bahia, Santa Catarina state; Teresópolis, Rio de Janeiro state, Brazil.

Diagnosis

Species of *Issoca* with the dorsum exhibiting two pairs of dark stripes. Fibers of the subneural muscle cross the retractor muscle conspicuously. The prostatic vesicle is bifurcate. The penis papilla is conical and stubby, with a length half of its diameter. The papilla projects almost vertically from the roof of the atrium towards the gonopore. A female atrium does not exist.

Type locality. Teresópolis, Rio de Janeiro state, Brazil.

Material studied. **Type material. Syntype MNRJ 8927**. P. Schirch Coll, 1929, Teresópolis, Rio de Janeiro state, preserved in 80% ethanol. Studied through micro-computed tomography. **Additional specimens**. **F0024 (MZUSP PL. XXXX)**: F. Carbayo *et al*., campus Cidade Universitária Armando Salles de Oliveira, São Paulo, São Paulo state, 05 February 2002: horizontal sections of a portion anterior to the ovaries on 3 slides. **F0545 (MZUSP PL. XXXX)**: campus Cidade Universitária Armando Salles de Oliveira, São Paulo, São Paulo state, J. Pedroni *et al*. 03 September 2005: sagittal sections of copulatory apparatus on 8 slides; sagittal sections of the pharynx on 9 slides; transverse sections of the cephalic region on 6 slides; sagittal sections of the ovarian region on 7 slides; transverse sections of pre-pharyngeal region on 6 slides. **F0648 (MZUSP PL. XXXX)**: Gardens of the Fundação Maria Luisa e Oscar Americano, São Paulo, São Paulo state, D. Banhado *et al*. col., 05 December 2005: horizontal sections of the cephalic region on 3 slides; transverse sections of a portion anterior to the ovaries on 8 slides. **F0795 (MZUSP PL. XXXX)**: campus Cidade Universitária Armando Salles de Oliveira, São Paulo, São Paulo state, J. Pedroni *et al*., 19 December 2005: sagittal sections of the copulatory apparatus on 24 slides; sagittal sections of the pharynx on 15 slides; transverse sections of the cephalic region on 9 slides; transverse sections of a portion posterior to ovaries on 10 slides; horizontal sections of the ovarian region on 3 slides; transverse sections of pre-pharyngeal region on 11 slides. **F3595 (MZUSP PL. XXXX)**: Grassland in Morretes, Paraná state, F. Carbayo *et al*., 07 April 2009: sagittal sections of the copulatory apparatus on 4 slides.

Distribution

Rio de Janeiro, Teresópolis (Rio de Janeiro State); Mongaguá, São Paulo, Ubatuba (São Paulo State). Baía de Paranaguá (Paraná State); Blumenau, Itajaí (Santa Catarina State).

External morphology

The live animals are approximately 30-45 mm in length and 2-3 mm in width. The body is elongated with parallel margins (Fig. 3A–D). The shape of the cephalic region (2.5% of the body length) resembles an inverted spoon: it is slightly dilated dorsally and latero-laterally (Fig. 3) and concave ventrally. The anterior tip is rounded or truncated, depending on the degree of muscular contraction. The remaining, main body portion is convex dorsally, rounded in the margins and flattened ventrally. The posterior extremity is pointed. The largest preserved adult measured 39 mm in length, 2.4 mm in width and 0.8 mm in height.

The color of the living specimens is brown red in the cephalic region and in the posterior tip (Fig. 3A-C). The remaining body displays a pastel yellow ground color with a pair of paramedian black stripes (each with 11% of the width of the body) and a pair of lateral black stripes (18%). The stripes extend from the level of the cephalic region to nearly the posterior end. The ground color of the preserved syntype is beige and the stripes beige (Fig. 3D-E).

The eyes are formed by one pigmented cup 25 µm in diameter. They contour the anterior extremity of the body in a row of 1–2 eyes along the first 2 millimeters (Fig. 3E). Backwards, they spread progressively on each side of the dorsum to form a band with 42% of the body width until the end of the anterior half of the body. Backwards they become progressively more scarce until the posterior extremity of the body. Eyes occurring in the longitudinal paramedian bands are in small halos.

The relative mouth:body length ratio is 62-64% and that of gonopore:body length ratio is 75-80%.

Internal morphology

The width of the creeping sole equals 81-93% of body width at the pre-pharyngeal region. The sensory pits are 22.5 µm deep, and are

distributed in a single ventro-lateral row, from the very anterior tip of the body up to at least 6.5 mm behind (equal to 17% of body length).

Scarce cell glands producing erythrophil granules pierce dorsal epithelium of the pre-pharyngeal region. Rhabditogen cells pierce dorsal and marginal epithelium, in the latter being more abundant. Ventral epidermis is pierced scarcely by two types of gland cells, secreting erythrophil and xanthophil granules, respectively. A glandular margin is not present.

The cutaneous musculature is composed of three layers, i.e., a subepithelial circular (one-fiber thick), a diagonal with decussate bundles (7.5 µm thick) and an innermost longitudinal layer (37.5 µm thick dorsally and ventrally, the latter arranged in compact bundles that in the anterior extremity of the body form the retractor muscle of the cephalic region (see below). The cutaneous musculature, measured in four specimens, is as thick as 9-15% of body height.

In the pre-pharyngeal region (Fig. 4A), there are four parenchymal muscle layers: a dorsal layer with diagonal decussate fibers (20 µm thick, or 3% of the body height, specimen F0545), a transverse supraintestinal layer (25 µm, or 3.7%), a transverse subintestinal layer (15 µm, or 2.2%), and a transverse subneural layer (30 µm, or 4%). Dorso-ventrally oriented parenchymal fibers are abundant in this region.

In the anterior extremity of the body, the muscle fibers of the ventral cutaneous longitudinal layer originate the retractor muscle of the cephalic region (Fig. 4B-C; 5). At 1428 µm (F0795) (equal to 3.7% of body length) from the anterior extremity of the body, this layer becomes thinner towards the body margins and occupies 80% of the body width. Here, the subintestinal muscle layer is absent and dorso-ventral parenchymal muscle fibers are abundant and gathered in small bundles running obliquely in the transverse plane.

At 930 µm from the anterior extremity, the median region of the ventral cutaneous longitudinal muscle layer is sunken into the parenchyma and gives rise to the retractor of the cephalic region, which here is bell-shaped in transverse section (Fig. 5A).

At 550 µm from anterior extremity, the retractor is constituted of a medial, gross, cylindrical bundle and a few small, lateral bundles that detach from the gross bundle to run to the body sides (Fig. 5B). The small bundles run together and parallel to bundles of the subneural layer so that they are hardly distinguished from each other. Other fibers of this subneural muscle run laterally gathered in bundles traversing the retractor muscle (Fig. 5C-D). Here, this subneural parenchymal layer is well developed whereas the remaining parenchymal layers are insignificant.

At 460-360 µm (Fig. 5C-D), the gross bundle is ellipse-shaped in cross section. Shortly anteriorly, the fibers of its dorsal side also detach and run obliquely towards the dorsum and sides of the body.

At 320-260 µm (Fig. 5E-F) from the anterior extremity, oblique muscle fibers are relatively abundant and dorso-ventral parenchymal fibers acquire highest density. Here, the retractor is less apparent. It disappears close to the anteriormost extremity of the body.

The glandular surface of the ventral epidermis of the concave cephalic region widens towards the anterior extremity of the body as the muscle fibers of the retractor concentrate medially. This glandular surface is richly pierced by gland cells producing erythrophil granules, and by scarce glands producing cyanophil granules.

The mouth is situated in the middle of the pharyngeal pouch (Fig. 6). The pharynx is bell-shaped, with the dorsal insertion placed backwards by a distance equal to 70% of pharyngeal length so that it lays dorsal to the mouth. The lining epithelium of the pharyngeal pouch is flat, non-ciliated, and is surrounded by a 10-µm thick circular muscle.

The outer and inner pharyngeal epithelia are flat and ciliated. The outer epithelium is underlain by a longitudinal muscle (5 µm thick) followed by a circular muscle (30–45 µm), the latter with some longitudinal fibers interspersed. The inner epithelium is surrounded by a circular muscle (17.5–47.5 µm), followed by a longitudinal muscle (10–45 µm, specimen F0545). A ventral nerve plate is present.

The testes are located beneath the supraintestinal transverse muscle layer, between the intestinal diverticula (Fig. 4A). They extend from 8 mm behind anterior extremity of the body (27% of body length) to nearly the root of the pharynx. The sperm ducts run between the subintestinal parenchymal muscle fibers, dorso-laterally to the ovovitelline ducts. Close to the penis bulb, these ducts bend dorsally and medially to penetrate the dorso-proximal section of penis bulb, subsequently opening into the anterior section of the respective branch of the prostatic vesicle (Fig. 7). The prostatic vesicle is bifurcate, each branch long, and wider in its with mid-region. The branches run posteriorly and slightly ventrally, their distal half is placed within the penis papilla. As the paired branches merge, they open into an irregular cavity, or ejaculatory duct, running downwards to open at the tip of the penis papilla. The prostatic vesicle is lined with a ciliated, columnar epithelium. Anteriormost portion of the branches receive some glands producing erythrophil granules. Most prostatic vesicle is pierced by glands producing conspicuous xanthophil granules (Fig. 8A-B). The vesicle surrounded by criss-crossed muscles. The ejaculatory duct is lined with a cuboidal epithelium and is surrounded by a 2-um thick circular muscle.

The penis papilla is conical and stubby, with a length half of its diameter. The papilla projects almost vertically from the roof of the atrium towards the gonopore (Fig. 7A-B; 8A) and is lined with a cuboidal, non-ciliated epithelium. This epithelium is surrounded by a 10-um thick muscle of criss-crossed fibers. Numerous glands discharge erythrophil granules through the papillar epithelium,

excepting that around the ejeculatory duct. Bodies of these glands are located outside the penis bulb. The penis papilla occupies most of the male atrium. This atrium is smooth and the gonopore is located in its mid-region. This atrium is lined with a columnar, non-ciliated epithelium, which is pierced by numerous glands producing fine erythrophil granules. A 10-µm-thick circular muscle followed by a 5-um-thick longitudinal muscle surrounds the atrial epithelium.

The ovaries are 310 µm long in the antero-posterior body axis and 140 µm wide (Fig. 8C). They are located immediately above the ventral nerve plate, at a distance from the anterior tip equivalent to 25% of body length. The ovovitelline ducts arise from the lateral surface of the anterior portion of the ovaries, and run backwards above the ventral nerve plate. They ascend laterally to the gonopore canal to join dorsally to the female genital canal to form a common ovovitelline duct. The distal half of the ascending portion of these paired ducts receives shell glands. The common ovovitelline duct runs backwards progressively bending to the ventral side to communicate with the female genital canal. This long canal (270 µm in specimen F0648) runs anteriorly, slightly ventrally, to open into the posterior section of the male atrium. A female atrium does not exist. This long canal is lined with a columnar, ciliated epithelium that contains fine erythrophil granules, and is underlain by a criss-crossed, 8-um-thick muscle.

A muscle coat of fibers orientated as a net wraps the prostatic vesicle, the male atrium and the anterior portion of the female genital canal.

Remarks

This is the only species of the genus. The species is abundant in yards and gardens across Southeast and South Brazil. It was not found in the forest. For this reason, it might have been dispersed by human activity.

Genus ***Supramontana*** Carbayo & Leal-Zanchet, 2003

Synonymy

Luteostriata Carbayo, 2010, **syn. nov.**

Winsoria Negrete *et al*., 2019, **syn. nov.**

Type species: *Supramontana irritata* Carbayo & Leal-Zanchet, 2003

3.2.2. *Supramontana jandaia* (Froehlich, 1955) comb. nov.

Synonymy

Issoca jandaia Froehlich, 1955a. sp. n., p. 230-234. pls. VIII.

Not *Issoca jandaia* in Carbayo *et al*. (2013) and specimens MZUSP PL 1015, and MZUSP PL 1213 in the Genbank.

Type locality. Monte do Jaraguá, São Paulo State, Brazil.

Material studied. **Type material**. **Syntype 1** (‘1’ as slides are labeled with “verme 1”): Monte do Jaraguá, São Paulo, São Paulo state, Froehlich & Froehlich, August 1951, sagittal sections of copulatory apparatus on slides S1525-S1527 (illustrated on Fig. 52 in Froehlich, 1955). **Syntype 2** (‘2’ as slides are labeled with “verme 2”): idem, sagittal sections of copulatory apparatus on slides S1528-S1529. **Unlabeled syntype (either 1, 2 or 3)**: sagittal sections of the pharynx (illustrated on Fig. 53 in Froehlich, 1955) on slide S1530; sagittal sections of the cephalic region on slides S1533-S1535; transverse sections of the cephalic region on sides S1536, S1538-S1540; transverse sections of the cephalic region on sides S1541-S1545.

Distribution

Only known from the type locality.

Diagnosis

Species of *Supramontana* with three dorsal stripes of which the mid-stripe is narrower. Female atrium length : male atrium length ratio is 1.3; the prostatic vesicle length : copulatory apparatus length ratio ranges between 0.2-0.3; the copulatory apparatus height : body height ratio is 0.4; the ejaculatory duct runs ventro-posteriorly; the male epithelium is pierced by numerous erythrophil glands.

External morphology

See original description and Fig. 9 of this paper.

Internal morphology

The sensory pits are 25 µm deep and are distributed in a simple ventro-lateral row, from the very anterior extremity up to at least 5.3% of body length. In the pre-pharyngeal region (Fig. 10), the dorsal and marginal epithelium are pierced by rhabditogen cells, glands cells producing erythrophil granules and abundant and apparent cell glands producing cyanophil granules. There is not a well delimited glandular margin. The ventral epidermis is pierced by scarce gland cells secreting fine erythrophil and cyanophil granules.

The cutaneous musculature comprises the three typical layers of Geoplaninae, i.e., a subepithelial circular layer followed by a double diagonal layer with decussate fibers, and a strongly developed longitudinal layer, 50 µm thick dorsally and 80 µm ventrally. The fibers of the latter muscle layer are gathered into compact bundles. The cutaneous musculature thickness relative to body height at the pre-pharyngeal region is 15.9%.

Four parenchymal muscle layers are present throughout the body: a dorsal layer of diagonal decussate fibers (25 µm thick, or 2.8% of the body height), a transverse supraintestinal layer (30 µm, or 3.4%), a transverse subintestinal layer (25 µm, or 2.8%), and a subneural layer (40 µm, or 4.5%) of transverse muscles. Dorso ventral oriented

parenchymal muscle fibers are abundant in the pre-pharyngeal region.

The muscular organization of the cephalic region differs from that of the remaining body. Bundles of ventral longitudinal cutaneous muscles gradually concentrate medially to give rise to the cephalic retractor muscle (Fig. 11). Approximately at 1 mm from the anterior extremity, the retractor resembles a lens in cross-section (Fig. 11A-B). Here the four parenchymatic muscle layers are well developed, specially the dorso-diagonal and the subneural layers. Closer to the anterior extremity the retractor muscle becomes rounded and all its fibers are gathered in a compact mass. In this region, parenchymatic muscle layers are inconspicuous, with the exception of the subneural layer, strongly developed and organized in conspicuous bundles running transversally over the retractor muscle (Fig. 11C). A few fibers of this layer seemingly are interwoven with dorsalmost fibers of retractor muscle. From this region towards anterior extremity fibers of the retractor muscle progressively detach in bundles that run to the body sides (Fig. 11D-F). As they detach, the retractor muscle acquires a cross section shape resembling a vertically oriented lens (Fig. 11E-F) and becomes less apparent until it disappears close to the anteriormost extremity of the body. All parenchymal muscles fade out near the anteriormost body portion. Dorso-ventral parenchymal muscle fibers are abundant in the cephalic region and they are frequently gathered in bundles of 4–10 fibers each. These fibers connect dorsal epidermis with the ventral glandular epidermis. Medially, some fibers run obliquely from the dorsal epidermis of one side of the body to anchor to the ventral glandular epidermis of the other body side, thereby rimming the retractor muscle.

The glandular surface of the cephalic ventral epidermis, widens towards anterior extremity of the body as the muscle fibers of the retractor concentrate medially. This surface is incompletely bipartite (Fig. 9B) and is richly pierced by gland cells producing erythrophil

granules, and by scarce glands producing xanthophil granules (Fig. 11).

The mouth is situated at a distance from the root of the pharynx equivalent to 38,4% of pharyngeal pocket length (Fig. 12A). An esophagus is absent. The pharynx is cylindrical, with dorsal insertion posterior to the ventral and located anteriorly to the mouth level. The lining epithelium of the pharyngeal pouch is squamous, non-ciliated, surrounded by a layer of circular fibers (22.5 µm thick). The outer and inner pharyngeal epithelia are flat and ciliated. The outer epithelium is underlain by a simple longitudinal muscle, followed by a circular muscle (25 µm). The inner epithelium is surrounded by a circular muscle (30 – 40 µm), followed by a longitudinal muscle (15 µm). The central nervous system mainly consists of a ventral nerve plate.

The testes are located under the supraintestinal transverse muscle layer, mostly between the intestinal diverticula (Fig. 10). The position of anteriormost testes was not measured since the body portion containing it was not available. Posteriormost testes lay nearly the root of the pharynx. The sperm ducts run between the subintestinal parenchymal muscle layer, dorso-internally to the ovovitelline ducts. Each sperm duct opens into a thin and short diverticulum projected from the antero-lateral aspect of the prostatic vesicle. This vesicle is extrabulbar and consists of a dilated proximal portion dorso-anterior orientated and a tubular distal portion, initially ventral and then ascending (Fig. 12B). The prostatic vesicle penetrates the anterior aspect of the penis bulb (Fig. 12B; 13-AB). The prostatic vesicle receives abundant fine erythrophil granular secretions derived from glands in the parenchyma. Prostatic vesicle lined with ciliated, columnar epithelium, which is surrounded by a strongly developed circular muscle with some longitudinal fibers interspersed. The prostatic vesicle passes into the ejaculatory duct. Proximally, this duct is sinuous and 50 µm in diameter; distally, 30 um. Ejeculatory duct lined with a ciliated, cuboidal epithelium surrounded by circular

muscle. The ejaculatory duct terminates at the base of a large sheath that simulates a penis papilla). A penis papilla is absent. This sheath occupies almost the entire male atrium. The sheath is lined with a cuboidal, non-ciliated epithelium, pierced by two types of gland cells producing cyanophil and erythrophil granules, respectively; the latter being most abundant. The epithelium is underlain by a 5-um-thick muscle of longitudinal fibers.

The male atrium is mostly occupied by the sheath and large folds. One of these folds is a transverse, annular-shaped fold located halfway of the atrial length. From the roof of the distal portion of the male atrium, a large fold projects laterally and continues along the female atrium. The male atrium is lined with a columnar, non-ciliated erythrophil epithelium. This epithelium is pierced by gland cells producing cyanophil granules and by very abundant gland cells producing erythrophil granules. A circular muscularis (5 µm thick) encircles the male atrium, followed by a one-fiber-thick longitudinal muscle.

Position and measurements of ovaries were not measured since the body portion presumably containing them was not available. The ovovitelline ducts arise from the dorso-anterior surface of the anterior portion of the ovaries, and run backwards above the ventral nerve plate. They ascend posteriorly to the gonopore region, and subsequently unite dorsally to form a common ovovitelline duct dorsally to the female atrium (Fig. 12B). The distal fourth of the ascending portion of these paired ducts receives shell glands. The glandular ovovitelline duct runs posteriorly and communicates with the female genital canal. This canal is curved ventro-posteriorly to communicate with the posterior section of the female atrium. Female genital canal lined with a columnar epithelium the subapical surface of it is erythrophil. The female atrium is an irregular, spacious cavity, gradually dilated towards male atrium. Walls of the female atrium are folded and partially projected into its lumen. One of these folds is

continuous with a fold coming from the male atrium (Fig. 12B; 13). The female atrium is lined with a cuboidal-to-columnar epithelium. The muscularis of the female atrium consists of two muscle layers, a 5-um-thick longitudinal muscle followed by a 15-um thick circular muscle, both partially intermingled. The female atrium receives gland cells producing erythrophil granules. The common muscle coat is well-developed; dorsal to the gonopore, this muscle coat is divided into a male and female coat.

Remarks

Among the species of the genus, only S. *jandaia* exhibits five thin stripes with the medial one being thinner than the remaining stripes. Regarding the internal morphology, only *S. 3* and S. *2* sp. n. are similar to S. *jandaia* in the general shape of the copulatory organ with respect to the female atrium length : male atrium length (around 1.3), the prostatic vesicle length : copulatory apparatus length (around 0.2-0.3), and the copulatory apparatus height: body height (around 0.4). However, in S. *2* sp. n., the ejaculatory duct runs more or less horizontally (*vs.* ventro-posteriorly in S. *jandaia*), whereas *S. 3* differs from *S. jandaia* in that the male epithelium is pierced by a relatively low number of erythrophil glands (*vs.* very numerous in S. *jandaia*).

3.2.3. *Supramontana piranga* (Froehlich, 1955) comb. nov.

Synonymy

Issoca piranga Froehlich, 1955a. sp. n., p. 232-234. pls. VIII.

Type locality. Teresopolis, Rio de Janeiro State, Brazil.

Material studied. **Holotype**, Parque Nacional da Serra dos Órgãos, Teresópolis, Rio de Janeiro state. Froehlich & Froehlich, June 1952. (MZUSP PL. XXXX): transverse sections of cephalic region on slides S1511-1515, S1701-S1702; horizontal sections of the ovarian region on 3 slides; transverse sections of a portion posterior to ovaries on 5 slides; transverse sections of pre-pharyngeal region on 6 slides; sagittal sections of the pharynx (illustrated on Fig. 58 in Froehlich, 1955) on slides S1506-1507; sagittal sections of copulatory apparatus (illustrated on Fig. 57 in Froehlich, 1955) on slides S1508-S1510.

Diagnosis

Species of *Supramontana* with the cephalic region notably expanded laterally; the dorsum is decorated with a pair of black paramedian bands and a pair of inconspicuous lateral stripes; the male atrium is as long as the female atrium; the prostatic vesicle has about 30% of the length of the copulatory apparatus; the ejaculatory duct opens at the tip of a penis papilla.

Description

External morphology

Live specimen (Fig. 14A) measured 37 mm in length and 3 mm in width. Preserved, measured 25 mm in length and 3 mm in width. The body is elongated with nearly parallel margins. The cephalic region is enlarged and has a constriction separating it from the rest of the body. The creeping sole is as wide as 2/3th of body width. The mouth

lays at a distance from the anterior extremity equal to 60% of body length; the gonopore at 76%.

The eyes are formed by one pigmented cup with 25 µm in diameter. The eyes contour the anterior end in an irregular row along the first two millimeters; backwards, they spread progressively on each side of the dorsum.

Internal morphology

The sensory pits are 20µm deep and are distributed in a simple ventro-lateral row, from the very anterior extremity up to at least 14% of body length. In the pre-pharyngeal region (Fig. 14B), rhabditogen cells producing erythrophil granules and abundant and very apparent cell glands producing xanthophil granules open through the dorsal epithelium and marginal epithelium; necks of xanthophil glands are 25 µm in width. The ventral epidermis is pierced by scarce gland cells secreting fine erythrophil granules.

The cutaneous musculature comprises the three typical layers of Geoplaninae, i.e., a simple subepithelial circular layer followed by a double diagonal layer with decussate fibers, and a strongly developed longitudinal layer, 70 µm thick dorsally and 85 µm ventrally. The fibers of the latter muscle layer are gathered into compact bundles (Fig. 14A-C). The cutaneous musculature thickness relative to body height at the pre-pharyngeal region is 14.7%.

The three usual parenchymal muscle layers are present throughout the body: a dorsal layer of diagonal decussate fibers (25 µm thick, or 4.3% of the body height), a transverse supraintestinal layer (32.5 µm, or 5.4%), and a transverse subintestinal layer (10 µm, or 1.7%). Additionally, there is a subneural layer (35 µm, or 5,8%) of transverse muscles.

The muscular organization changes (Fig. 15) towards the anterior region of the body with respect to that of the pre-pharyngeal region. Bundles of ventral longitudinal cutaneous muscles gradually

concentrate medially to give rise to the cephalic retractor muscle. At 1.6–1.8 mm from the anterior extremity, the retractor resembles a lens in cross-section horizontally located (Fig. 15A-B). Muscle fibers of the retractor muscle are gathered in few but thick bundles. Here the dorso-diagonal and subintestinal parenchymatic muscle layers are weak, whereas the supraintestinal and the subneural layers are well developed. More anteriorly, the retractor muscle becomes rounded and all its fibers are gathered in a compact mass (Fig. 15B). In this region, parenchymatic muscle layers are inconspicuous, with the exception of the subneural layer, developed and organized in conspicuous bundles running transversally over the retractor muscle. Apparently, some fibers of this layer abut or intertwine with the most dorsal fibers of the retractor muscle. From this region towards anterior extremity fibers of the retractor muscle progressively detach in bundles that run to the body sides (Fig. 15C-D). As they detach, the retractor muscle acquires a cross section shape resembling a vertically oriented lens and becomes less apparent until it disappears close to the anteriormost extremity of the body. All parenchymal muscles fade out near the anteriormost body portion. Dorso-ventral parenchymal muscle fibers are abundant in the cephalic region and they are frequently gathered in bundles of 3–15 fibers each. These fibers connect dorsal epidermis with the ventral glandular epidermis. Medially, some fibers run obliquely from the dorsal epidermis of one side of the body to anchor to the ventral glandular epidermis of the other body side, thereby rimming the retractor muscle. The glandular surface of the ventral epidermis widens towards the anterior extremity of the body as the muscle fibers of the retractor concentrate medially. This surface is incompletely bipartite and is richly pierced by gland cells (with 7.5–10 µm thick necks) producing erythrophil granules.

The mouth is situated at a distance from the root of the pharynx equivalent to 37.2% of pharyngeal pocket length (Fig. 16A). An

esophagus is present with 12.8% of pharynx length. The pharynx is cylindrical, with dorsal insertion posterior to the ventral and located anteriorly to the mouth level. The lining epithelium of the pharyngeal pouch is squamous, non-ciliated, surrounded by a layer of circular fibers (12.5 µm thick). The outer and inner pharyngeal epithelia are flat and ciliated. The outer epithelium is underlain by a simple longitudinal muscle, followed by a circular muscle (15 µm). The inner epithelium is surrounded by a circular muscle (15–37.5 µm), followed by a longitudinal muscle (12.5 µm). The central nervous system mainly consists of a ventral nerve plate.

The testes are located under the supraintestinal transverse muscle layer, between the intestinal diverticula. They extend from 8 mm behind anterior extremity of the body (32% of body length) to nearly the root of the pharynx. The sperm ducts run between the subintestinal parenchymal muscle layer, dorso-medially to the ovovitelline ducts. Each sperm duct opens into a thin and short diverticulum projected from the lateral aspect of the prostatic vesicle. This vesicle is extrabulbar and consists of a dilated proximal portion and a tubular, sinuous, distal portion (Fig. 16B). The prostatic vesicle penetrates the dorso-anterior aspect of the penis bulb. The prostatic vesicle receives fine erythrophil granular secretions derived from glands in the parenchyma. Prostatic vesicle lined with ciliated, columnar epithelium, which is surrounded by a strongly developed circular muscle (75µm). The prostatic vesicle passes into the ejaculatory duct. Proximally, this duct is sinuous with 30 µm in diameter; distally straight, 25 µm. Ejeculatory duct lined with a ciliated, cuboidal epithelium surrounded by circular muscle. The protrusible penis papilla is conical, slightly inclined ventrally, and with its dorsal insertion posterior to the ventral insertion (Fig. 16B-C). The penis papilla occupies only the proximal portion of the male atrium. The penis papilla is lined with a cuboidal, non-ciliated epithelium, pierced by glands producing erythrophil granules.

The male atrium is mostly occupied by the penis papilla and by large folds. One of these folds is a transverse, annular-shaped fold that separates the male and female atrium. The male atrium is lined with a columnar, non-ciliated epithelium. This epithelium is pierced by gland cells producing erythrophil granules. A circular muscularis (7.5 µm thick) encircles the male atrium, followed by a one-fiber-thick longitudinal muscle.

The ovaries are 245 – 290 µm long in the antero-posterior body axis and 100 – 125 µm wide. They are located immediately above the ventral nerve plate, at a distance from the anterior tip equivalent to 28,6% of body length. The ovovitelline ducts ascend laterally to the gonopore region, and subsequently unite dorsally to form a common ovovitelline duct dorsally to the female atrium. In the middle of the ascending portion of these paired ducts it receives shell glands. The glandular ovovitelline duct, long, runs straight posteriorly and communicates with the female genital canal. This canal is curved ventro-posteriorly to communicate with the posterior section of the female atrium (Fig. 16D). The female atrium is an irregular, spacious cavity, gradually dilated towards male atrium. Walls of the female atrium are folded and partially projected into its lumen. The female atrium is lined with a cuboidal-to-columnar epithelium. The muscularis of the female atrium consists of two muscle layers, a 5-um-thick longitudinal muscle followed by a 15-um thick circular muscle, both partially intermingled. The female atrium receives gland cells producing erythrophil granules. The common muscle coat is well-developed; dorsal to the gonopore, this muscle coat is divided into a male and female coat.

Remarks

Externally, *I. piranga* differs from its congeners in that the cephalic region is notably expanded laterally and the dorsum is ornated with a pair of black paramedian bands and a pair of inconspicuous lateral stripes. Internally, the species resembles *S. jandaia, S. 2* sp. n.*, S. 3* and *S. 4* sp. n. in the general shape of the copulatory apparatus in that the male and female atria have the same relative length, and the prostatic vesicle has about 0.3 times the length of the copulatory apparatus. However, only in S. *piranga* there is a penis papilla with the ejaculatory duct opening at its tip.

3.2.4. *Supramontana potyra* (Froehlich, 1957) comb. nov.

Synonymy:

Issoca potyra Froehlich, 1958. sp. n.

Type locality. Eldorado (formerly Xiririca), São Paulo state, Brazil.

Material studied. Type material. **Holotype**, Otto Schubart, 21 November 1952. Sagittal sections of the cephalic region (illustrated on Fig. 35 in Froehlich, 1957) on slides S1516-S1517; transverse section of a body region immediately behind the cephalic region on slide S1520; sagittal sections of portion containing ovaries on 41 slides; horizontal sections of portion posterior to ovaries on 22 slides;

transverse sections of the pre-pharyngeal region on slides S1518-S1519; transverse sections of pre-pharyngeal region on 25 slides; sagittal sections of the pharynx (illustrated on Fig. 36 in Froehlich, 1957) on slides S1523-S1525; sagittal sections of the copulatory apparatus (illustrated on Fig. 37 in Froehlich, 1957) on slides S1521-S1522;

Diagnosis

Species of *Supramontana* with a pair of black bands dorsally; the female atrium has half the length of the male atrium length; the prostatic vesicle length is 10% of that of the copulatory apparatus; the penis papilla is as long as the male atrium.

Description

External morphology

See original description and Fig. 17 in this paper.

Internal morphology

The sensory pits are 20 µm deep and are distributed in a simple ventro-lateral row, from the very anterior extremity up to at least 13.6% of body length. In the pre-pharyngeal region (Fig. 18A), rhabditogen cells producing erythrophil granules and abundant and very apparent cell glands producing erythrophil granules open through the dorsal epithelium and marginal epithelium; necks of erythrophil glands are 12.5 µm in width. The ventral epidermis is pierced by cells producing erythrophil granules and scarce cells secreting fine cyanophil granules.

The cutaneous musculature comprises the three typical layers of Geoplaninae, i.e., a subepithelial circular layer followed by a double diagonal layer with decussate fibers, and a strongly developed longitudinal layer, 100 – 150 µm thick dorsally and 85 µm ventrally. The fibers of the latter muscle layer are gathered into compact

bundles (Fig. 18A-B). The cutaneous musculature thickness relative to body height at the pre-pharyngeal region is 12 – 23%.

The three usual parenchymal muscle layers are present throughout the body: a dorsal layer of diagonal decussate fibers (50 µm thick, or 4.7% of the body height), a transverse supraintestinal layer (60µm, or 5.6%), and a transverse subintestinal layer (30 µm, or 2.8%). Additionally, there is a subneural layer (50µm, or 4.7%) of transverse muscles.

The muscular organization changes (Fig. 18C) towards the anterior region of the body with respect to that of the pre-pharyngeal region. Bundles of ventral longitudinal cutaneous muscles gradually concentrate medially to give rise to the cephalic retractor muscle. In this region, parenchymatic muscle layers are inconspicuous, with the exception of the supraintestinal and subneural layer. The subneural layer is organized in conspicuous bundles running transversally over the retractor muscle. A few fibers of this layer seemingly are interwoven with dorsalmost fibers of retractor muscle. From this region towards anterior extremity fibers of the retractor muscle progressively detach in bundles that run to the body sides. All parenchymal muscles fade out near the anteriormost body portion. Dorso-ventral parenchymal muscle fibers are abundant in the cephalic region and they are frequently gathered in bundles of 3–10 fibers each. These fibers connect dorsal epidermis with the ventral glandular epidermis. The glandular surface of the ventral epidermis widens towards the anterior extremity of the body as the muscle fibers of the retractor concentrate medially. This surface is richly pierced by gland cells (with 10–12.5 µm thick necks) producing xanthophil and cyanophil granules, and by scarce glands producing erythrophil granules.

The mouth is situated at a distance from the root of the pharynx equivalent to 29.6% of pharyngeal pocket length (Fig. 19A). An

esophagus is absent. The pharynx is bell-shaped, with dorsal insertion posterior to the ventral and located posterior to the mouth level. The lining epithelium of the pharyngeal pouch is squamous, non-ciliated, surrounded by a layer of circular fibers (7.5 µm thick). The outer and inner pharyngeal epithelia are flat and ciliated. The outer epithelium is underlain by a simple longitudinal muscle, followed by a circular muscle (20 µm), with some longitudinal fibers interspersed. The inner epithelium is surrounded by a circular muscle (40 – 100 µm), followed by a longitudinal muscle (20 µm). The central nervous system mainly consists of a ventral nerve plate.

The testes are located under the supraintestinal transverse muscle layer. They extend from 11.5 mm behind the anterior extremity of the body (29.5% of body length) to nearly the root of the pharynx.

The sperm ducts run between the subintestinal parenchymal muscle layer, dorso-internally to the ovovitelline ducts. Each sperm duct opens into the antero-lateral aspect of the prostatic vesicle. This vesicle is extrabulbar and dilated, and penetrates the anterior aspect of the penis bulb. The prostatic vesicle receives fine erythrophil granular secretions derived from glands in the parenchyma. Prostatic vesicle lined with ciliated, cuboidal epithelium, which is surrounded by a simple longitudinal muscle, followed by a circular muscle (20 µm) with some longitudinal fibers interspersed. The prostatic vesicle passes into a sinuous ejaculatory duct. Ejeculatory duct lined with a ciliated, cuboidal epithelium surrounded by circular muscle. The ejaculatory duct terminates at the ventral penis papilla region (Fig. 20). The protrusible penis papilla is conical, slightly inclined ventrally, and with its dorsal insertion posterior to the ventral insertion. The penis papilla is as long as the male atrium. The penis papilla occupies most of the male atrium. Penis papilla is lined with a cuboidal, non-ciliated epithelium, pierced by glands producing erythrophil granules, and underlain by a simple layer of circular fibers.

The male atrium is mostly occupied by the penis. From the roof of the distal portion of the male atrium, a large fold projects laterally and continues along the female atrium. The male atrium is lined with a columnar, non-ciliated epithelium. This epithelium is pierced by gland cells producing erythrophil granules. A simple circular layer encircles the male atrium, followed by a one-fiber-thick longitudinal muscle.

The ovaries are 450 µm long in the antero-posterior body axis and 220 µm wide. They are located immediately above the ventral nerve plate, at a distance from anterior tip equivalent to 28.5% of body length (Fig. 19B). The ovovitelline ducts arise from the dorso-lateral surface of the ovaries, and run backwards above the ventral nerve plate. They ascend anteriorly to the gonopore region, and subsequently unite dorsally to form a common ovovitelline duct dorsally to the female atrium. The distal fourth of the ascending portion of these paired ducts receives shell glands. The glandular ovovitelline duct runs posteriorly and communicates with the female genital canal. This canal is dilated (200 µm wide) and curved ventro-posteriorly to communicate with the posterior section of the female atrium. Female genital canal lined with a columnar, non-ciliated epithelium. The female atrium is an irregular, spacious cavity, gradually dilated towards male atrium (Fig. 20). Walls of the female atrium are folded and partially projected into its lumen. One of these folds is continuous with a fold coming from the male atrium. The muscularis of the female atrium consists of two muscle layers, a longitudinal muscle followed by a circular muscle, both partially intermingled. The female atrium receives gland cells producing erythrophil granules. The common muscle coat is well-developed; dorso-anteriorly to the gonopore, this muscle coat is divided into a male and female coat.

Remarks

The external aspect of *S. potyra* only confounds with that of *S. 1* sp. n. in that the dorsum of both species presents a pair of black bands. Nevertheless, the bands are closer to each other in *S. potyra*. With regard to the copulatory apparatus only *S. arturi* and *S. 1* sp. n. resemble *S. potyra* in that the female atrum is more or less half the length of the male atrium and in that the relative length of the prostatic vesicle is roughly 0.1 times as long as the copulatory apparatus. However, the copulatory apparatus of *S. arturi* is relatively longer and lacks a penis papilla, whereas in *S. 1* sp. n., the prostatic vesicle is elongate (*vs.* short in *S. potyra*) and the penis papilla is as long as the male atrium (*vs.* shorter in *S. potyra*).

3.2.5. *Supramontana 1* sp. n.

Type locality. Intervales State Park, Ribeirão Grande, São Paulo State, Brazil.

Material studied. Type material. Intervales State Park (-24.27 -48.41), Ribeirão Grande, São Paulo State, Brazil. **Holotype F3754g (MZUSP PL. XXXX)** (MZUSP PL. XXXX) F. Carbayo *et al*., col., 6 July 2009: transverse sections of cephalic region on 3 slides; horizontal sections of portion anterior to ovaries on 7 slides; sagittal sections of portion containing ovaries on 15 slides; transverse sections of pre-pharyngeal region on 14 slides; sagittal sections of pharynx region on 26 slides; sagittal sections of copulatory apparatus on 21 slides. **Paratype F2690 (MZUSP PL. XXXX)** F. Carbayo *et al*., col., 25 July 2008: transverse sections of cephalic region on 35 slides; horizontal sections of portion containing ovaries on 15 slides; horizontal sections of portion posterior to ovaries on 11 slides; transverse sections of pre-pharyngeal region on 26 slides; sagittal sections of portion containing pharynx and copulatory apparatus region on 54 slides. **Paratype F2691 (MZUSP PL. XXXX)** F. Carbayo *et al*., col., 25 July 2008: sagittal sections of copulatory apparatus on 12 slides. **Paratype F3083 (MZUSP PL. XXXX)** F. Carbayo *et al*., col., 12 December 2008: horizontal sections of cephalic region on 4 slides; horizontal sections of portion anterior to ovaries on 4 slides; horizontal sections of portion containing ovaries on 4 slides; transverse sections of pre-pharyngeal region on 7 slides; sagittal sections of pharynx region on 9 slides; sagittal sections of copulatory apparatus on 12 slides. **Paratype F3136 (MZUSP PL. XXXX)** F. Carbayo *et al*., col., 13 December 2008: sagittal sections of portion containing pharynx and copulatory apparatus region on 38 slides.

Cantareira State Park, Tres Cruzes, São Paulo State, Brazil. **Paratype F2941 (MZUSP PL. XXXX)** F. Carbayo *et al*., col., 26 October 2008: transverse sections of cephalic region on 13 slides; sagittal sections of copulatory apparatus on 10 slides. **Paratype F3029 (MZUSP PL. XXXX)** F. Carbayo *et al*., col., 14 December 2008: horizontal sections of portion containing ovaries on 12 slides; transverse sections of pre-pharyngeal region on 8 slides; sagittal sections of pharynx region on 12 slides; sagittal sections of copulatory apparatus on 36 slides. **Paratype F3047 (MZUSP PL. XXXX)** F. Carbayo *et al*., col., 14 December 2008: horizontal sections of cephalic region on 2 slides; horizontal sections of portion containing ovaries on 2 slides; transverse sections of portion posterior to ovaries on 12 slides; transverse sections of pre-pharyngeal region on 3 slides; sagittal sections of portion containing pharynx and copulatory apparatus region on 22 slides. **Paratype F3515** F. Carbayo *et al*., col., 26 March 2009: horizontal sections of cephalic region on 9 slides. **Paratype F3525 (MZUSP PL. XXXX)** F. Carbayo *et al*., col., 26 March 2009: transverse sections of cephalic region on 7 slides; horizontal sections of portion anterior to ovaries on 4 slides; sagittal sections of portion containing ovaries on 10 slides; transverse sections of pre-pharyngeal region on 11 slides; sagittal sections of pharynx region on 14 slides; sagittal sections of copulatory apparatus on 14 slides.

Diagnosis

Species of *Supramontana* with a pair of black bands on the yellowish color of the dorsum; the female atrium length: male atrium length ratio is 0.5; the prostatic vesicle length: copulatory apparatus length ratio is 0.3; the ejaculatory ducts crosses the penis papilla to open subterminally.

Description

External morphology

Largest fixed specimen (specimen F3083) is 54mm in length and 3.5mm in width and 1 mm high. The body is elongated with parallel margins (Fig. 21). The cephalic region (1/50th of the body length) has a constriction which separates it from the rest of the body (Fig. 21B). The anterior end is slightly laterally dilated, before converging to the rounded extremity of the body, and its ventral surface is slightly concave). The posterior extremity is pointed. The dorsum is convex, the ventral side is flattened, and the body margins are rounded, so that the section of the body is elliptic. The creeping sole is as wide as 73 – 83% of body width at the pre-pharyngeal region. The mouth lays at a distance from anterior extremity equal to 64 – 67% of body length; the gonopore at 89 – 94% (specimen F3083 and F3754g, respectively).

The ground color is pastel yellow with paste orange color in the extremities, and two paramedian black stripes (3/19th of body width) (Fig. 21A-C). The stripes extend from the level of the cephalic constriction to nearly the posterior end. The ventral side is beige in color, with the margins pastel yellow (Fig. 21D).

The eyes are formed by one pigmented cup with 35-65 µm in diameter in the center of halos. Anteriormost eyes are larger and fine along the antero-posterior body axis. The eyes contour the anterior end in a row of 2-3 eyes along the first two millimeters; backwards, they spread progressively on each side of the dorsum in a band with 3/5th of the body width until the end of the anterior half of the body. Posterior to this region, they are scarcer and the band narrows until posterior tip.

Internal morphology

The sensory pits are 25-30µm deep and are distributed in a simple ventro-lateral row, from the very anterior extremity up to at least 19% of body length. In the pre-pharyngeal region (Fig. 22), numerous rhabditogen cells pierce dorsal and marginal epithelium. Very apparent cell glands producing xanthophil granules open through the dorsal and marginal epithelium; necks of xanthophil glands are 15 µm in width. The ventral epidermis is pierced by cells producing xanthophil granules and scarce cells secreting fine erythrophil granules. A defined glandular margin is absent; the glands piercing the margins continue dorsally.

The cutaneous musculature comprises the three typical layers of Geoplaninae, i.e., a subepithelial circular layer followed by a double diagonal layer with decussate fibers, and a strongly developed longitudinal layer, 85 – 200 µm thick dorsally and 80 – 150 µm ventrally. The fibers of the latter muscle layer are gathered into compact bundles (Fig. 22). The cutaneous musculature thickness relative to body height at the pre-pharyngeal region is 22–26%.

The three usual parenchymal muscle layers are present throughout the body: a dorsal layer of diagonal decussate fibers (60-75 µm thick, specimens F3083 and F2690, respectively, or 5 – 6% of the body height), a transverse supraintestinal layer (65 – 100 µm, or 6 – 7%), and a transverse subintestinal layer (40 – 50 µm, or 3 – 4%). Additionally, there is a subneural layer (25 – 40µm, or 2.5 – 2.7%) of transverse muscles. Obliquely oriented parenchymal fibers are abundant in the pre-pharyngeal region.

The muscular organization changes (Figs. 23-24) in the anterior region of the body with respect to that of the pre-pharyngeal region. Bundles of ventral longitudinal cutaneous muscles gradually concentrate medially to give rise to the cephalic retractor muscle. At

1.9–1.4 mm from the anterior extremity, the retractor resembles a lens in cross-section (Fig. 23A-B). Here the supra and subtinestinal parenchymatic muscle layers are weak, whereas the dorso-diagonal and the subneural layers are well developed. At 0.9 mm from the anterior extremity, the retractor muscle becomes more or less rounded and all its fibers are gathered in a compact mass (Fig. 23C). In this region, parenchymatic muscle layers are inconspicuous, with the exception of the supraintestinal and subneural layer. The subneural layer is organized in conspicuous bundles running transversally over the retractor muscle (Fig. 23A-D). From this region towards anterior extremity fibers of the retractor muscle progressively detach in bundles that run to the body sides. The glandular surface of the ventral epidermis widens towards the anterior extremity of the body as the muscle fibers of the retractor concentrate medially. This surface is incompletely bipartite and is pierced by very abundant gland cells (with 10–12 µm thick necks) producing erythrophil granules.

The mouth is situated at a distance from the root of the pharynx equivalent to 49.5% of pharyngeal pocket length (Fig. 25A). An esophagus is inconspicuous. The pharynx is bell-shaped, with dorsal insertion posterior to the ventral and located above to the mouth level. The lining epithelium of the pharyngeal pouch is squamous, non-ciliated, surrounded by a layer of circular fibers (10 µm thick, F3754g). The outer and inner pharyngeal epithelia are flat and ciliated. The outer epithelium is underlain by a simple longitudinal muscle, followed by a circular muscle (25 µm, F3754g), with some longitudinal fibers interspersed. The inner epithelium is surrounded by a circular muscle (20–30 µm), followed by a longitudinal muscle (10 µm). The central nervous system mainly consists of a ventral nerve plate.

The testes are located under the supraintestinal transverse muscle layer. They extend from 12 mm behind the anterior extremity of the body (30% of body length) to nearly the root of the pharynx.

The sperm ducts run between the subintestinal parenchymal muscle layer, dorso-internally to the ovovitelline ducts. Each sperm duct opens laterally into the proximal aspect of the prostatic vesicle. This vesicle is extrabulbar and consists of a dilated proximal portion and a tubular, sinuous, distal portion. The prostatic vesicle receives fine erythrophil granular secretions derived from glands in the parenchyma. The prostatic vesicle is lined with ciliated, cuboidal epithelium, which is surrounded by a simple longitudinal muscle, followed by a circular muscle (25µm) with some longitudinal fibers interspersed. The prostatic vesicle passes into a sinuous ejaculatory duct in the point of penetrating the anterior aspect of the penis bulb (Fig. 25B-C). The ejaculatory duct is lined with a ciliated, cuboidal epithelium which is surrounded by a circular muscle. The ejaculatory duct opens ventrally two-third-way of the penis papilla length.

The protrusible penis papilla is conical, slightly inclined ventrally, and with its dorsal insertion shifted to the ventral insertion (Fig. 25B-C). The penis papilla is as long as the male atrium or shorter. The penis papilla occupies most of the male atrium. The penis papilla is lined with a cuboidal, non-ciliated epithelium. This epithelium is pierced by glands producing erythrophil granules, and is underlain by a 5-um thick circular muscle followed by a longitudinal muscle 5-7 µm thick.

The male atrium is ample. Some specimens exhibit a small ventral fold. From the roof of the distal portion of the male atrium, a large fold projects laterally and continues along the female atrium. The male atrium is lined with a columnar, non-ciliated epithelium. This epithelium is pierced by gland cells producing erythrophil granules. A 5-um-thick circular muscle encircles the male atrium, followed by an equally thick longitudinal muscle.

The ovaries are 480-500 µm long in the antero-posterior body axis and 150-170 µm wide. They are located immediately above the ventral nerve plate, at a distance from the anterior tip equivalent to 23% of body length. The ovovitelline ducts arise from the dorso-lateral surface of the ovaries, and run backwards above the ventral nerve plate. They ascend laterally to the female atrium, and subsequently unite dorsally to form a common ovovitelline duct dorsally to the female atrium (Fig. 25C). The distal fourth of the ascending portion of these paired ducts receives shell glands. The common glandular ovovitelline duct runs posteriorly and communicates with the female genital canal. This canal is 200 µm long and is projected antero-dorsally from the dorso-posterior section of the female atrium. The female genital canal is lined with a columnar, non-ciliated epithelium. The female atrium is an irregular, spacious cavity, gradually dilated towards the male atrium. Walls of the female atrium exhibit longitudinal folds. The female atrium is lined by a 35 µm high columnar epithelium which is pierced by glands producing erythrophil granules. The subapical section of the lining cells is stained weaker. The muscularis of the female atrium consists of two muscle layers, circular and longitudinal, respectively, partially intermingled. The female atrium receives gland cells producing erythrophil granules. The common muscle coat is well-developed; dorsal to the gonopore, this muscle coat is divided into a male and female coat.

Remarks

Supramontana 1 sp. n. resembles S. *potyra* and S. *bipatria* in the dorsal color pattern consisting of a pair of black bands on a yellowish ground color. However, these bands are relatively closer to each other in S. *potyra*. Interestingly, *S. 1* sp. n. and S. *bipatria* are not distinguishable by the color pattern. With respect to the copulatory apparatus, *S. 1* sp. n. compares only with S. *arturi* and S. *irritata* in that the species share the same ratio female atrium length : male

atrium length (roughly 0.5), and in that the prostatic vesicle is 0.3 times as long as the copulatory apparatus. However, the copulatory apparatus of S. *arturi* is relatively longer and lacks a penis papilla, whereas S. *irritata* bears a conical penis papilla.

3.2.6. *Supramontana 2* sp. n.

Type locality. Intervales State Park, Ribeirão Grande, São Paulo State, Brazil.

Material studied.

Type material. Intervales State Park, Ribeirão Grande, São Paulo State, Brazil. **Holotype F2766 (MZUSP PL. XXXX)** F. Carbayo *et al*., col., 28 July 2008: horizontal sections of cephalic region on 3 slides; horizontal sections of portion containing ovaries on 5 slides; transverse sections of portion posterior to ovaries on 8 slides; transverse sections of pre-pharyngeal region on 18 slides; sagittal sections of portion containing pharynx and copulatory apparatus region on 9 slides. **Paratype F2689** (MZUSP PL. XXXX) F. Carbayo *et al*., col., 25 July 2008: transverse sections of cephalic region on 7 slides; horizontal sections of portion containing ovaries on 3 slides; transverse sections of portion posterior to ovaries on 6 slides; sagittal sections of pharynx region on 17 slides; sagittal sections of copulatory apparatus on 8 slides.

Diagnosis

Species of *Supramontana* with an ivory ground color dorsally and five equidistant dorsal stripes, os which the paramedian ones are wider; the female atrium is 1.1-1.4 times as long as the male one; the prostatic vesicle has 0.3-0.4 times the length of the copulatory apparatus; the sperm ducts open into the mid-region of the prostatic vesicle; the ejaculatory duct runs horizontally.

Description

External morphology

The preserved specimens measured 36 mm in length and 2.5mm in width and 1 mm high. The body is elongated with parallel margins (Fig. 26). The cephalic region (1/24th of the body length), is slightly laterally expanded to acquire an inverted spoon-shape. Behind it, the body narrows to form a constriction, or ‘neck’, then gradually widens until the pharyngeal region, subsequently narrows to the pointed posterior tip. The dorsum is convex. Ventral cephalic region is slightly concave. The remaining ventral side is flattened, and the body margins are rounded, so that the section of the body is elliptic. The creeping sole is as wide as 78% of body width at the pre-pharyngeal region. The mouth lays at a distance from the anterior extremity equal to 59% of body length; the gonopore at 77%.

Ground color ivory with orangish extremities, and five longitudinal black stripes: a thin median black line (1/13th of body width), two lateral stripes (2/13th of body width) and two marginal stripes (3/26th of body width) (Fig. 26). The stripes extend from the level of the cephalic constriction to nearly the posterior end. The ventral side is signal white in color.

The eyes are formed by one pigmented cup 40-45 µm in diameter. They contour the anterior extremity of the body in a single row along the first 2 millimeters. Backwards, the eyes spread progressively on each side of the dorsum to form a band with a maximum width

equivalent to 29% of the body width in mid body length. Behind the band becomes narrower until the posterior tip of the body.

Internal morphology

The sensory pits are 30µm deep and are distributed in a simple ventro-lateral row, from the very anterior extremity up to at least 14% of body length. In the pre-pharyngeal region (Fig. 27), dorsal and marginal epithelia are pierced by rhabditogen cells, glands cells producing erythrophil granules and abundant and very apparent cell glands producing xanthophil granules. Necks of xanthophil glands are 25 µm in width. Two types of glands producing pinkish and cyanophil granules, respectively, also pierce dorsal epithelium. There is not a well delimited glandular margin. The ventral epidermis is pierced by scarce cells secreting fine erythrophil granules.

The cutaneous musculature comprises the three typical layers of Geoplaninae, i.e., a subepithelial circular layer followed by a double diagonal layer with decussate fibers, and a strongly developed longitudinal layer, 75 µm thick dorsally and 100 µm ventrally. The fibers of the latter muscle layer are gathered into compact bundles (Fig. 27). The cutaneous musculature thickness relative to body height at the pre-pharyngeal region is 20%.

Four parenchymal muscle layers are present throughout the body: a dorsal layer of diagonal decussate fibers (50 µm thick, or 6% of the body height, specimen F2766), a transverse supraintestinal layer (60 µm, or 7%), a transverse subintestinal layer (50 µm, or 6%), and a subneural layer (30 µm, or 3,5%) of transverse muscles. Obliquely oriented parenchymal muscle fibers are abundant in the pre-pharyngeal region.

The muscular organization of the cephalic region differs from that of the remaining body (Fig. 28-29). Bundles of ventral longitudinal cutaneous muscles gradually concentrate medially to give rise to the cephalic retractor muscle. Between 2 mm and 0.38 mm from the

anterior extremity, the retractor resembles a lens in cross-section horizontally located. Muscle fibers of the retractor muscle are gathered in few but thick bundles. Here the four parenchymatic muscle layers are well developed, specially the dorso-diagonal and the subneural layers. At 0.37 mm from the anterior extremity, the retractor muscle becomes rounded and all its fibers are gathered in a compact mass. In this region, parenchymatic muscle layers are inconspicuous, with the exception of the subneural layer, strongly developed and organized in conspicuous bundles running transversally over the retractor muscle. A few fibers of this layer seemingly are interwoven with dorsalmost fibers of retractor muscle. From this region towards anterior extremity fibers of the retractor muscle progressively detach in bundles that run to the body sides. As they detach, the retractor muscle becomes less apparent until it disappears close to the anteriormost extremity of the body. All parenchymal muscles fade out near the anteriormost body portion.

The glandular surface of the cephalic ventral epidermis widens towards the anterior extremity of the body as the muscle fibers of the retractor concentrate medially. This surface is incompletely bipartite (Fig. 28) and is richly pierced by gland cells (with 10–12 µm thick necks) producing erythrophil granules.

The mouth is situated at a distance from the root of the pharynx equivalent to 28% of pharyngeal pocket length (Fig. 30A). Esophagus is 9% of pharynx length. The pharynx is cylindrical, with dorsal insertion posterior to the ventral and located anteriorly to the mouth level. The lining epithelium of the pharyngeal pouch is squamous, non-ciliated, surrounded by a layer of circular fibers (15 µm thick, F2766). The outer and inner pharyngeal epithelia are flat and ciliated. The outer epithelium is underlain by a simple longitudinal muscle, followed by a circular muscle (30 µm, F2766). The inner epithelium is surrounded by a circular muscle (10–25 µm), followed by a

longitudinal muscle (7,5 µm). The central nervous system mainly consists of a ventral nerve plate.

The testes are located under the supraintestinal transverse muscle layer, mostly between the intestinal diverticula. Position of anteriormost testes was not measured since tissue was digested for DNA extraction. Posteriormost testes lay nearly the root of the pharynx. The sperm ducts run between the subintestinal parenchymal muscle layer, dorso-internally to the ovovitelline ducts. Each sperm duct opens into a thin and short diverticulum projected from the antero-lateral aspect of the prostatic vesicle. This vesicle is extrabulbar and consists of a dilated proximal portion and a tubular, sinuous, distal portion. The prostatic vesicle penetrates the anterior aspect of the penis bulb (Fig. 30B, 31. The prostatic vesicle receives fine erythrophil granular secretions derived from glands in the parenchyma. Prostatic vesicle lined with ciliated, columnar epithelium, which is surrounded by a strongly developed circular muscle (40µm) with some longitudinal fibers interspersed. The prostatic vesicle passes into the ejaculatory duct. Proximally, this duct is 35 µm in diameter; distally, 10 um. Ejeculatory duct lined with a ciliated, cuboidal epithelium surrounded by circular muscle. The ejaculatory duct terminates at the tip of a small penis papilla (Figs. 30B, 31A-C; 32A-B). The protrusible penis papilla is conical, slightly inclined ventrally, and with its dorsal insertion posterior to the ventral insertion. The penis papilla occupies 21% of the male atrium length. This small penis papilla is housed in a large sheath (Figs. 31A-B; 32A-B). This sheath is almost as long as twice that of the penis papilla. Penis papilla and sheath are lined with a cuboidal, non-ciliated epithelium, pierced by glands producing erythrophil granules, and underlain by a 4-um-thick muscle of apparently longitudinal fibers.

The male atrium is mostly occupied by large folds. One of these folds is a transverse, annular-shaped fold located halfway of the atrial length. The male atrium is lined with a columnar, non-ciliated

erythrophil epithelium, the subapical surface of it is stained paler. This epithelium is pierced by gland cells producing erythrophil granules. A circular muscularis (5 µm thick) encircles the male atrium, followed by a one-fiber-thick longitudinal muscle.

The ovaries are 400µm long in the antero-posterior body axis and 210µm wide. They are located immediately above the ventral nerve plate, at a distance from anterior tip equivalent to 21% of body length. The ovovitelline ducts arise from the dorso-anterior surface of the anterior portion of the ovaries, and run backwards above the ventral nerve plate. They ascend laterally to the gonopore region, and subsequently unite dorsally to form a common ovovitelline duct dorsally to the female atrium (Figs. 30B, 31A). The distal fourth of the ascending portion of these paired ducts receives shell glands. The glandular ovovitelline duct runs posteriorly and communicates with the female genital canal. This canal is very long and curved anteriorly to communicate with the posterior section of the female atrium. Female genital canal lined with a columnar epithelium, whose subapical surface is erythrophil. The female atrium is an irregular, spacious cavity, gradually dilated towards male atrium. Walls of the female atrium are folded and partially projected into its lumen (Figs. 30C, 31A, D; 32A, C). The female atrium is lined with a cuboidal-to-columnar epithelium. The muscularis of the female atrium consists of two muscle layers, a 5-um-thick longitudinal muscle followed by a 15-um thick circular muscle, both partially intermingled. The female atrium receives gland cells producing erythrophil granules. The common muscle coat is well-developed; dorsal to the gonopore, this muscle coat is divided into a male and female coat.

Remarks

Supramontana graffi and *S. 3* resemble S. *2* sp. n. in having five dorsal stripes, of which the paramedian is wider. However, in S. *graffi*, the stripes are not equidistant from each other (*vs.* equidistant in. S. *2*

sp. n.), whereas in *S. 3* the ground color is beige (*vs.* ivory in S. *2* sp. n.). The copulatory apparatus of S. *2* sp. n. compares with that of S. *jandaia* and *S. 4* sp. n. in that they have a female atrium 1.1-1.4 as long as the male one and in that the prostatic vesicle length equals 0.3-0.4 tiems that of the copulatory apparatus. However, the ejaculatory duct of S. *jandaia* runs postero-ventrally (*vs.* horizontally in S. *2* sp. n.), and in *S. 4* sp. n. the sperm ducts open into the anterior region of the prostatic vesicle (*vs.* mid-region in S. *2* sp. n.).

3.2.7. *Supramontana 3* sp. n.

Synonymy

Issoca jandaia: Carbayo *et al*., (2013).

Type locality. Serra da Bocaina National Park, São José do Barreiro, Rio de Janeiro State, Brazil.

Material studied. **Type material. Holotype F2042 (MZUSP PL. XXXX)** F. Carbayo *et al*., col., 9 February 2007: horizontal sections of cephalic region on 3 slides; sagittal sections of portion containing ovaries on 3 slides; transverse sections of pre-pharyngeal region on 2 slides; sagittal sections of copulatory apparatus on 6 slides. **Paratypes: F2043 (MZUSP PL.XXXX)** F. Carbayo *et al*., col., 9 February 2007: transverse sections of cephalic region on 3 slides; transverse sections of portion anterior to ovaries on 4 slides; transverse sections of pre-pharyngeal region on 3 slides; sagittal

sections of pharynx region on 12 slides. **F2799 (MZUSP PL. XXXX)** F. Carbayo *et al*., col., 7 September 2008: transverse sections of a body portion behind copulatory apparatus on 4 slides. **F2815 (MZUSP PL. XXXX)** F. Carbayo *et al*., col., 8 September 2008: Transverse sections of cephalic region on 5 slides; sagittal sections of portion containing ovaries on 6 slides.

Diagnosis

Species of *Supramontana* with a beige dorsum ornated five equidistant dorsal stripes, of which the paramedian ones are wide; the female atrium is 1.1 times as long as the male atrium; the prostatic vesicle is 0.2 times as long as the copulatory apparatus; the ejaculatory duct runs postero-dorsally; a penis papilla is absent; the male atrium receives scarce erythrophil gland cells.

Description

External morphology

The living specimen F2042 measured 29 mm in length and 2 mm in width; preserved, it measured 16 mm in length, 2 mm in width and 1 mm height. The body displays the typical shape of the genus, i. e., subcylindrical, elongate with parallel margins and the cephalic region (6% of the body length) spoon-shaped (Fig. 33A-C). The creeping sole is approximately as wide as 80% of the body width at the pre-pharyngeal region. The mouth lays at a distance from anterior extremity equal to 56% of body length; the gonopore at 75% (specimen F2042).

The ground body color is beige, red orange in the cephalic region, and five longitudinal black stripes: a thin median line (6% of the body width), two paramedian stripes (16%) and two marginal stripes (8%) (Fig. 33). The stripes extend from the level of the cephalic constriction to nearly the posterior end, where the paired stripes converge. The dorsal ground color of the dorsum passes gradually to the signal grey

of the ventral side (Fig. 33A). In the preserved specimens the stripes kept their color whereas the ground color faded to yellowish (Fig. 33B-D).

The eyes are monolobated, 25 µm in diameter, distributed marginally in a single row surrounding the anterior extremity of the body; 0.5 mm behind they are arranged in a marginal row of 4-5 eyes in a same transverse plane and behind they turn progressively scarcer and spread onto the dorsum to the external margin of the paramedian stripes until the posterior tip of the body. The sensory pits are ~25 µm deep, and are distributed ventro-laterally in a uniserial row that contours the anterior extremity of the body; they extend posteriorly to at least the equivalent of 3% of the body length.

Internal morphology

The sensory pits are 20 µm deep and are distributed in a simple ventro-lateral row, from the very anterior extremity up to at least 2% of body length. In the pre-pharyngeal region, dorsal and marginal epithelium are pierced by rhabditogen cells, and by two types of cells producing erythrophil and xanthophil granules, respectively. In the horizontal and sagittal sections examined, no glandular margin was observed. The ventral epidermis is pierced by scarce cells of two types secreting fine xanthophil and basophil granules, respectively.

The cutaneous musculature comprises the three typical layers of Geoplaninae, i.e., a subepithelial circular layer followed by a double diagonal layer with decussate fibers, and a strongly developed longitudinal layer, 60 µm thick dorsally and 30 µm ventrally._The cutaneous musculature thickness relative to body height at the pre-pharyngeal region is 13%.

Four parenchymal muscle layers are present throughout the body: a dorsal layer of diagonal decussate fibers (25 µm thick, or 2.5% of the body height, specimen F2043), a transverse supraintestinal layer (25

µm, or 2.5%), a transverse subintestinal layer (25 µm, or 2.5%), and a subneural layer (60 µm, or 6.5%) of transverse muscles.

The organization of the musculature in the cephalic region is like that of *I. jandaia* in terms of s in terms of organization and relative development (Fig. 34A-B). The glandular cushions of the ventral cephalic region bear numerous gland cells producing erythrophil granules (Figs. 33C; 34A).

The mouth is situated at a distance from the root of the pharynx equivalent to 50% of pharyngeal pocket length (Fig. 34C). The dorsal insertion of the pharynx is shifted to the posterior region of the body to level with the mouth, so that the pharynx is bell-shaped and an esophagus becomes apparent. The outer and inner pharyngeal epithelia are flat and ciliated. The outer epithelium is underlain by a simple longitudinal muscle, followed by a circular muscle (15 µm, F2042). The inner epithelium is surrounded by a circular muscle (15 µm), followed by a longitudinal muscle (3 µm). The central nervous system mainly consists of a ventral nerve plate.

The testes are located under the supraintestinal transverse muscle layer, mostly between the intestinal diverticula. Anteriormost testes shortly behind the ovaries (20 µm in F2042) and at a distance from the anterior tip of the body equal to 30.6% of body length. Posteriormost testes lay 200 µm before the root of the pharynx. The sperm ducts run between the subintestinal parenchymal muscle layer, internally to the ovovitelline ducts.

Each sperm duct opens laterally in the anterior portion of the prostatic vesicle. This vesicle is extrabulbar and consists of a somewhat ovoid structure, with its central region narrowed. The posterior portion of the vesicle communicates with the ejaculatory duct in the anterior aspect of the penis bulb. The prostatic vesicle receives fine erythrophil granular secretions derived from glands in the parenchyma, and is lined with ciliated, cuboidal-to-columnar

epithelium, which is surrounded by a criss-crossed muscle (40µm, F2042) followed by a 10-um thick longitudinal muscle (Fig. 35 A-C).

The anterior portion of the sinuous and thin ejaculatory duct runs postero-dorsally; its distal portion descends to open into the antero-dorsal aspect of the male atrium. The ejaculatory duct is lined with a ciliated, cuboidal epithelium, and is surrounded by a 10-um thick circular muscle. A penis papilla is lacking (Fig. 35A, C-D).

The male atrium is mostly occupied by large folds. Folds of the anterior section of the atrium (1/3rd of its length) converge and are lined with a low (1 µm thick), non-ciliated epithelium with sunken nuclei and pierced by glands producing fine erythrophil granules. Muscle fibers underlining this epithelium are inconspicuous. The posterior section (2/3th) presents larger 2-3 folds, which are lined with a non ciliated 8-15 µm high epithelium; this epithelium is crossed by two types of glands, one type producing fine erythrophil granules; and another, scarcer type, producing slightly cyanophil granules. A circular 10-um-thick muscle encircles the male atrium, followed by a 10-um-thick longitudinal muscle.

The ovaries are more or less rounded, 170-180 µm in diameter. They are located immediately above the ventral nerve plate, at a distance from the anterior tip equivalent to 29.4% (F2042) of body length. The ovovitelline ducts arise from the dorsal surface of the ovaries, and run backwards above the ventral nerve plate. They ascend laterally to the gonopore region, and subsequently unite dorsally to the anterior region of the female atrium to form a common ovovitelline duct (Fig. 35A). The very distal portion of the paired ducts receives shell glands. The glandular ovovitelline is relatively long, 200 um, and runs posteriorly to communicate with the female genital canal. This canal, ciliated, is 100 µm long and communicates with the postero- dorsal section of the female atrium. The female atrium is as long as the male atrium, and provided with transverse folds filling its lumen (Fig. 35A,

C-D). The lining epithelium of the female atrium is columnar epithelium. Numerous glands of two types, empty xanthophil and erythrophil granules, respectively into the atrial lumen. The muscularis of the female atrium consists of two muscle layers, a 5-um-thick longitudinal muscle followed by a 5-um thick circular muscle. The common muscle coat is well-developed; dorsal to the gonopore.

Remarks

With respect to the general appearance, only S. *graffi* and S. *2* sp. n. confounds with *S. 3* as they have five dorsal stripes, of which the paramedian ones are wider. However, in S. *graffi* the stripes are not equidistant from each other (*vs.* equidistant in. *S. 3*), whereas in S. *2* sp. n. the ground color is ivory (*vs.* beige in *S. 3*). Regarding the copulatory apparatus, S. *jandaia*, S. *multilineata*, S. *piranga* and *S. 4* sp. n. resemble *S. 3* in having a female atrium roughly 1.1-1.4 times long as the male atrium and in that the prostatic vesicle is more or less 0.2 times as long as the copulatory apparatus. Nonetheless, in S. *2* sp. n. and *S. 4* sp. n. the ejaculatory ducts runs roughly horizontally (*vs.* postero-dorsally in *S. 3*), in S. *piranga* the ejaculatory duct opens at the tip of the penis papilla (*vs.* in the male atrium in *S. 3*), and in S. *jandaia* the male atrium receives ventrally and laterally very numerous erythrophil gland cells (*vs.* scarce in *S. 3*).

3.2.8. *Supramontana 4* sp. n.

Type locality. Serra da Bocaina National Park, São José do Barreiro, São Paulo State, Brazil.

Material studied.

Type material. Serra da Bocaina National Park, São José do Barreiro, São Paulo State, Brazil. **Holotype F2102 (MZUSP PL. XXXX)** F. Carbayo *et al*., col., 10 February 2008: transverse sections of cephalic region on 8 slides; horizontal sections of portion containing ovaries on 7 slides; transverse sections of pre-pharyngeal region on 3 slides; sagittal sections of portion containing pharynx and copulatory apparatus region on 6 slides.

Diagnosis

Species of *Supramontana* with three black dorsal stripes; the female atrium length : male atrium ratio length is 0.9; the prostatic vesicle length : copulatory apparatus length ratio is 0.4; the sperm ducts open in the anterior region of the prostatic vesicle.

Description

External morphology

The live animal measured 46 mm in length and 2.5 mm in width. Preserved it is approximately 25 mm long and 3 mm wide. The body is elongated with parallel margins (Fig. 36A). The anterior extremity is rounded to truncate, roof gable-shaped when creeping (Fig. 36A) and pointed in the preserved specimen (Fig. 36C). The posterior extremity is pointed. The dorsum is convex, the flattened ventral side becomes slightly concave in the anterior extremity (Fig. 36B). The body margins are rounded. The width of the creeping sole equals 75% of the body width in the pre-pharyngeal region. The mouth lays at a

distance from the anterior extremity more or less equal to 68% of body length; the gonopore is at 82%.

The dorsal ground color of the living specimen is honey yellow (RAL 1005), darker in both extremities, with a paramedian black stripe on each side of the body (each with 20% of the width of the body) and a mid stripe with chestnut brown color (RAL 8015; 5%) (Fig. 36A-B); the ventral side is 'brownish grey' (J. Pedroni, pers. obs.). In the preserved specimen the dorsal color became slightly paler; the ventral side ivory (RAL 1014), darker along a marginal band on each side of the body, which progressively spread medially (Fig. 36C). The very anterior extremity which is chestnut brown.

The eyes are formed by one pigmented cup 20-25 µm in diameter. They contour the anterior extremity of the body in a single row along the first 2 millimeters (Fig. 36B). Backwards, the eyes spread progressively on each side of the dorsum to form a band with a maximum width equivalent to 20% of the body width in mid body length. Behind the band becomes narrower until the posterior tip of the body.

Internal morphology

The sensory pits are approximately 18-22 µm deep. The ventral epithelium of the very anterior tip (ca. 1 mm long) is detached from the body and the distribution of the pits in the region could not be observed. Posterior to this region, the sensory pits are distributed in a single ventro-lateral row.

Abundant rhabditogen cells and gland cells producing xanthophil granules pierce dorsal and marginal epithelium of the pre-pharyngeal region (Fig. 37A). Here the ventral epidermis is pierced by two types of scarce gland cells, producing erythrophil and xanthophil granules, respectively. A glandular margin is absent.

The cutaneous musculature comprises the three typical layers of Geoplaninae, i.e., a subepithelial circular (one-fiber thick), followed by

a double diagonal with decussate bundles (10 µm thick) and an innermost longitudinal layer (47-50 µm thick dorsally and ventrally) (Fig. 37A). The longitudinal muscle is arranged in compact bundles (35-90 fibers each) that in the anterior extremity of the body form the retractor muscle of the cephalic region. The cutaneous musculature is as thick as 14% of the body height.

In the pre-pharyngeal region (Fig. 37A) are four parenchymal muscle layers, all well developed: a dorsal layer with diagonal decussate fibers (30 µm thick, or 3% of the body height), a transverse supraintestinal layer (4.1%), a transverse subintestinal layer (3%), and a transverse subneural layer (5%).

The cephalic region was sectioned transversely, though sections of the anteriormost region are horizontal as a result of twisting of the body when fixed. In this cephalic region, the muscle fibers of the ventral cutaneous longitudinal layer originate the retractor muscle of the cephalic region.

Very approximately at 1 mm (equal to 4% of body length) from the anterior extremity of the body, this layer is 84 µm thick and becomes thinner towards the body margins, occupying 53% of the body width (Fig. 37B).

At 0.5 mm from the anterior extremity, the histological sections are between transverse and horizontal. Here the ventral cutaneous longitudinal muscle is delta-shaped in the transverse section and 40% of the body width (Fig. 37C-D). Here only the dorsal and the subneural parenchymal muscle layers are apparent. Further towards the anterior tip of the body the sections are horizontal and the ventral longitudinal parenchymal muscle forms the retractor of the cephalic region, apparently sunken into the parenchyma and as wide as 17% of the body (Fig. 37E). Here dorso-ventral parenchymal muscle fibers are abundant. The retractor is constituted of bundles of fibers that progressively detach from it to run obliquely towards the body sides.

Some of these bundles cross from one side of the body to the other. Other bundles run transversely together with fibers of the parenchymal subneural muscle. Further anteriorly, the retractor becomes less apparent by detachment of its bundles (Fig. 37F).

The dark surface of the ventral epidermis of the cephalic region (Fig. 36C), is pierced by numerous gland cells producing xanthophil granules (Fig. 37B-D). Necks of these gland cells are situated behind and are located dorsally and ventrally to the parenchymal subintestinal muscle. Surrounded by these xanthophil gland cells are other gland cells producing cyanophil granules. The opening of the latter could not be determined.

The mouth is situated at a distance from the root of the pharynx equivalent to 31% of pharyngeal pocket length (Fig. 38A). The pharynx is cylindrical, with the dorsal insertion placed backwards (Fig. 38A-B). The outer epithelium is underlain by a longitudinal muscle (30 µm thick) with circular muscle fibers interspersed. The inner epithelium is surrounded by a circular muscle (21 µm), followed by a longitudinal muscle (3 µm). A ventral nerve plate is present.

The testes are located beneath the supraintestinal transverse muscle layer, between the intestinal diverticula (Fig. 37A). They extend from 5 mm behind the anterior extremity of the body (20% of body length) to nearly the root of the pharynx. The sperm ducts run between the subintestinal parenchymal muscle fibers, dorso-laterally to the ovovitelline ducts. Close to the penis bulb, these ducts bend medially to open into the lateral section of the mid region of the prostatic vesicle. The prostatic vesicle is pear-shaped (Figs. 38C, 39A). The distal portion of the prostatic vesicle is tubular and runs dorsally to penetrate the anterior region of the penis bulb and subsequently continues with the ejaculatory duct (Fig. 38C). This duct is a relatively wide duct with a pleated wall. The ejaculatory duct opens into the male atrium through a small penis papilla projecting from the anterior

region of this atrium. This small fold is contained in an intermediate-sized fold posterior to which is another large annular fold. Posterior third of the male atrium is narrower than the anterior.

The prostatic vesicle is lined with a ciliated, columnar epithelium which is pierced by glands producing fine erythrophil granules. The vesicle is surrounded by a 25 µm thick layer of criss-crossed and circular muscle fibers. The ejaculatory duct is lined with a cuboidal epithelium and is surrounded by a 8-12-µm thick circular muscle.

The lining epithelium of the male atrium changes gradually from cuboidal in the small penis papilla to columnar in the distal region of the atrium. Short-necked gland cells producing erythrophil granules pierce the entire male atrium epithelium and are particularly abundant in the small pensi papilla (Fig. 39A). Gland cells with long necks and producing xanthophil granules exhibit the same distribution, but are especially abundant in the larger fold. No muscle fibers are underlying the epithelium of the small papilla fold. The epithelium of the larger fold is underlain by a 8 µm thick circular muscle followed by a 5 µm thick longitudinal muscle. The epithelium lining the remaining atrium is underlain by only a 10 µm thick circular muscle.

The ovaries are 410 µm long in the antero-posterior body axis and 180 µm wide. They are located immediately above the ventral nerve plate, at a distance from anterior tip equivalent to 20% of body length. The ovovitelline ducts arise from the dorso-lateral surface of the anterior portion of the ovaries, and run backwards above the ventral nerve plate. They ascend laterally to the gonopore canal to join dorsally to the female atrium to form the common ovovitelline duct (Fig. 38C). The distal quarter of the ascending portion of these paired ducts receives shell glands. The common ovovitelline duct is relatively long and bends postero-ventrally to communicate with the female genital canal. This long canal is relatively long and is C-shaped

in lateral view. This canal communicates with the postero-ventral section of the female atrium through a large lateral fold (Fig. 39B). The female atrium is elongated, with 80% of the length of the male atrium and provided with lateral folds narrowing the lumen. The female atrium is lined with a columnar epithelium, and epithelial cells vary in height so giving to the atrial surface an irregular aspect (Fig. 39B). The atrial epithelium is pierced by gland cells producing erythrophil granules, and is underlain by 5-µm thick longitudinal muscle followed by a 18-µm thick circular muscle.

Remarks

With respect to the external appearance, only some morphotypes of S. muelleri resemble *S. 4* sp. n. in that both species have three dorsal stripes (see Carbayo, 2010). However, in three-striped morphotypes of *Supramontana* muelleri the paramedian stripes are ferruginous in color (*vs.* black in *S. 4* sp. n.). Regarding the internal morphology, only S. *2* sp. n. compares *S. 4* sp. n. and S. *bipatria* in the female atrium length : male atrium length ratio (roughly 0.9) and in the length of the prostatic vesicle relative to that of the copulatory apparatus (0.3). Nonetheless, in S. *2* sp. n. the sperm ducts open laterally into the mid-anterior region of the prostatic vesicle (*vs.* anterior region in *S. 4* sp. n.), and S. *bipatria* presents a well developed penis papilla. Unfortunately, DNA sequences are not available. Therefore, an independent test of the nature of this species is lacking.

4. DISCUSSION

4.1. On the phylogeny

Our ML phylogenetic tree agrees with the two previous works in the general topology. Carbayo's *et al*. (2013) trees were inferred from one mitochondrial gene fragment (COI) and three nuclear gene fragments (28S, 18S, EF), from each gene alone and from all genes concatenated and three different optimality criteria. All species were also monophyletic (except *L. graffi*, with one of the two specimens identified by means of only the external morphology); *Issoca* and *Luteostriata* were polyphyletic; *Supramontana* was nested within a group with some *Issoca* representatives; and *I. rezendei* was sister to the remaining LIS (i.e. *Luteostriata, Issoca, Supramontana*) members (Carbayo *et al*., 2013). Negrete's *et al* (2019) produced similar results in their phylogenies inferred from a concatenated data matrix (COI and 18S), even the position of *Winsoria* as a sister member of *I. jandaia* (here renamed as *S. 3*), this clade nested in the paraphyletic *Luteostriata*. As in the present paper, not all clades in those two studies were recovered with full statistical support. This situation could be in part explained by the fact that COI is too saturated for inferring ancient interrelationships (Álvarez-Presas *et al*., 2008).

4.2. On the diagnostic attributes of the genera

In spite of the statistical limitations of the trees, the topology of the ML tree is congruent with the morphological attributes. Moreover, morphological evidence supporting the non-monophyletic status of *Issoca* was already provided (Araujo & Carbayo, 2018).

Species in the clade LWIS (*Luteostriata*, *Winsoria*, *Issoca*, and *Supramontana*) compare to each other. Among the diagnostic traits of the genera (or traits present in the species but not included in the diagnoses) we leave out putative symplesiomorphic characters (e. g.,

body slender, parallel body margins, eyes and sensory pits contouring the cephalic region). The four genera are diagnosed by rather similar features: the ventral cephalic region is provided with a glandular surface; the muscle retractor of the cephalic region is derived from longitudinal ventral cutaneous fibers; this retractor muscle is partly sunk into the parenchyma; towards the anterior tip of the body, the retractor muscle dissipates in bundles running towards the margins of body; a transverse parenchymal sub-neural muscle is present; the female genital canal presents the proflex condition (i.e., projected anteriorly from the dorsal region of the female atrium).

Some of the characters vary among and/or within the genera in the details: The cephalic region may be spoon-shaped (*Issoca*), rounded (*Supramontana*, *Issoca*, *Luteostriata*) or blunt (*Winsoria*); sometimes it is gable roof-shaped when crawling (*Winsoria*, *Issoca*, *Luteostriata*, *Supramontana*). The cephalic glandular surface is lunate (*Issoca*), U-shaped (*Luteostriata*), V-shaped (*Issoca*, *Luteostriata*, *Winsoria*, as inferred from figures in the original description) or is absent (*Supramontana*). The transverse section of the cephalic retractor muscle varies in shape from lenticulate (*Supramontana*, *Luteostriata*) to rounded (*Issoca*, *Winsoria*) or almost circular (*Supramontana*); the transverse parenchymal sub-neural muscle is present either in the cephalic region and shortly behind only (*Winsoria*), or throughout the body (*Issoca*, *Luteostriata*, *Supramontana*). The cephalic retractor muscle dissipates towards the anterior extremity of the body in bundles that detach from it running towards margins of body only (*Issoca*, *Supramontana*) or also towards the dorsal side (*Luteostriata*). A penis papilla may be well developed (*Supramontana*, *Winsoria*, *Issoca*), small (*Issoca*) or absent (*Luteostriata*, *Issoca*). In this respect, Negrete and collaborators anticipated that the lack of resolution of their trees “might be attributable to a lack of taxonomic definitions of these genera” (Negrete *et al*., 2019). Most of the species of *Luteostriata* compares well in the shape of the copulatory apparatus

(prostatic vesicle very long; penis papilla absent; male atrium much longer than the female atrium), but the genus is paraphyletic.

Most of these traits exhibit continuous differences across the genera. In phylogenetic analysis, scoring continuous characters is challenging (e.g. Chappill, 1989; Stevens, 1991; Gift & Stevens, 1997; Wiens, 2001). Evident discrete, exclusive attributes of the LWIS genera are actually only one: the ventral longitudinal cutaneous musculature sunken into the parenchyma (*Supramontana*) or not (*Winsoria*, *Issoca*, *Luteostriata*).

Therefore, from the morphological perspective, the genera are poorly consistent. Moreover, *Issoca rezendei* clearly differs from the remaining members of LWIS in three exclusive discrete attributes: the subneural transverse parenchymatic muscle layer is interspersed with fibers of the cephalic retractor muscle (but in some species this muscle seem to be slightly intercrossed); the prostatic vesicle is intrabulbar; a female atrium is absent. On the other hand, the clade sister to *I. rezendei* poses a set of discrete attributes: the subneural transverse parenchymatic muscle layer above the cephalic retractor muscle; an extrabulbar prostatic vesicle; a female atrium well developed.

Despite these evident differences, species with such a morphological diversity can be fitted into *Issoca* because the diagnosis of the genus does not include traditionally important traits, such as the penis papilla, the male and female atria or female genital canal. Furthermore, the diagnostic attributes of the cephalic region in the genus are based only on the type species (Froehlich, 1955; Carbayo & Leal-Zanchet, 2003).

4.3. Taxonomic implications

Since Darwin's (1859) cornerstone contribution, the organization of the knowledge of biological diversity is expected to be based on evolutionary relationships. The genera *Issoca*, *Luteostriata* and *Supramontana* were originally proposed based on morphological data only (Froehlich, 1955; Carbayo & Leal-Zanchet, 2003; Carbayo, 2010), whereas *Winsoria* was suggested on an integrative approach. DNA sequences have been revealed to be a fundamental resource to independently test the morphology-based hypotheses of species and supra-specific taxa of land planarians. By doing so, cryptic species were discovered (Álvarez-Presas *et al*., 2015), the systematic position of many species could be reassessed, and non-monophyletic genera were uncovered (Carbayo *et al*., 2013). The integrative approach of this work points to the need to revise the taxonomic status of the LWIS members. We take advantage of the congruence between morphological and molecular data to propose the following taxonomic actions.

Rediagnosis of *Issoca*. The diagnosis of *Issoca* was originally proposed by Froehlich (1955) and later rediagnosed by Carbayo & Leal-Zanchet (2003). This diagnosis reads: Geoplaninae with elongated body; eyes and sensory pits contouring the entire cephalic region; large creeping sole, having a width greater than a third of the body width; cutaneous longitudinal musculature strong; longitudinal parenchymal musculature very weak or absent; cephalic extremity provided with a musculo-glandular organ, whose retractor originates from the ventral longitudinal cutaneous musculature and whose adhesive surface, concave in general, is simple or incompletely bipartite; sub-neural transverse parenchymatic muscle layer

interspersed with muscle fibres of the retractor; sensory papillae absent; copulatory apparatus lacking adenodactyls.

The diagnosis of *Issoca* should be complemented with the following: The prostatic vesicle is intrabulbar. The penis papilla is conical and stubby. A female atrium does not exist.

Rediagnosis of *Supramontana*. Geoplaninae with parallel body margins; creeping sole wide; eyes and sensory pits surround entire cephalic region; cephalic region with ventral longitudinal cutaneous musculature modified into a retractor muscle, sunken into the parenchyma, and dissipating towards the anterior extremity in bundles running towards the margins of body, sometimes towards the dorsal side too; a subneural transverse muscle present, which in the cephalic region is located above the cephalic retractor muscle; prostatic vesicle extrabulbar; penis papilla usually present; common glandular ovovitelline duct, dorsal to female atrium; female atrium present; female genital canal dorso-anteriorly oriented.

4.4. Summary of the nomenclatural acts

Supramontana has priority over *Luteostriata* and *Winsoria* since it is the oldest available name (Article 23 of the ICZN, 1999). An asterisk is used to mark species (re)described in this work.

Genus *Issoca* Froehlich, 1955
**Issoca rezendei* Froehlich, 1955
Genus *Supramontana* Carbayo & Leal-Zanchet, 2003
Synomymy:
Luteostriata Carbayo, 2010, syn. nov.
Winsoria Negrete *et al*., 2019, syn. nov.
S. abundans (Graff, 1899), comb. n.
S. argentina (Negrete *et al*., 2014), comb. n.
S. arturi (Lemos & Leal-Zanchet, 2008), comb. n.
S. assanga (Araujo & Carbayo, 2018)
**S. 1* sp. n.
S. bipatria (Negrete *et al*., 2019), comb. n.
S. caissara (E. M. Froehlich, 1955), comb. n.
S. ceciliae (E. M. Froehlich & Leal-Zanchet, 2003), comb. n.
S. ernesti (Leal-Zanchet & E. M. Froehlich, 2006), comb. n.
S. fita (Froehlich, 1959), comb. n.
S. graffi (E. M. Froehlich & Leal-Zanchet, 2003), comb. n.
S. irritata (Carbayo & Leal-Zanchet, 2003), comb. n.
**S. jandaia* (Froehlich, 1955), comb. n.
**S. 2* sp. n.
S. muelleri (Diesing, 1861), comb. n.
**S. piranga* (Froehlich, 1955), comb. n.
**S. potyra* (Froehlich, 1957), comb. n.
S. pseudoceciliae (Lemos & Leal-Zanchet, 2008), comb. n.
S. spatulata (Graff, 1899), comb. n.
S. subtilis (Amaral, Boll & Leal-Zanchet, 2019), comb. n.
**S. 4* sp. n.
**S. 3* sp. n.

CONCLUDING REMARKS

- In this study, we addressed the systematics of the land planarian genus *Issoca* (Platyhelminthes, Tricladida, Geoplanidae) and closely related taxa, namely *Luteostriata*, *Winsoria*, and *Supramontana,* by means of a morphological and molecular approach.
- Four species of Issoca are redescribed and four new species of *Supramontana* are described.
- The phylogenetic interrelationships of thirteen species are inferred from the Cytochrome Oxidase I (COI) gene and the nuclear gene (28S rDNA) concatenated. Our results contrast with the current classification of the species, with *Issoca* and *Luteostriata* polyphyletic, *Supramontana* is sister to *I. jandaia,* and in turn *Winsoria* is sister to *Supramontana* + *I. jandaia*.
- According to this results, the genera *Issoca* and *Supramontana* are re-diagnosed and the species reclassified. *Luteostriata* and *Winsoria* ar considerered junior synonym of *Supramontana*.
- These morphology-molecular-based taxonomic actions reveals the importance of testing morphology-based hypothesis of supra-specific groups (namely genera) with independent DNA-based phylogenies. Hopefully, a more complete representativeness of the group and additional molecular markers will help in a natural classification of these organisms.

REFERENCES

Álvarez-Presas, M., Baguñà, J., & Riutort, M. 2008. Molecular phylogeny of land and freshwater planarians (Tricladida, Platyhelminthes): from freshwater to land and back. Molecular phylogenetics and evolution, 47(2), 555-568.

Álvarez-Presas, M., Carbayo, F., Rozas, J., & Riutort, M. 2011. Land planarians (Platyhelminthes) as a model organism for fine- scale phylogeographic studies: understanding patterns of biodiversity in the Brazilian Atlantic Forest hotspot. Journal of Evolutionary Biology, 24(4), 887-896.

Álvarez-Presas, M., Amaral, S. V., Carbayo, F., Leal-Zanchet, A. M., & Riutort, M. 2015. Focus on the details: morphological evidence supports new cryptic land flatworm (Platyhelminthes) species revealed with molecules. Organisms Diversity & Evolution, 15(2), 379-403.

Araujo, A.P.G. & Carbayo, F. 2018. A new species of the land planarian *Issoca* (Platyhelminthes, Tricladida, Geoplaninae) sheds light on the polyphyletic status of the genus. ZooKeys, 752, 1-15.

Carbayo, F., & Leal-Zanchet, A. M. 2003. Two new genera of geoplaninid land planarians (Platyhelminthes: Tricladida: Terricola) of Brazil in the light of cephalic specialisations. Invertebrate Systematics, 17(3), 449-468.

Carbayo, F. 2010. A new genus for seven Brazilian land planarian species, split off from *Notogynaphallia* (Platyhelminthes, Tricladida). Belgian Journal of Zoology, 140 (Suppl.), 91-101

Carbayo, F., Álvarez-Presas, M., Olivares, C. T., Marques, F. P., Froehlich, E. M., & Riutort, M. 2013. Molecular phylogeny of Geoplaninae (Platyhelminthes) challenges current classification: proposal of taxonomic actions. Zoologica Scripta, 42(5), 508-528.

Cason, J. E. 1950. A rapid one-step Mallory-Heidenhain stain for connective tissue. Stain Technology, 25, 225-226.

Chappill, J. A. 1989. Quantitative characters in phylogenetic analysis. Cladistics, 5(3), 217-234.

Chisholm, L.A., Morgan, J.A.T., Adlard, R.D., Whittington, I.D., 2001. Phylogenetic analysis of the Monocotylidae (Monogenea) inferred from 28S rDNA sequences. International Journal for Parasitology, 31, 1253-1263.

ICNZ, 1999. International of Zoological Nomenclature. 4. ed. The International Trust for Zoological Nomenclature 1999.

Darwin, C. 1844. Brief descriptions of several terrestrial planariae, and of some remarkable marine species, with an account of their habits. Annals and Magazine of Natural History, Annales de Sciences Naturelles, (14), 241-251.

Darwin, C. 1859. On the Origin of Species by Means of Natural Selection Or the Preservation of Favoured Races in the Struggle for Life. International Book Company.

Ewing, B., & Green, P. 1998. Base-calling of automated sequencer traces using phred. II. Error probabilities. Genome Research, 8, 186-194.

Ewing B, Hillier L, Wendl MC, Green P. 1998. Base-calling of automated sequencer traces using phred. I. Accuracy assessment. Genome Research, 8, 175-185.

Fernández, R., Kvist, S., Lenihan, J., Giribet, & G., Ziegler, A. 2014. Sine systemate chaos? A versatile tool for earthworm taxonomy: non-destructive imaging of freshly fixed and museum specimens using micro-computed tomography. PloS ONE, 9(5), e96617.

Froehlich, C. G. 1955. Sobre morfologia e taxonomia das Geoplanidae. Boletim da Faculdade de Filosofia, Ciências e Letras. Série Zoologia, 19, 195-279.

Gift, N., & Stevens, P. F. 1997. Vagaries in the delimitation of character states in quantitative variation - an experimental study. Systematic Biology, 46(1), 112-125.

Gordon, D., Abajian, C., Green, P. 1998. Consed: a graphical tool for sequence finishing. Genome Research, 8, 195-202.

Gordon, D., Desmarais, C., Green, P. 2001. Automated finishing with autofinish. Genome Research, 11, 614-625.

Hall, T. A. 1999. BioEdit: a user-friendly biological sequence alignment editor and analysis program for Windows 95/98/NT. Nucleic Acid Symposium Series, 41, 95-98.

Heneberg, P. & Literák, I. 2013. Molecular phylogenetic characterization of Collyriclum faba with reference to its three host-specific ecotypes. Parasitology International, 62, 262-267.

Hurvich, C. M., & Tsai, C. L. 1989. Regression and time series model selection in small samples. Biometrika, 76(2), 297-307.

Katoh, K., Kuma, K., Toh, H., Miyata, T. 2002. MAFFT version 5: improvement in accuracy of multiple sequence alignment. Nucleic Acids Research, 33, 511-518.

Lanfear, R., Frandsen, P. B., Wright, A. M., Senfeld, T., & Calcott, B. 2017. PartitionFinder 2: new methods for selecting partitioned models of evolution for molecular and morphological phylogenetic analyses. Molecular biology and evolution, 34(3), 772-773.

Lázaro, E. M., Sluys, R., Pala, M., Stocchino, G. A., Baguña, J. & Riutort, M. 2009. Molecular barcoding and phylogeography of sexual and asexual freshwater planarians of the genus *Dugesia* in the Western Mediterranean (Platyhelminthes, Tricladida, Dugesiidae). Molecular Phylogenetics and Evolution, 52, 835-845.

Littlewood, D. T. j.; Rohde, K. & Chough, K. A. 1997. Parasite speciation within or between host species? - Phylogenetic

evidence from site-specific polystome monogeneans. International Journal for Parasitology, 27, 1289-1297.

Miller, M. A., Pfeiffer, W., and Schwartz, T. 2010. "Creating the CIPRES Science Gateway for inference of large phylogenetic trees" in Proceedings of the Gateway Computing Environments Workshop (GCE), 14 Nov. 2010, New Orleans, LA, 1-8.

Negrete, L., Leal-Zanchet, A. M. & Brusa, F. 2015. A new species of *Notogynaphallia* (Platyhelminthes, Geoplanidae) extends the known distribution of land planarians in Chacoan province (Chacoan subregion), South America. Zoological Studies, 54-58, 1-14. DOI 10.1186/s40555-015-0136-5

Negrete, L., Do Amaral, S. V., Ribeiro, G. G., Wolmann Gonçalves, J., Valiati, V. H., Damborenea, C., ... & Leal-Zanchet, A. M. 2019. Far away, so close! Integrative taxonomy reveals a new genus and species of land flatworm (Platyhelminthes: Geoplanidae) from southern South America. Zoological Journal of the Linnean Society, 189(3), 722-744.

Ogren, R. E. & Kawakatsu, M. 1990. Index to the species of the family Geoplanidae (Turbellaria, Tricladida, Terricola) Part I: Geoplaninae. Bulletin Fuji Women's College, Ser. I, 28, 79-166.

Ronquist, F., & Huelsenbeck, J. P. 2003. MrBayes 3: Bayesian phylogenetic inference under mixed models. Bioinformatics, 19(12), 1572-1574.

Silva, M. S., & Carbayo, F. 2020. X-ray microcomputed tomography applied to the taxonomic study of rare material: redescriptions of seven of Schirch’s Brazilian species of land planarians (Geoplanidae, Platyhelminthes). ZooKeys, 910, 1.

Stamatakis, A. 2016. The RAxML v8. 2. X Manual. Heidleberg Institute for Theoretical Studies. Available at: https://cme. h-its. org/exelixis/resource/download/NewManual. pdf.

Stevens, P. F. 1991. Character states, morphological variation, and phylogenetic analysis: a review. Systematic botany, 553-583.

Sunnucks, P., Blacket, M. J., Taylor, J. M., Sands, C. J., Ciavaglia, S. A., Garrick, R. C., ... & Pavlova, A. 2006. A tale of two flatties: different responses of two terrestrial flatworms to past environmental climatic fluctuations at Tallaganda in montane southeastern Australia. Molecular Ecology, 15(14), 4513-4531.

Tautz, D., Arctander, P., Minelli, A., Thomas, R. H., & Vogler, A. P. 2003. A plea for DNA taxonomy. Trends in Ecology & Evolution, 18(2), 70–74. doi:10.1016/s0169-5347(02)00041-1.

Tkach, V., Grabda-Kazubska, B., Pawlowski, J. & Swiderski, Z. 1999. Molecular and morphological evidence for close phylogenetic affinities of the genera *Macrodera*, *Lepdophallus*, *Metaleptophallus* and *Paralepoderma* (Digenea, Plagiorchiata). Acta Parasitologica, 44, 170-179.

Williams, S. T. & Ozawa, T. 2006. Molecular phylogeny suggests polyphyly of both the turban shells (family Turbinidae) and the superfamily Trochoidea (Mollusca: Vetigastropoda). Molecular Phylogenetics and Evolution, 39, 33-51.

Winsor, L. 1998. Aspects of taxonomy and functional histology in terrestrial flatworms (Tricladida: Terricola). Pedobiologia, 42(4), 12-432.

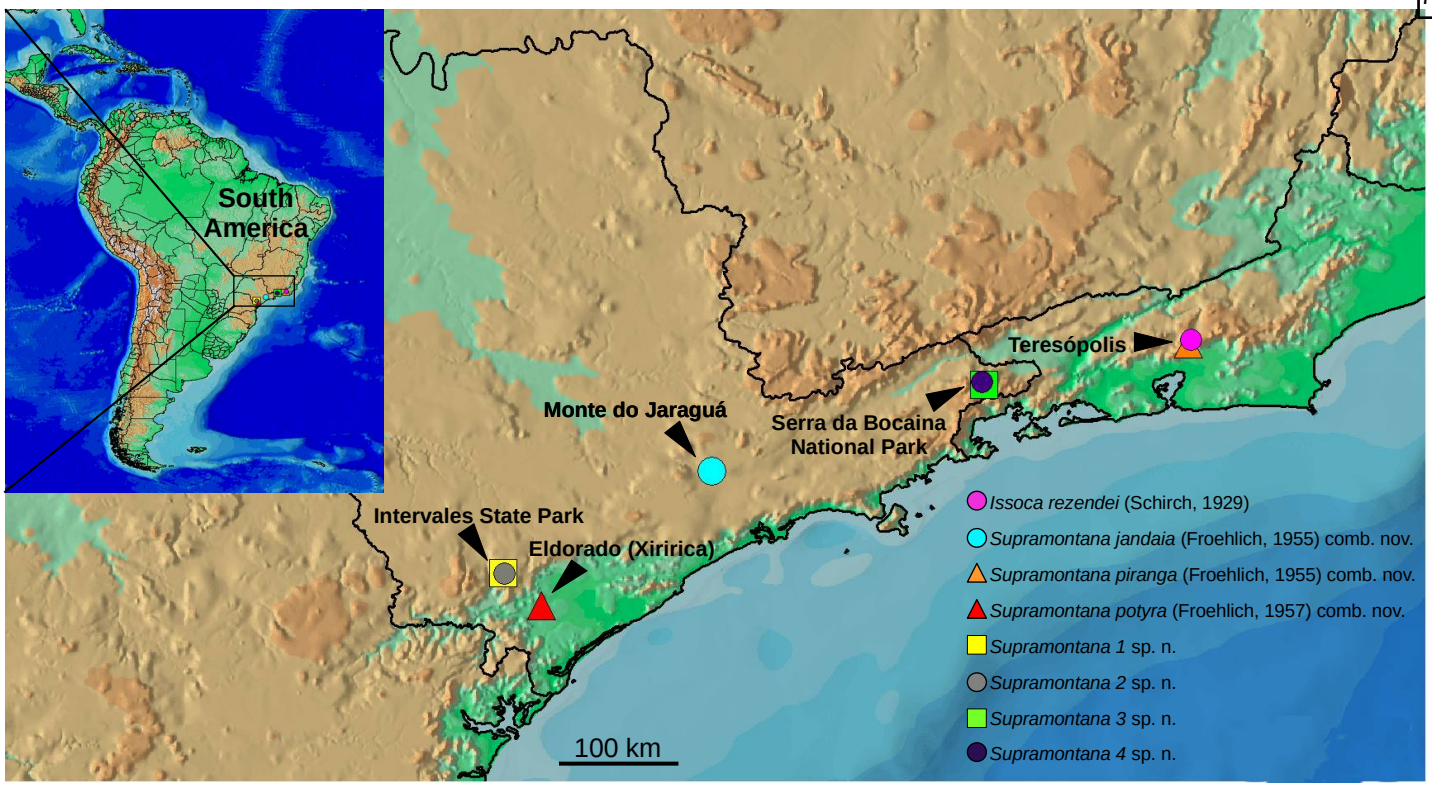

Fig. 1. Map showing the sampling sites of the eight species (re)described in this paper.

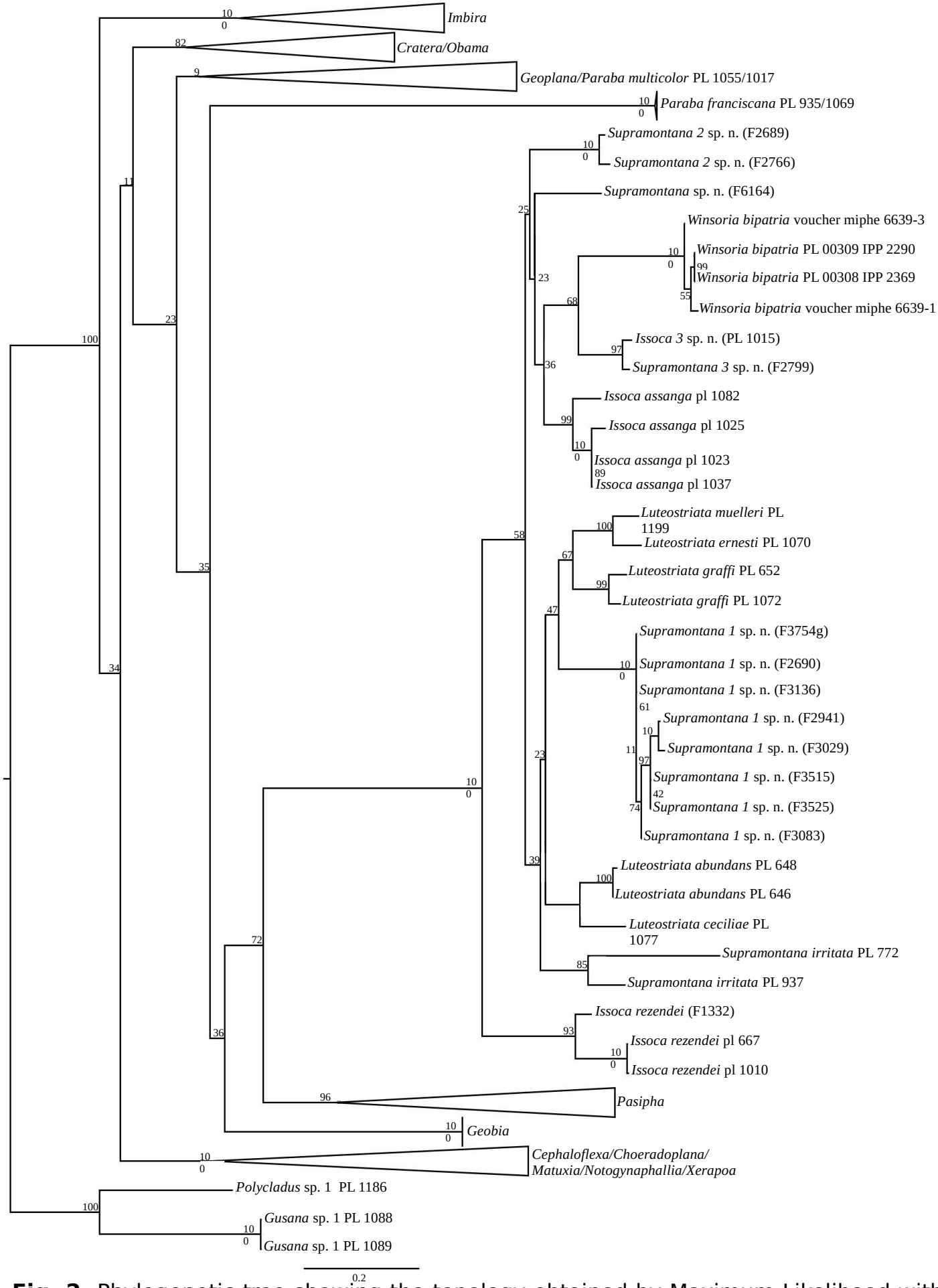

Fig. 2. Phylogenetic tree showing the topology obtained by Maximum Likelihood with the information of the concatenated two genes (18S rDNA + COI). Numbers at the nodes correspond to bootstrap values of the maximum likelihood analysis. Scale bar represents substitutions per site. Some clades of the outgroups are collapsed.

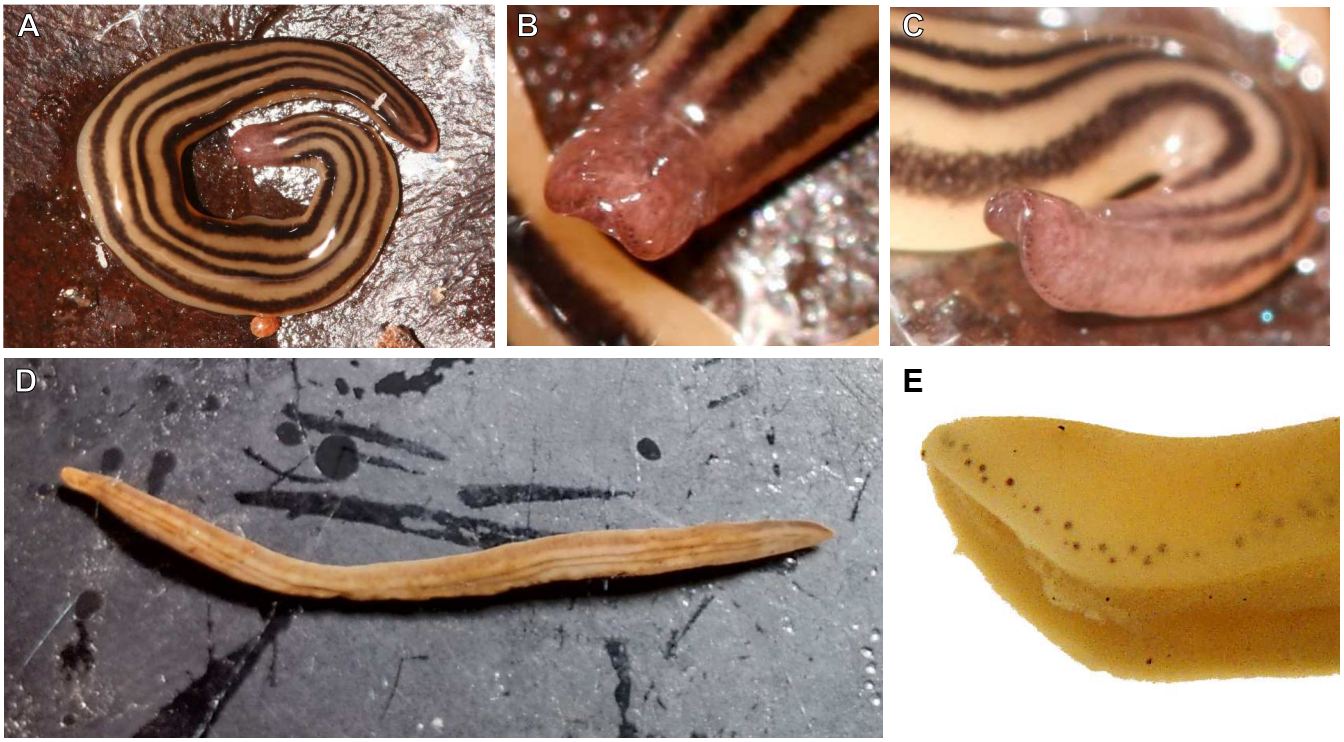

Fig. 3. *Issoca rezendei* (Schirch, 1929). (A): Dorsal view of a living specimen from São Paulo, São Paulo State. (B-C): Cephalic region of the same specimen. (D) Cephalic region of the preserved syntype MNRJ 8927-1 in lateral view; body length 33 mm. (E): Lateral view of the cephalic region of the preserved specimen F0715. Scale bars not available for Figs A-C, E.

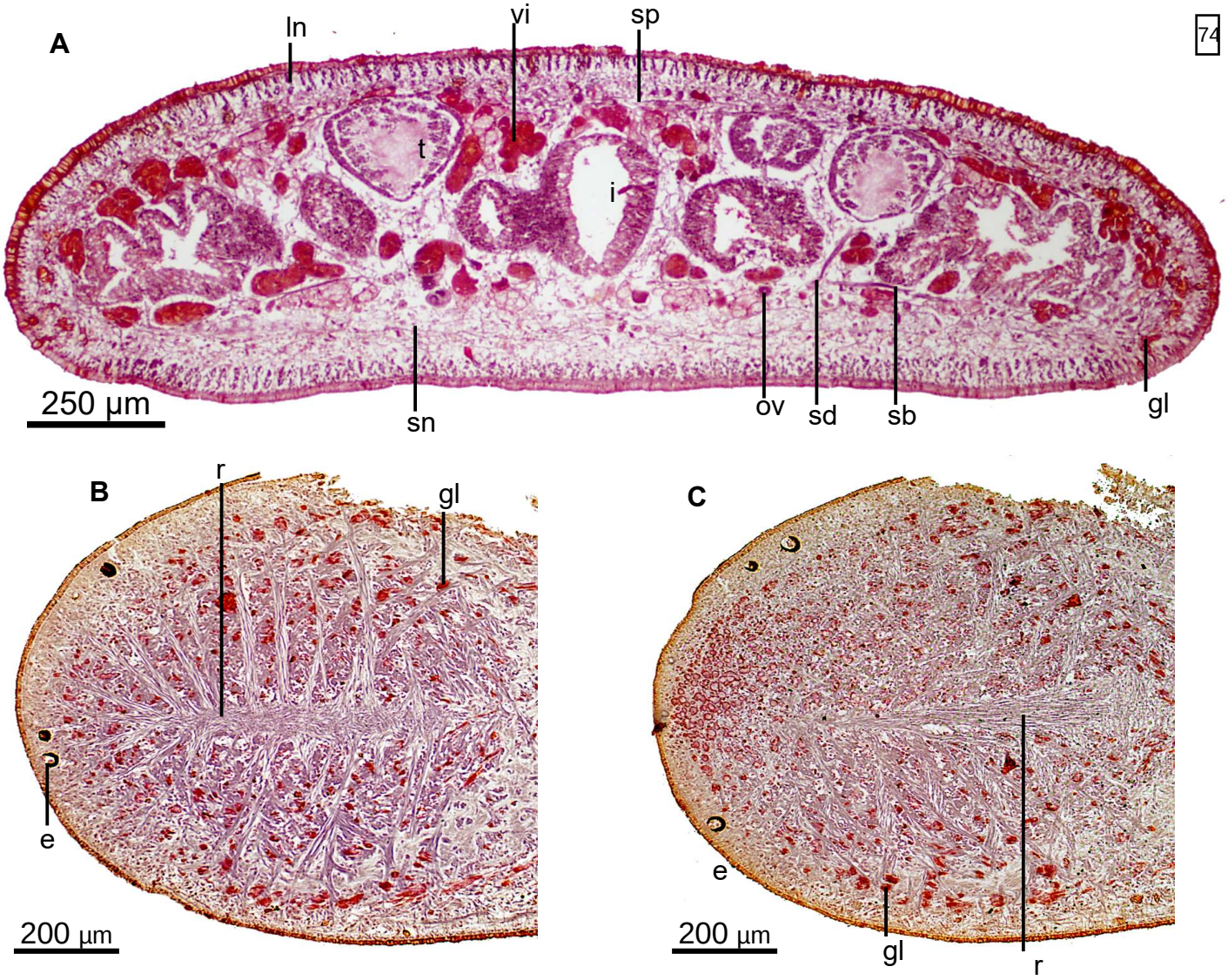

Fig. 4. *Issoca rezendei* (Schirch, 1929). Photomicrographs. (A): Transverse section of the pre-pharyngeal region of specimen F0795. (B-C) Horizontal sections of the cephalic region of specimen F0648.

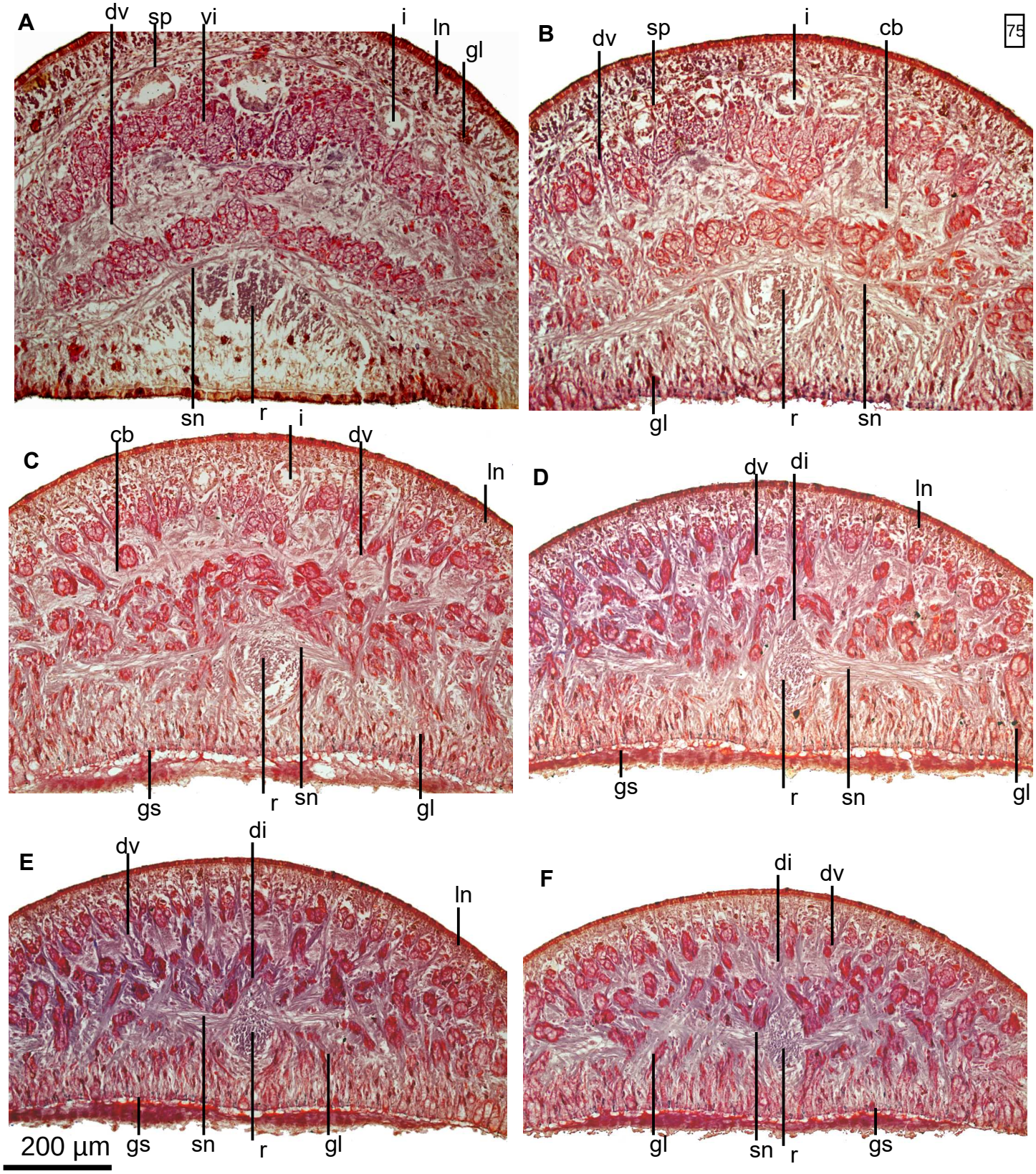

Fig. 5. *Issoca rezendei* (Schirch, 1929). Photomicrographs of transverse sections of the cephalic region of specimen F0795 at 930 µm (A), 550 µm (B), 460 µm (C), 360 µm (D), 320 µm (E), 260 µm (F), from the anterior extremity of the body.

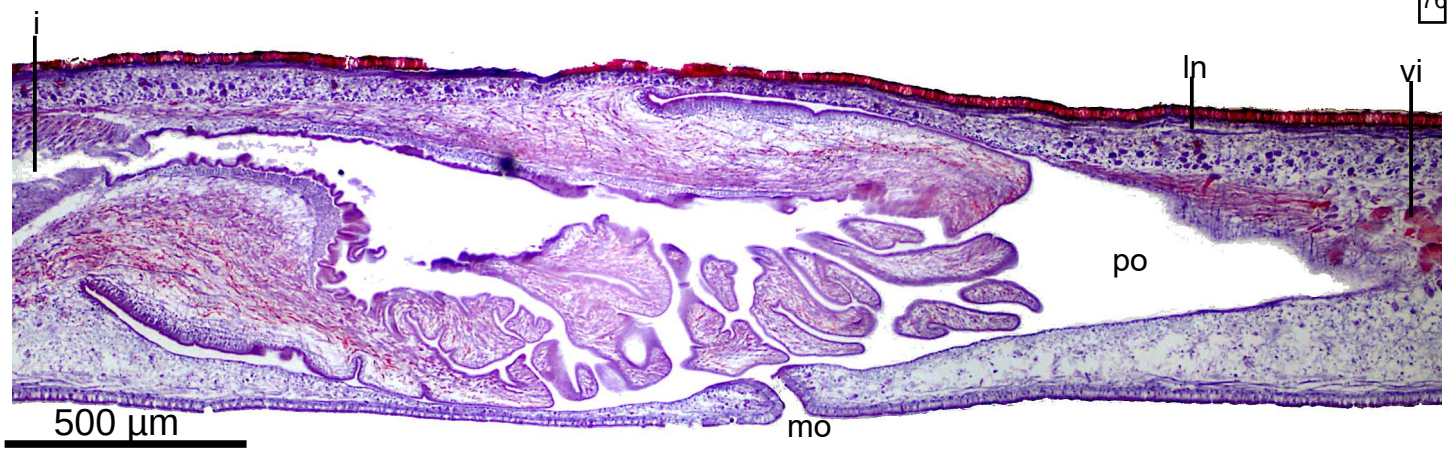

Fig. 6. *Issoca rezendei* (Schirch, 1929). Photomicrograph a sagittal section of the pharynx of specimen F0545.

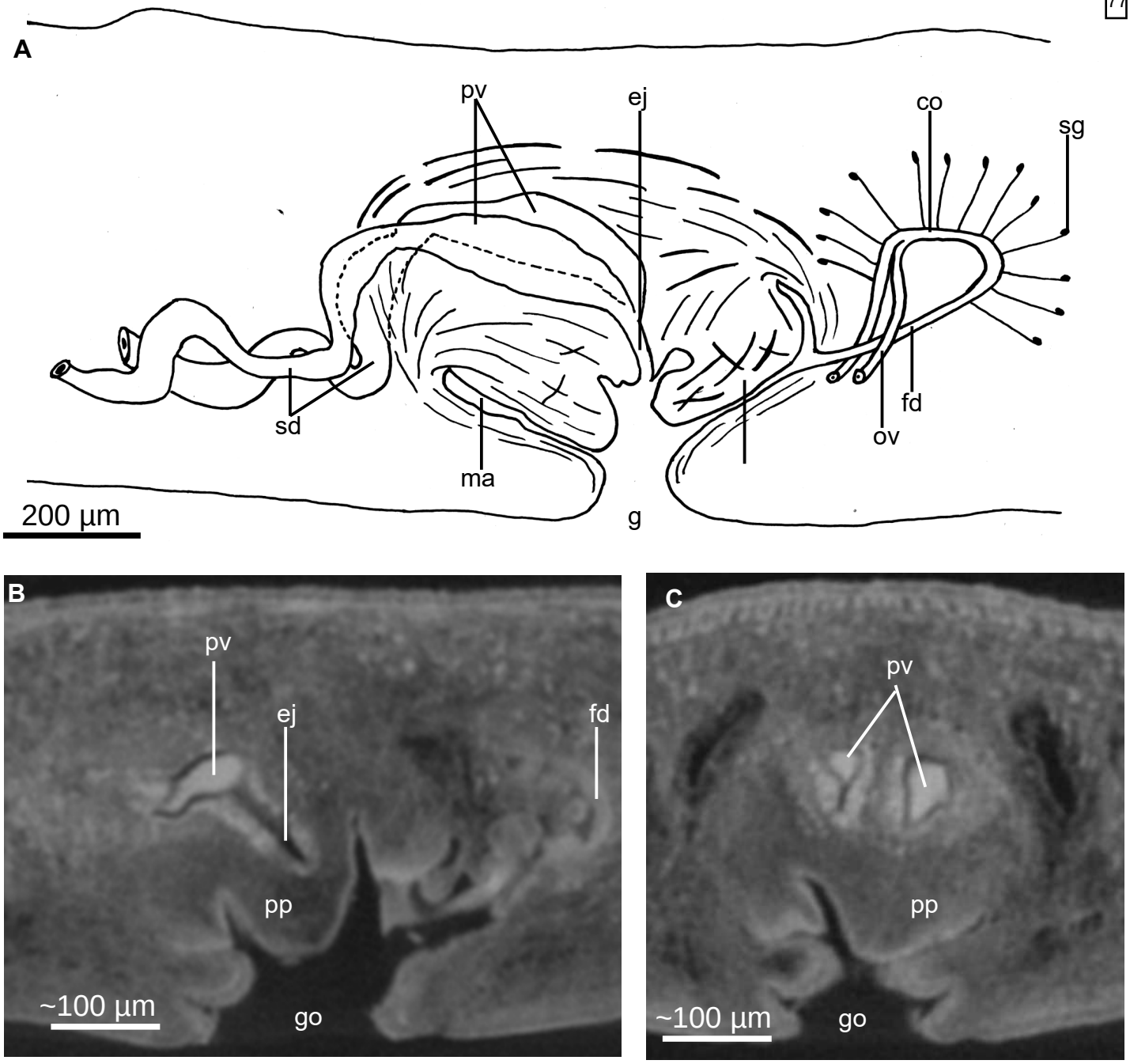

Fig. 7. *Issoca rezendei* (Schirch, 1929). (A) diagrammatic reconstruction of the copulatory apparatus of specimen F0648. (B-C): Sagittal (A) and transverse (B) µCT-derived images from syntype MNRJ 8927.

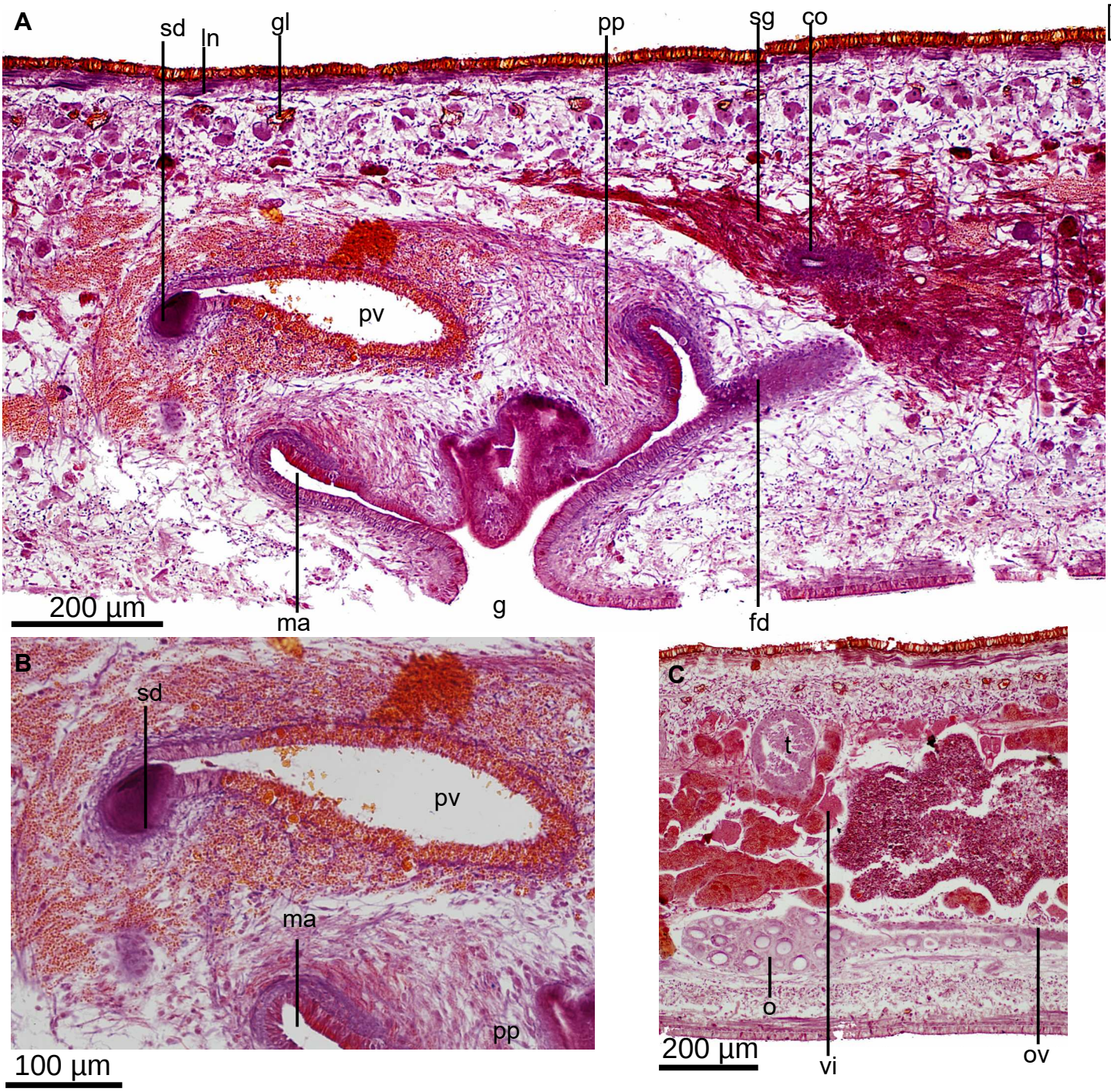

Fig. 8. *Issoca rezendei* (Schirch, 1929). Photomicrographs of sagittal sections of specimen F0648. (A): copulatory apparatus. (B): prostatic vesicle. (C): ovarian region.

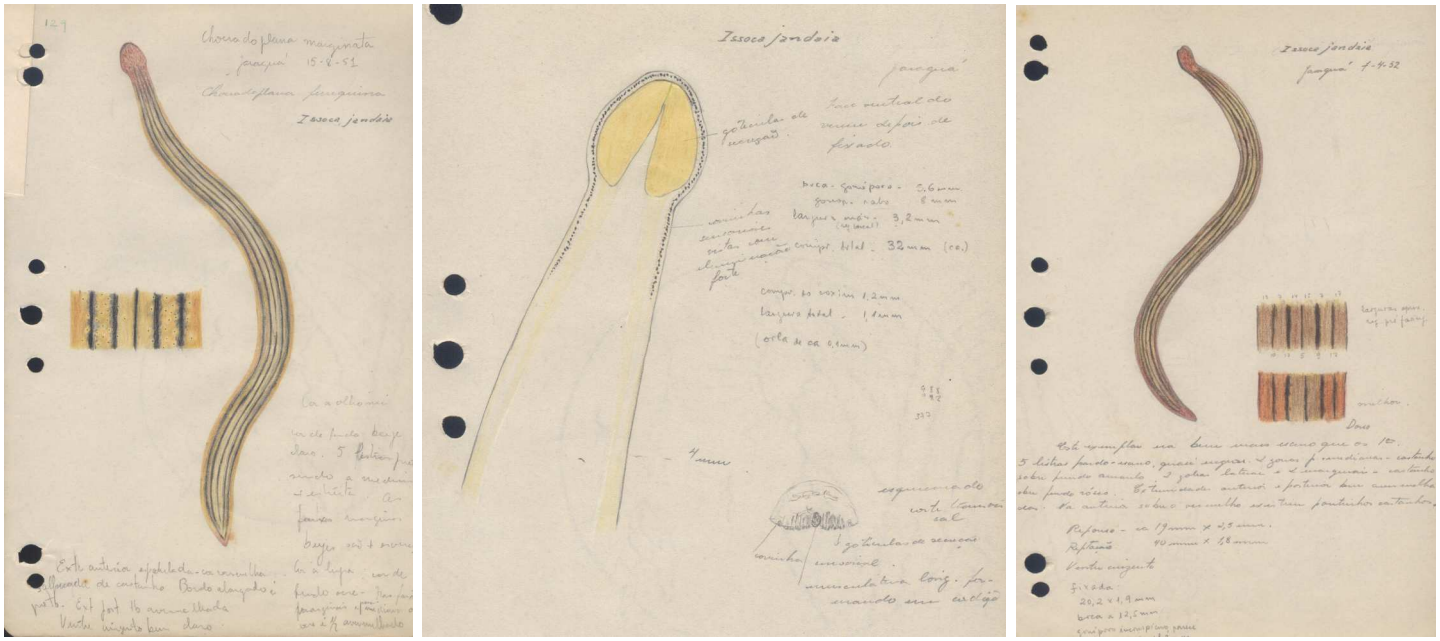

Fig. 9. *Supramontana jandaia* (Froehlich, 1955). Hand drawings by Froehlich, E.M. of the live type specimens.

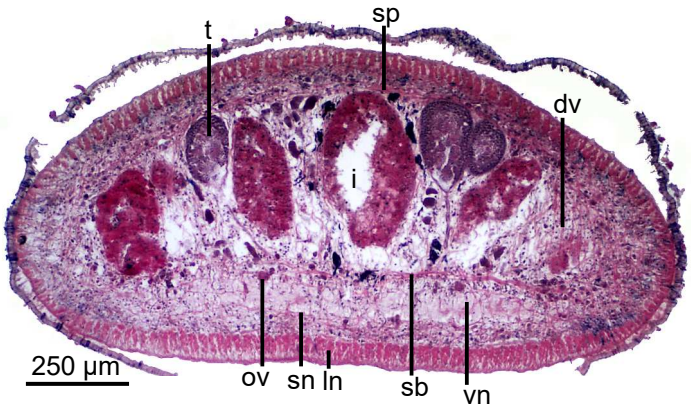

Fig. 10. *Supramontana jandaia* (Froehlich, 1955). (A): photomicrograph of a transverse section of the pre-pharyngeal region of an unlabelled syntype.

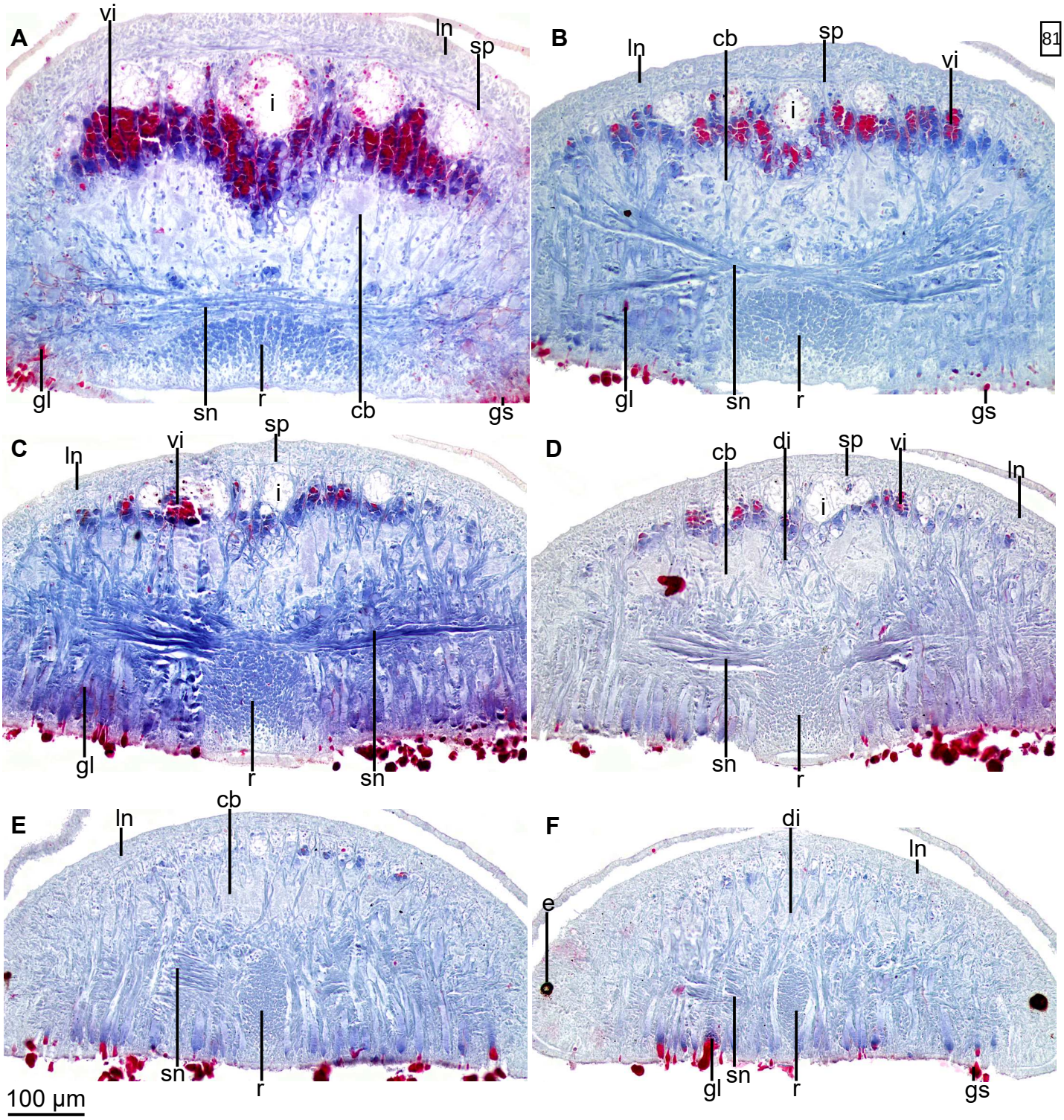

Fig. 11. *Supramontana jandaia* (Froehlich, 1955). Photomicrographs of transverse sections of the cephalic region of an unlabeled syntype arranged from furthest (A) to closest (F) distant from the anteriormost extremity of the body.

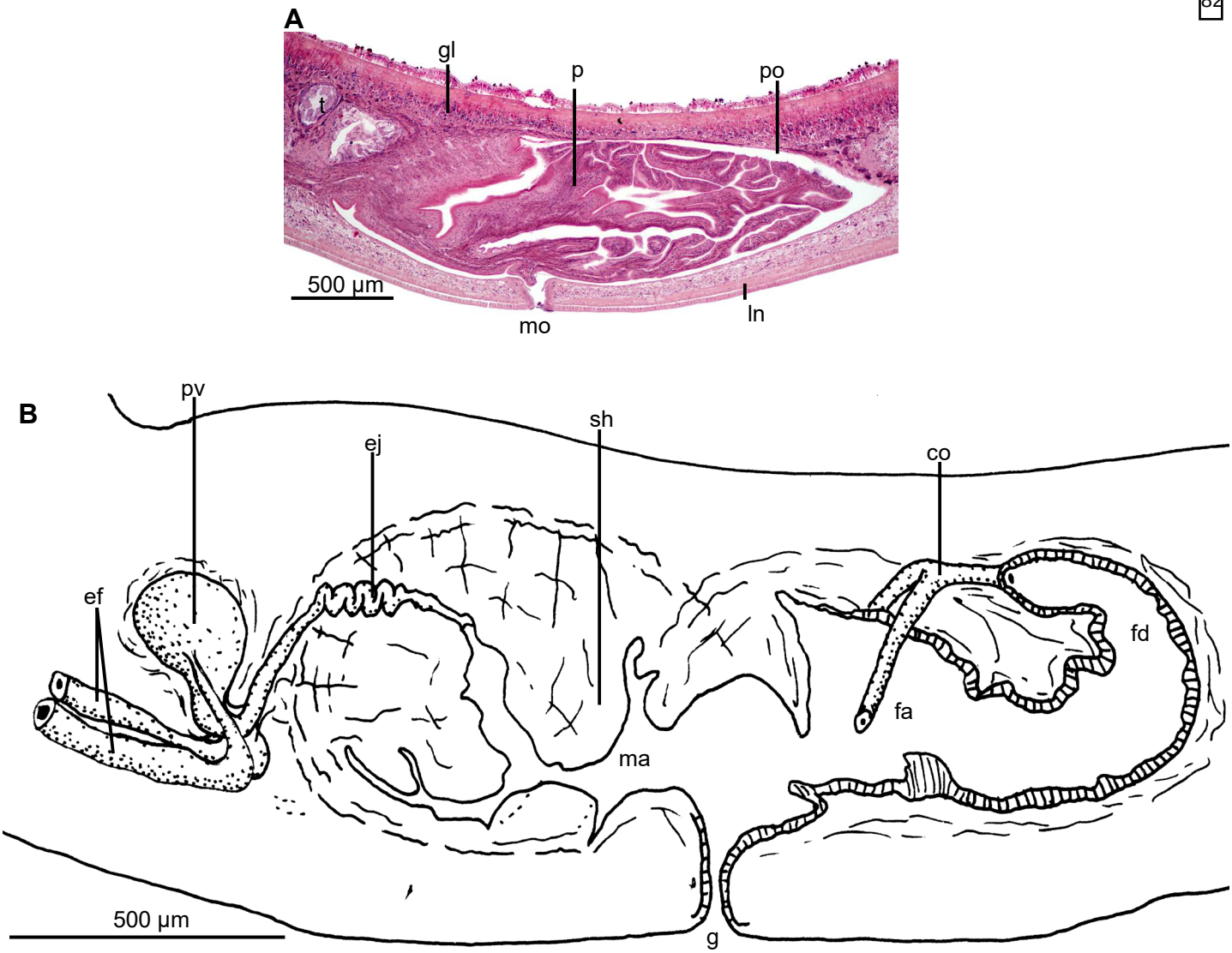

Fig. 12. *Supramontana jandaia* (Froehlich, 1955). (A): photomicrograph of a sagittal section of the pharynx of an unlabelled syntype. (B): Diagrammatic reconstruction of the copulatory apparatus of syntype 2.

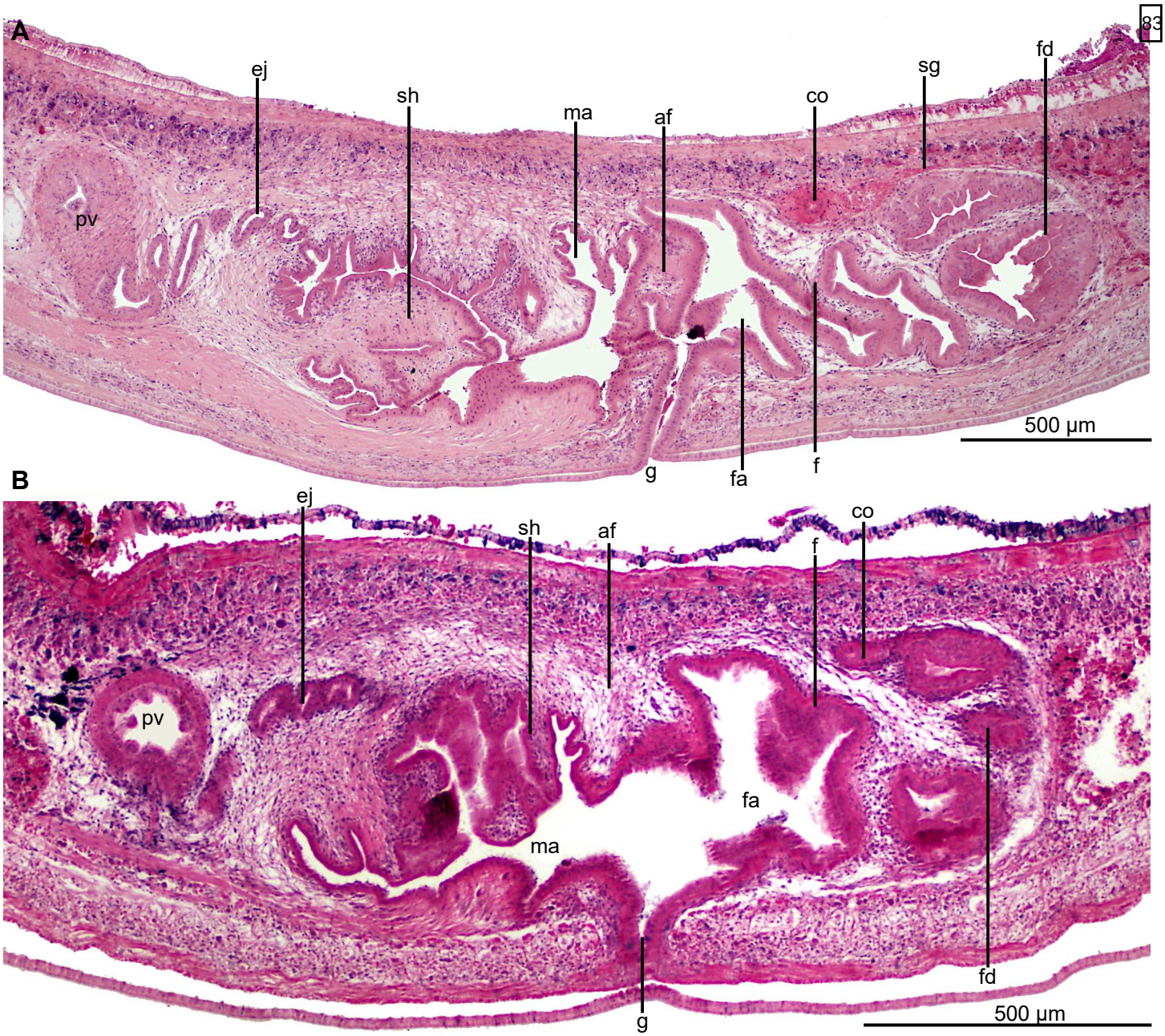

Fig. 13. *Supramontana jandaia* (Froehlich, 1955). (A-B): photomicrographs of sagittal sections of the copulatory apparatus of the syntypes 1 (A) and 2 (B).

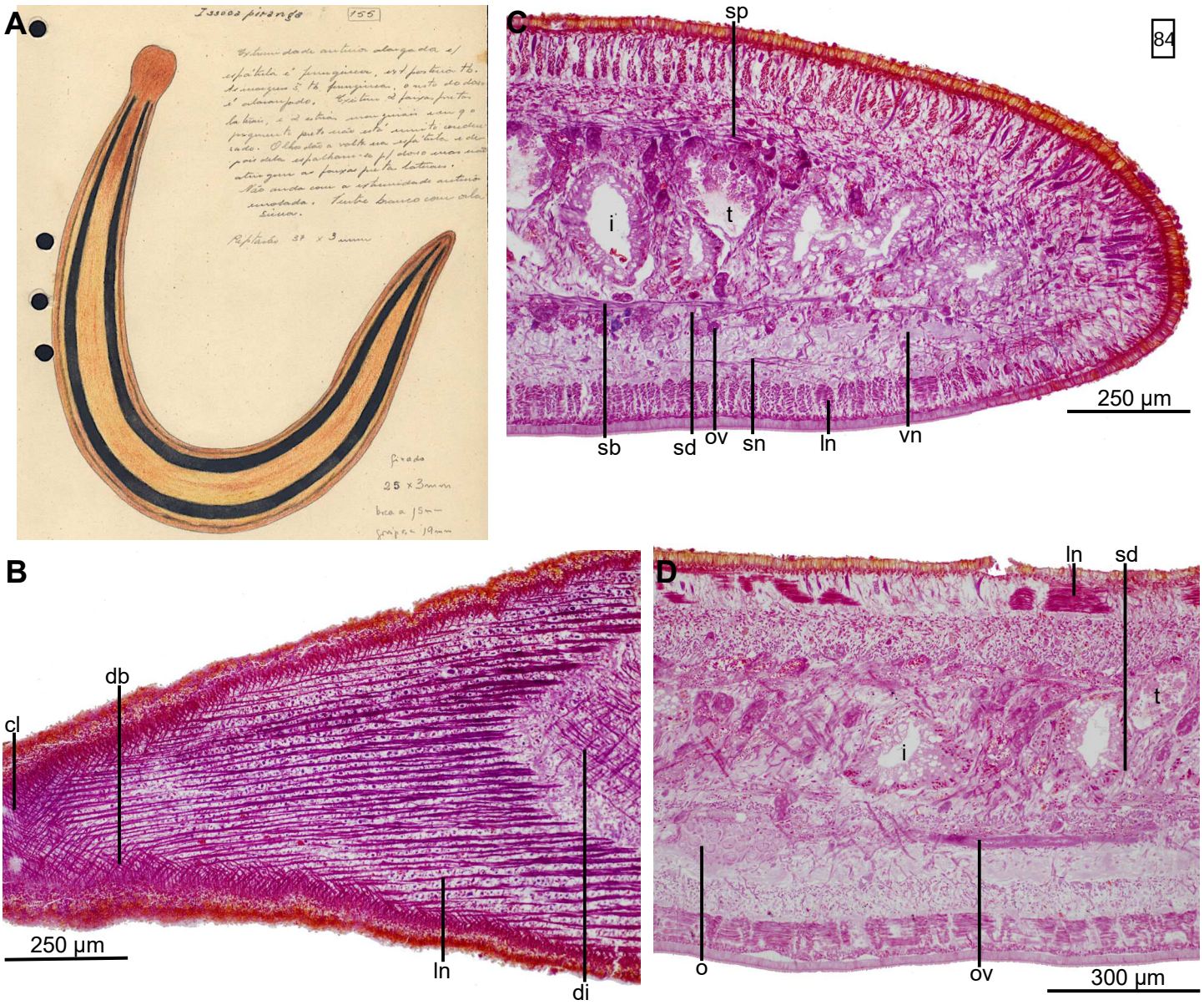

Fig. 14. *Supramontana piranga* (Froehlich, 1955). Holotype. (A): Hand drawing of the living specimen, by Froehlich, E.M. (B): photomicrograph of a horizontal section of the body. (C): photomicrograph of a transverse section of the pre-pharyngeal region. (D): photomicrograph of a sagittal section through and ovary.

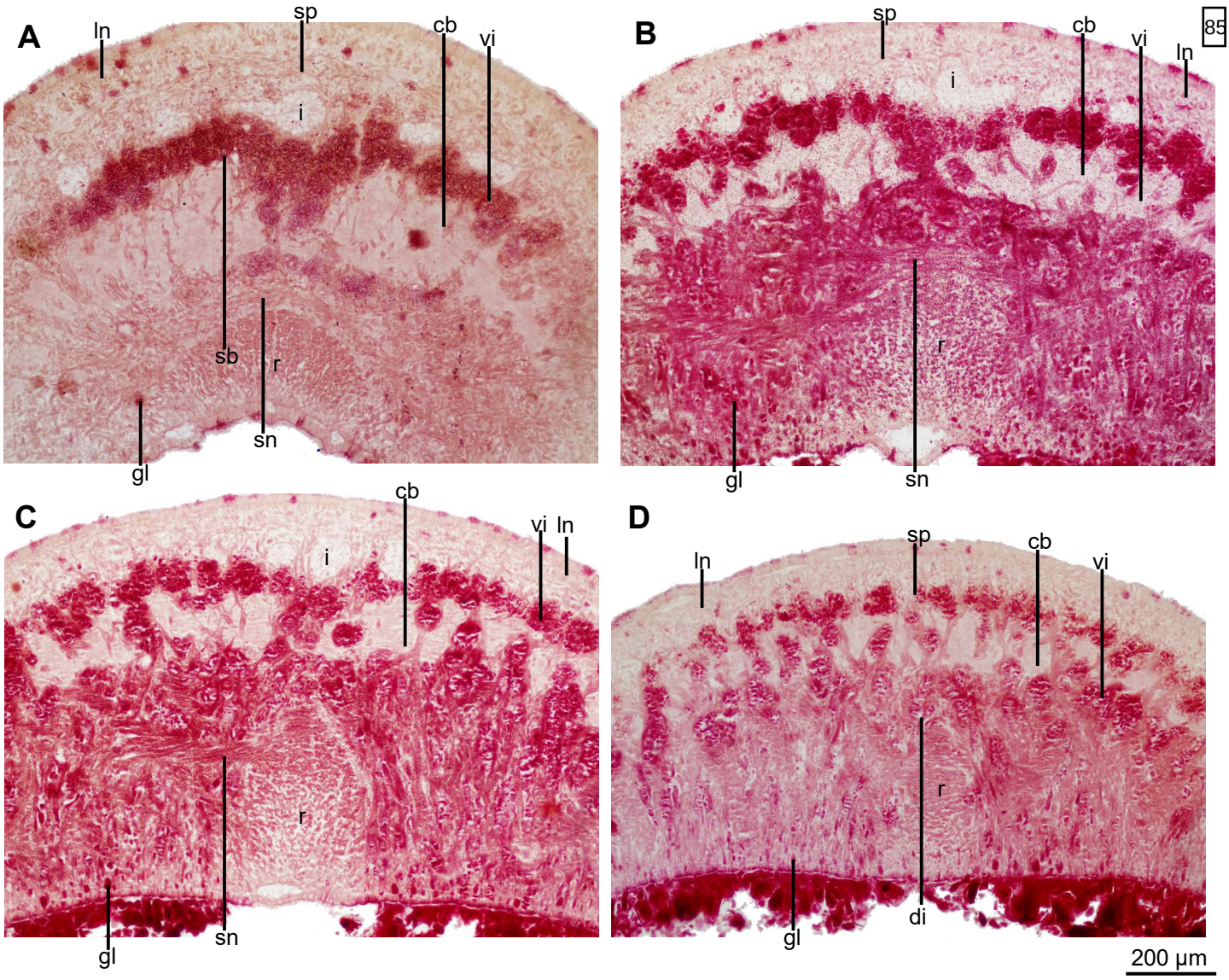

Fig. 15. *Supramontana piranga* (Froehlich, 1955). Holotype. Photomicrographs of transverse sections of the cephalic region arranged from furthest (A) to closest (D) distant from the anteriormost extremity of the body.

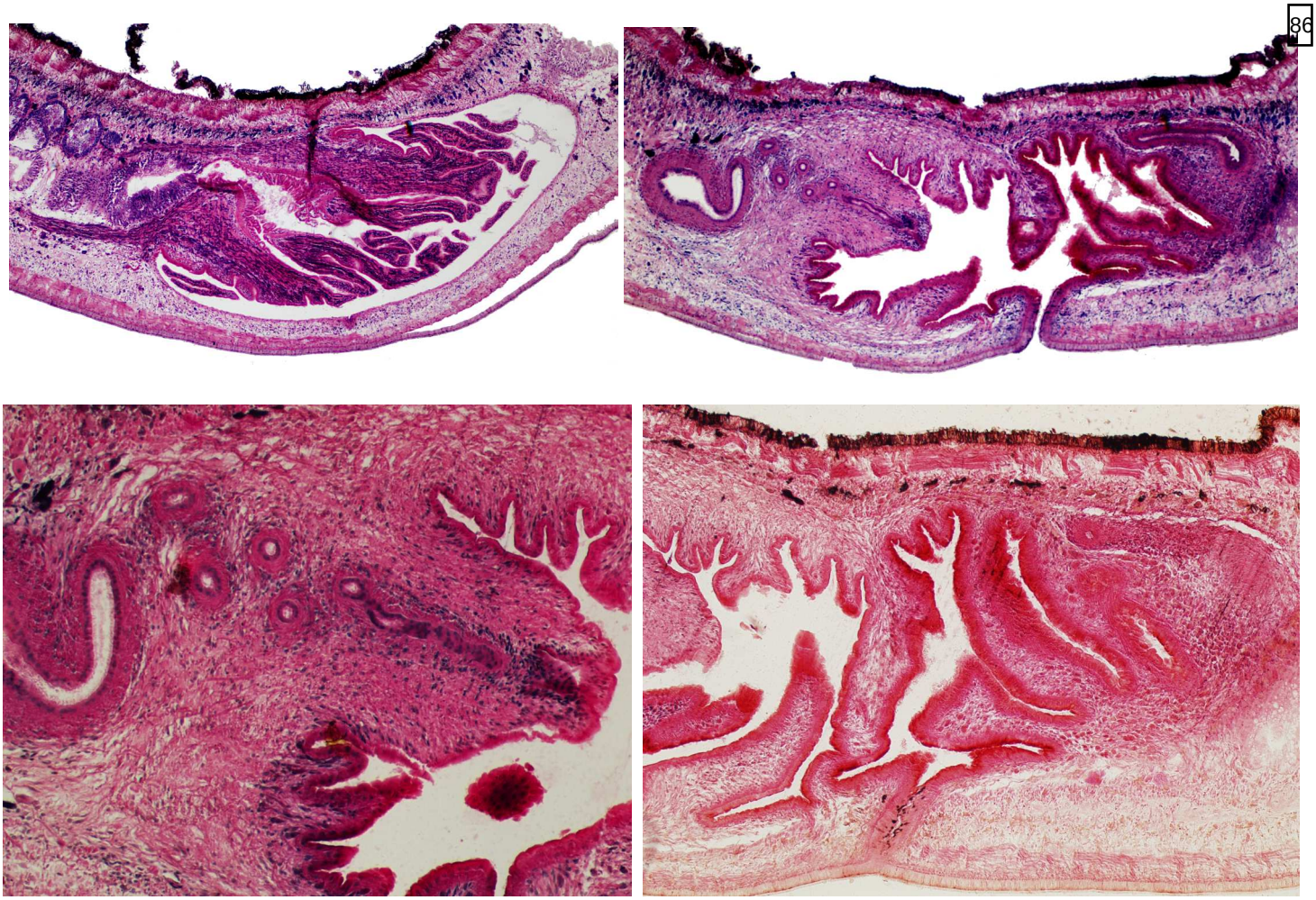

Fig. 16. *Supramontana piranga* (Froehlich, 1955). Holotype. Photomicrographs of sagittal sections. (A): pharynx; (B): copulatory apparatus; (C): penis papilla; (D): female atrium.

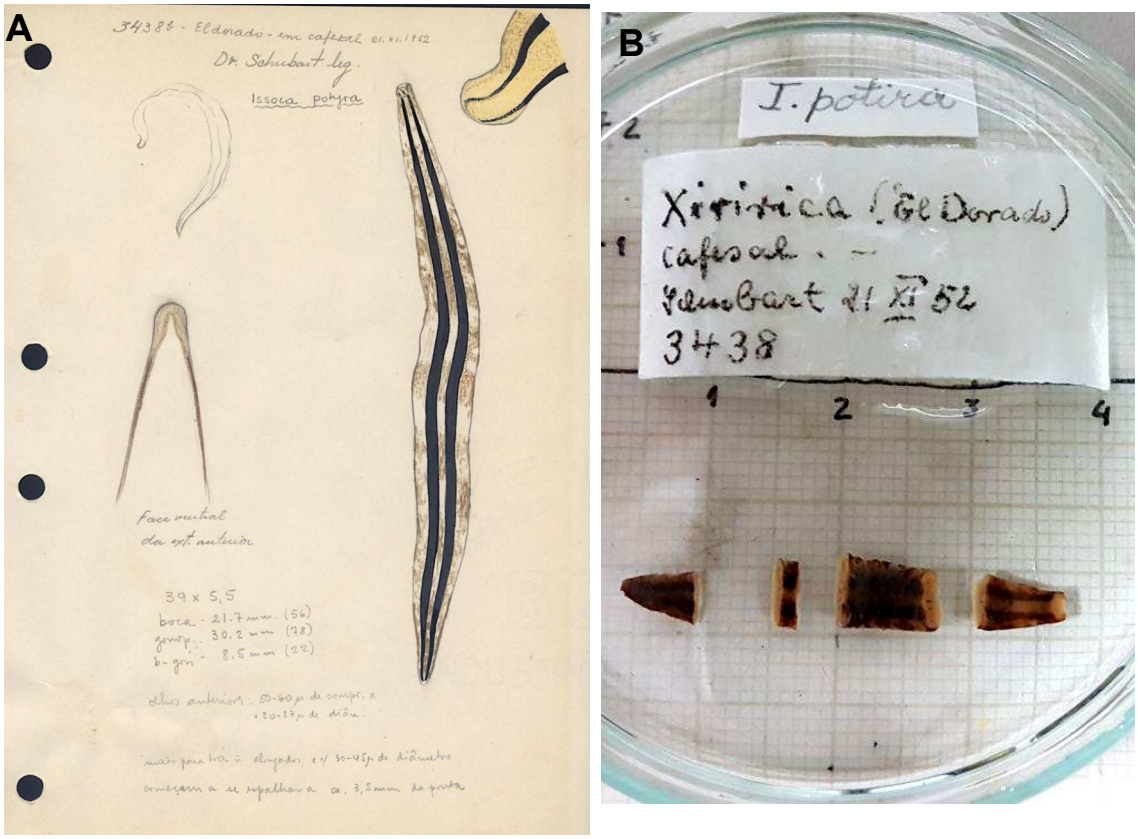

Fig. 17. *Supramontana potyra* (Froehlich, 1957). Holotype. (A): Hand drawing of the living specimen, by E. M. Froehlich. (B): Photograph of the remaining body portions in dorsal view, before newly histological processing for this study.

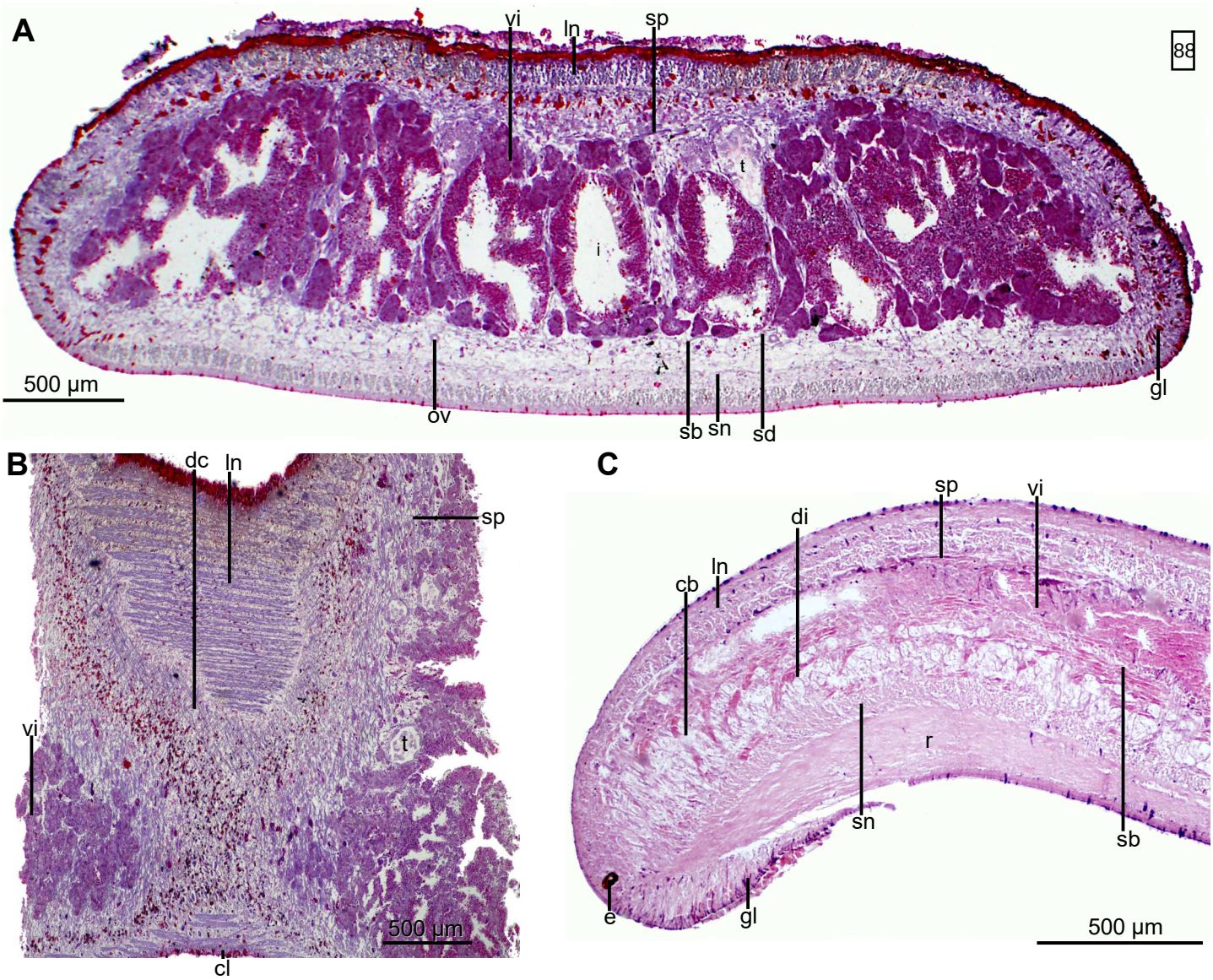

Fig. 18. *Supramontana potyra* (Froehlich, 1957). Photomicrographs of the holotype. (A): transverse section pre-pharyngeal region. (B): horizontal sections posterior to the ovaries. (C): sagittal section of the cephalic region.

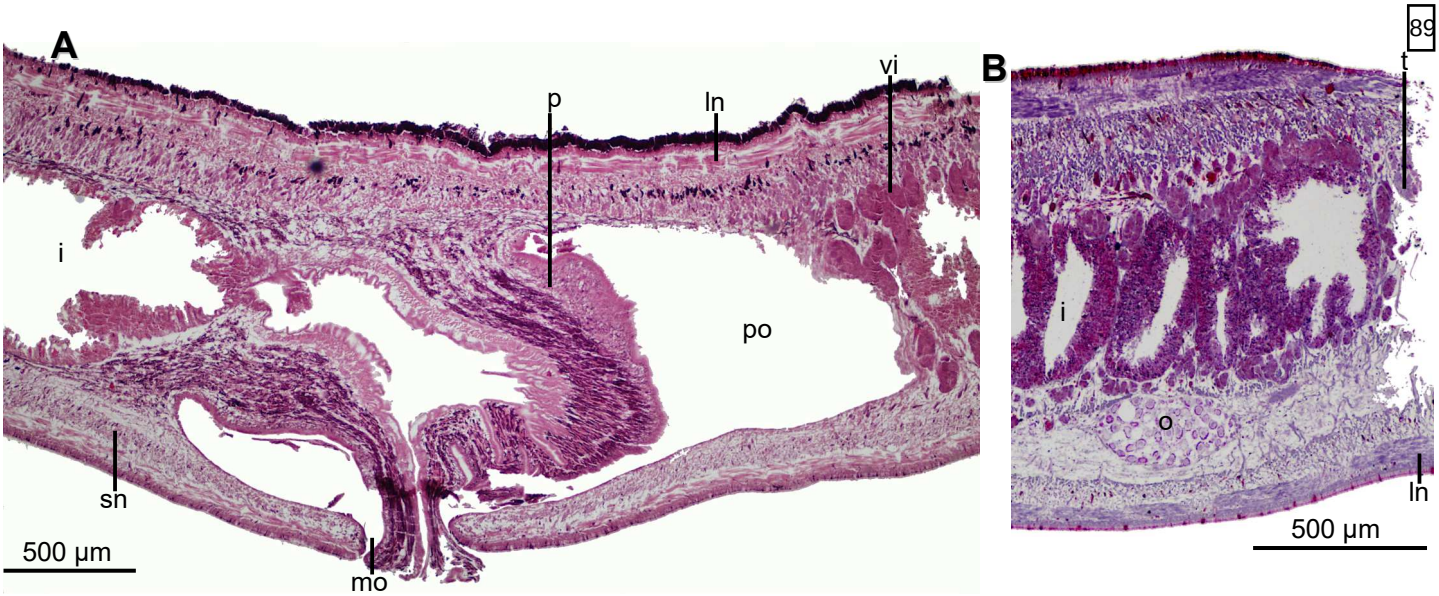

Fig. 19. *Supramontana potyra* (Froehlich, 1957). Holotype. Photomicrographs of sagittal sections. (A): pharynx. (B): ovary and anteriormost testes.

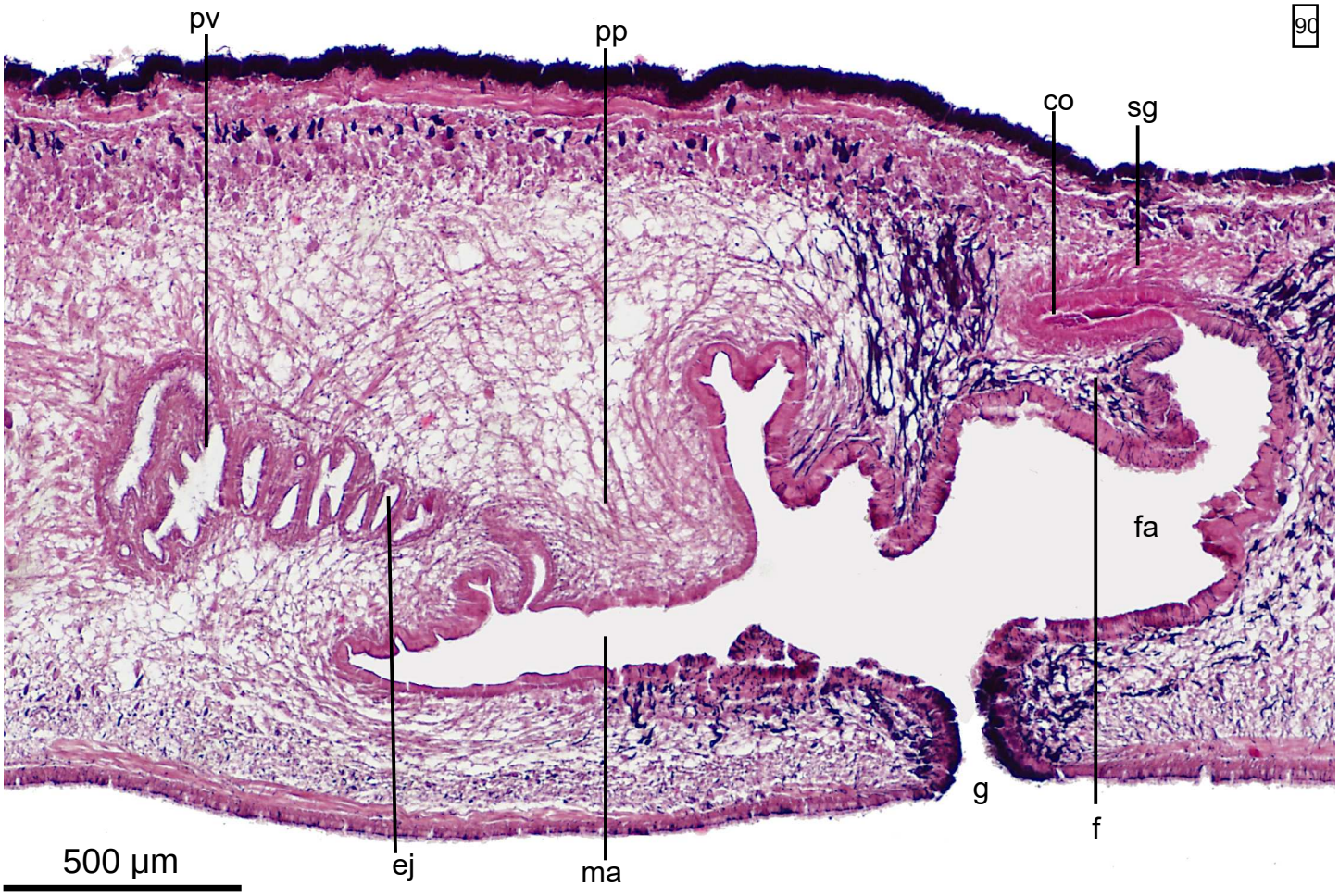

Fig. 20. *Supramontana potyra* (Froehlich, 1957). Holotype. Photomicrograph of sagittal section of the copulatory apparatus.

Fig. 21. *Supramontana 1* sp. n. Living specimens. (A): dorsal view of holotype. (B): cephalic region of holotype. (C): dorsal view of paratype F3083 (B): ventral view of paratype F2690.

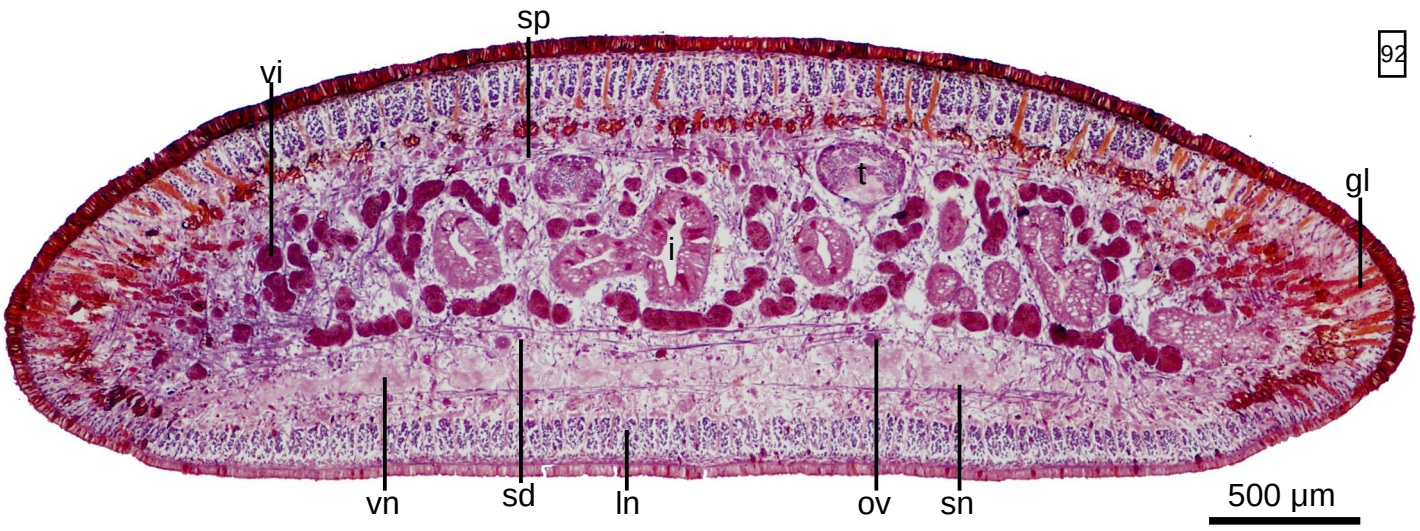

Fig. 22. *Supramontana 1* sp. n. Photomicrograph of a transverse section of the pre-pharyngeal region of the paratype F3083.

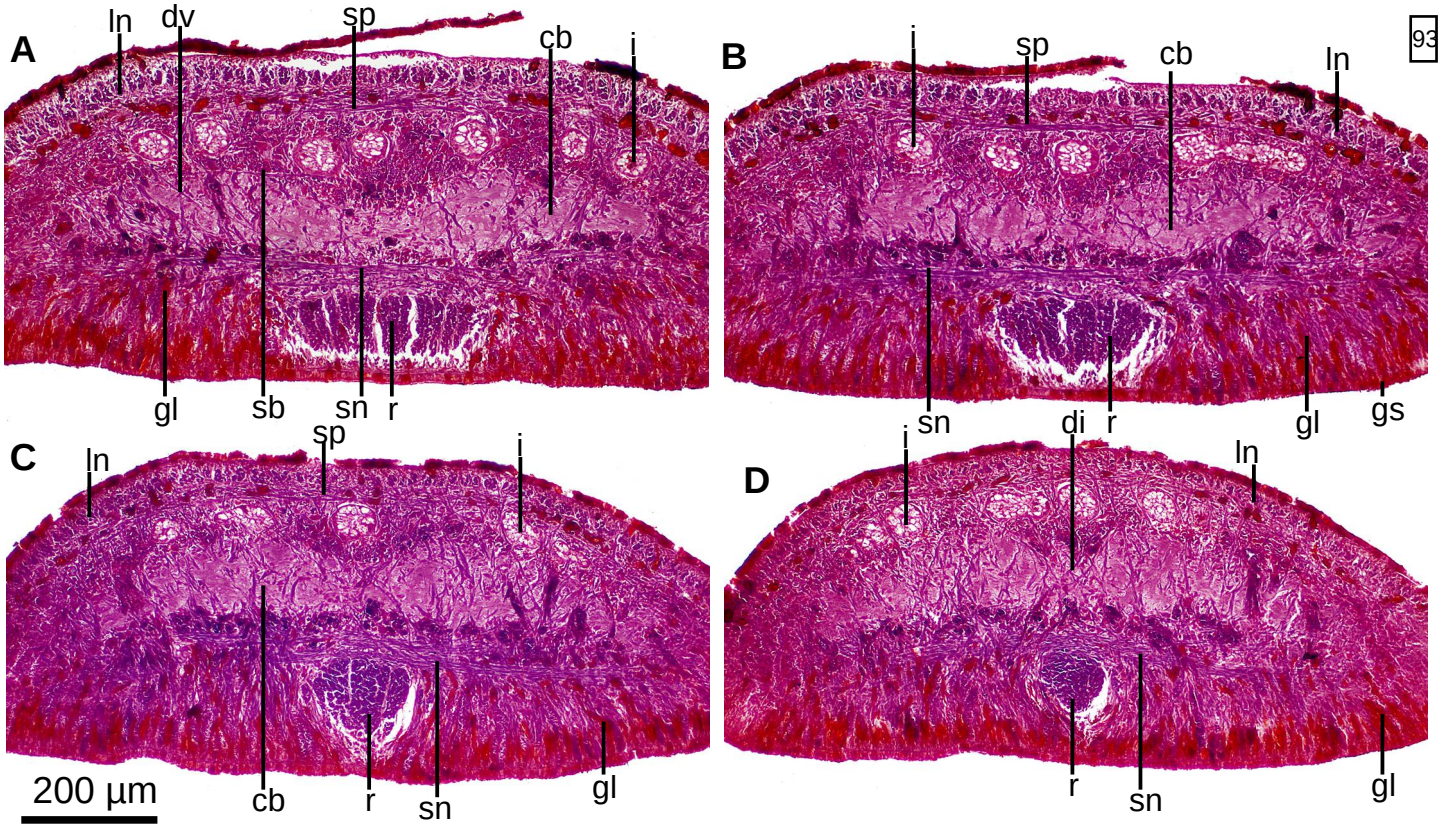

Fig. 23. *Supramontana 1* sp. n. Photomicrographs of transverse sections of the cephalic region of holotype F3754g arranged from furthest (A) to closest (D) distant from the anteriormost extremity of the body.

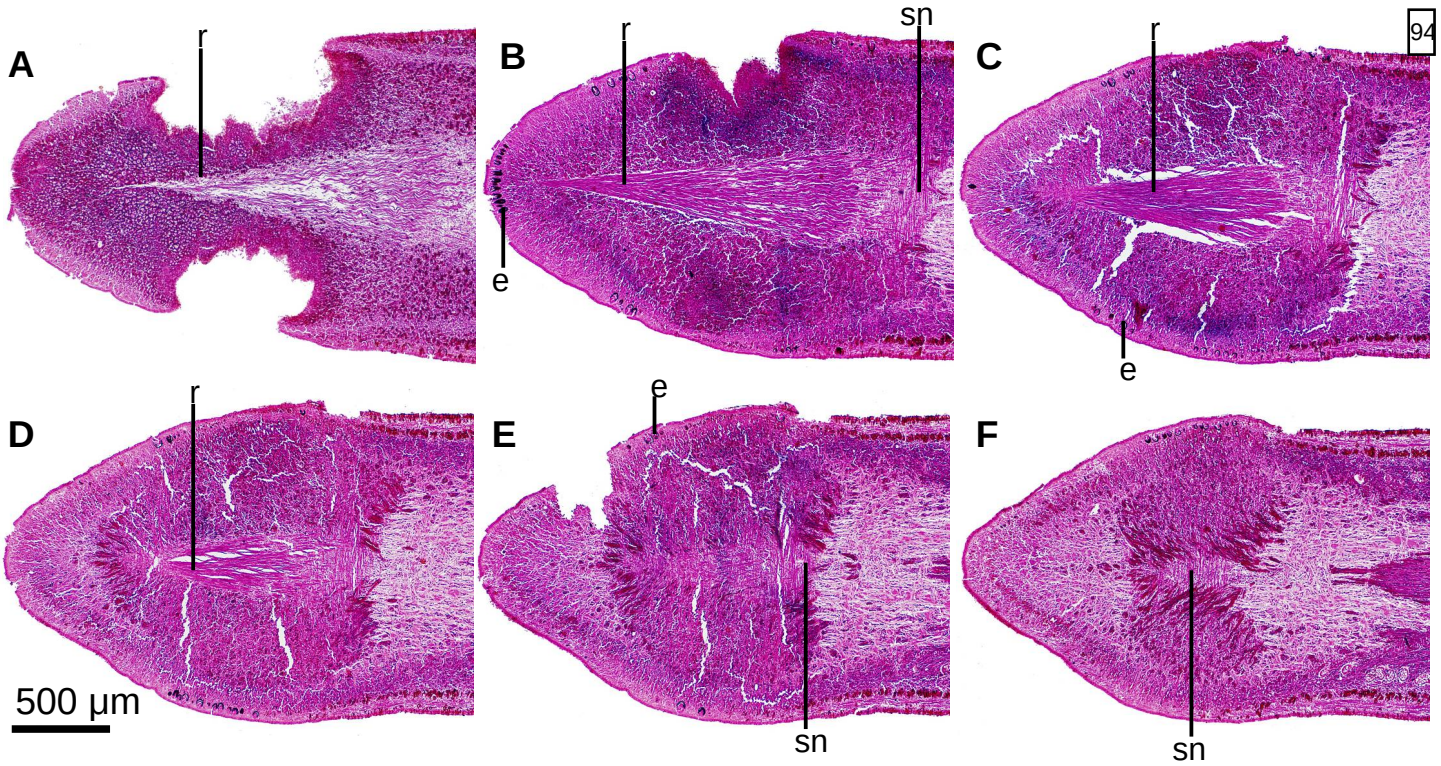

Fig. 24. *Supramontana 1* sp. n. (A-F): Photomicrographs of horizontal sections of the cephalic region of paratype F3083 from the ventralmost region (A) towards the dorsal side of the body (F).

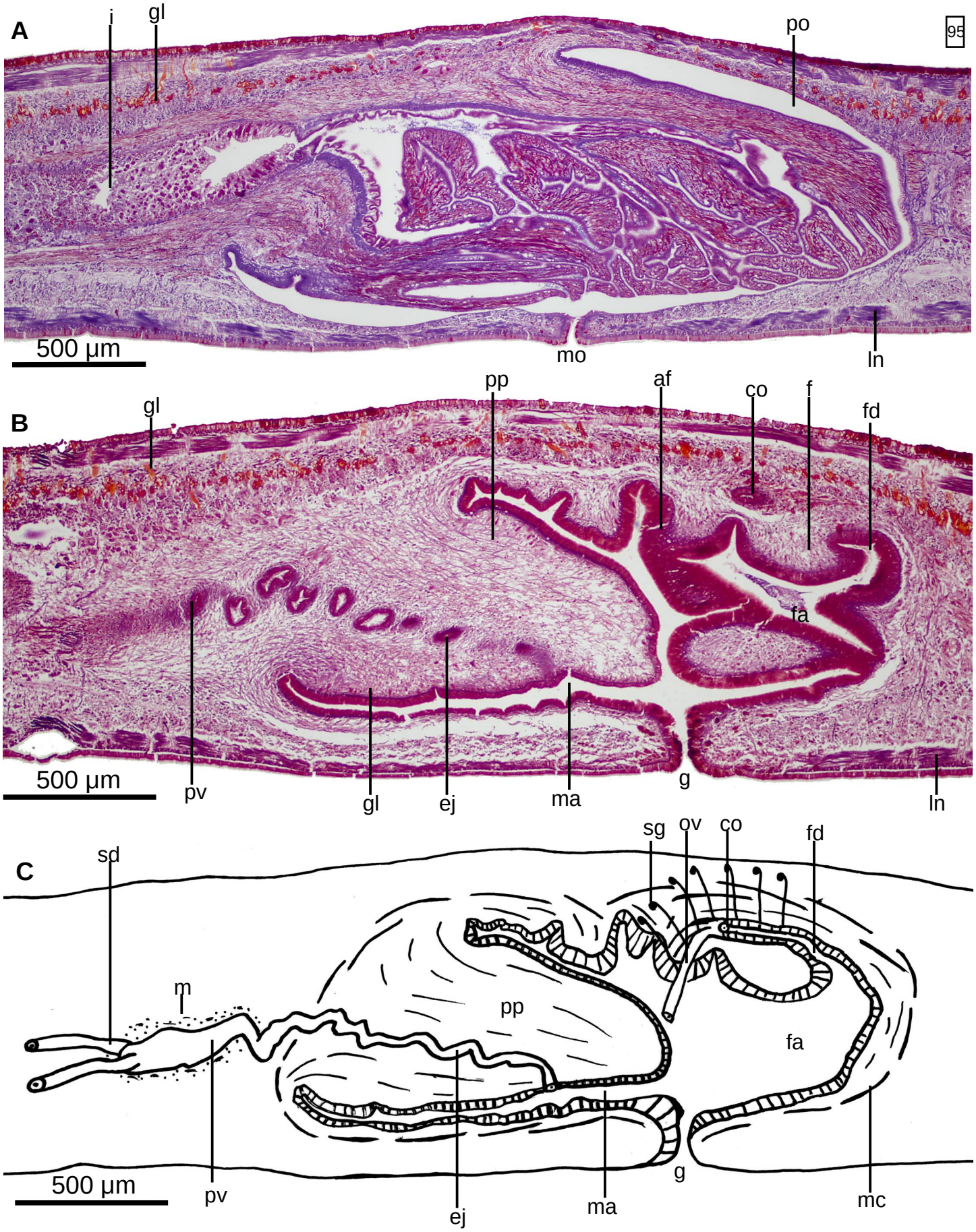

Fig. 25. *Supramontana 1* sp. n. (A) photomicrograph of a sagittal section of the pharynx. (B): photomicrograph of a sagittal section of the copulatory apparatus of holotype F3754g. (C): diagrammatic reconstruction of the copulatory apparatus of holotype F3754g.

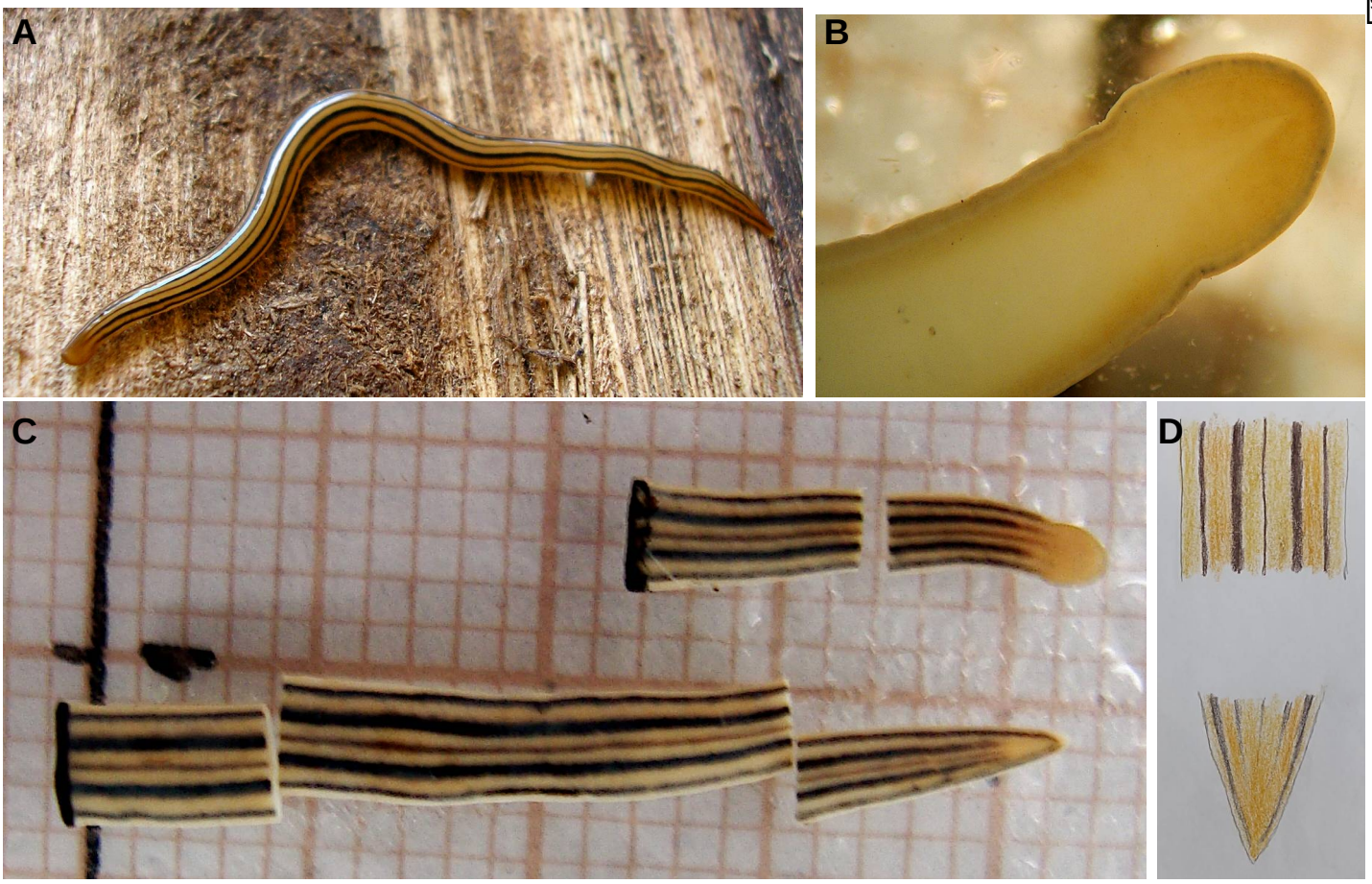

Fig. 26. *Supramontana 2* sp. n. (A) Live paratype F2689 in dorsal view. (B): ventral view of the cephalic region of the preserved holotype F2766. (C): preserved holotype on millimetered paper. (D): hand drawing of the dorsal side of paratype.

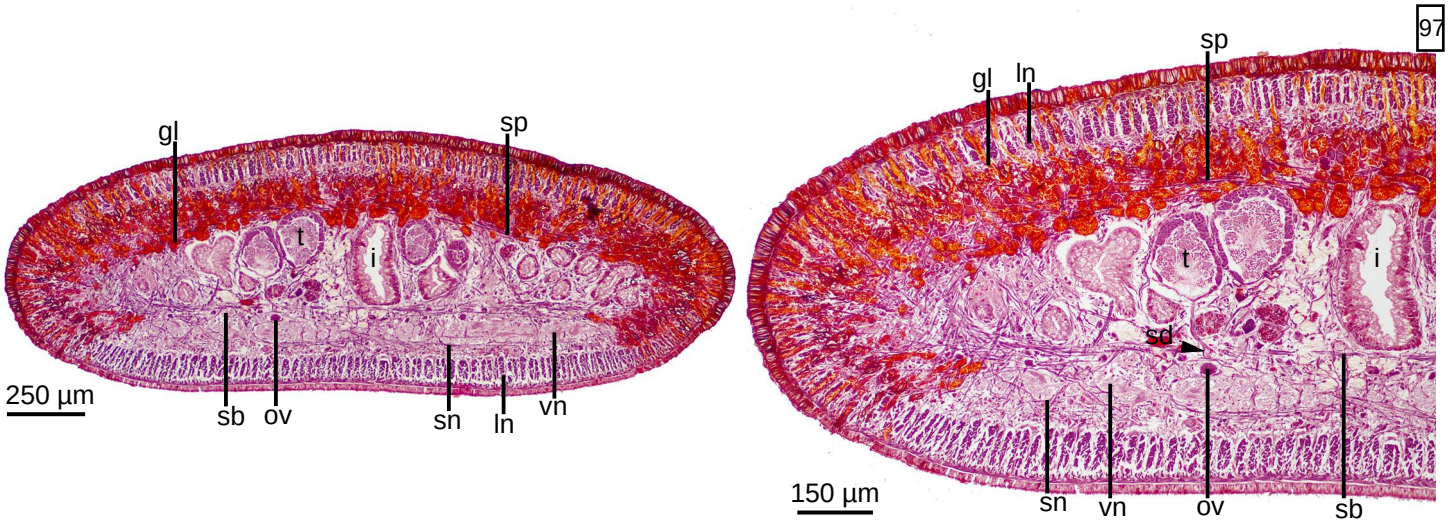

Fig. 27. *Supramontana 2* sp. n. (A-B): Photomicrograph of a transverse sections of the pre-pharyngeal region of the holotype F2766.

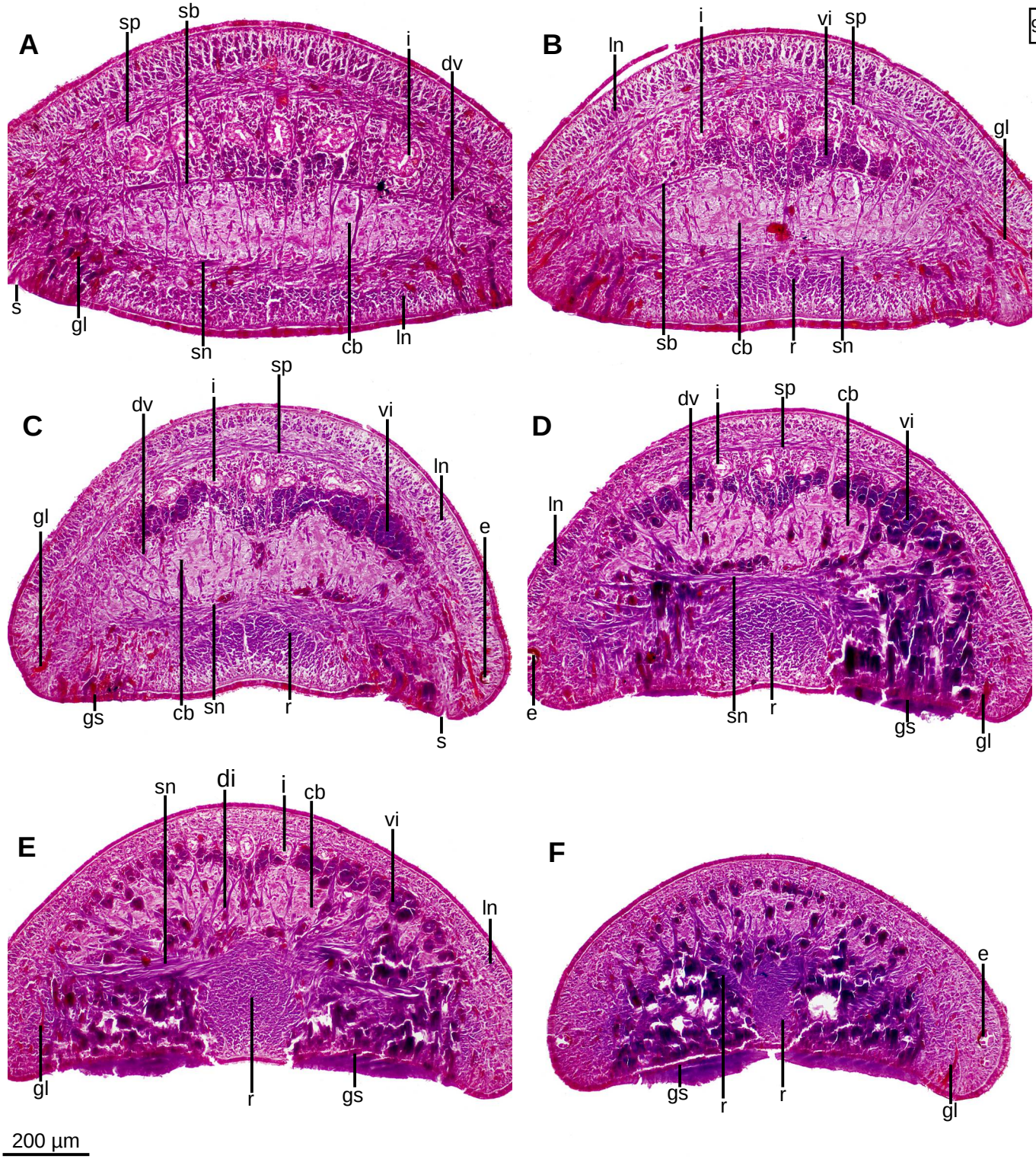

Fig. 28. *Supramontana 2* sp. n. Photomicrographs of transverse sections of the cephalic region of paratype F2689 arranged from furthest (A) to closest (F) distant from the anteriormost extremity of the body.

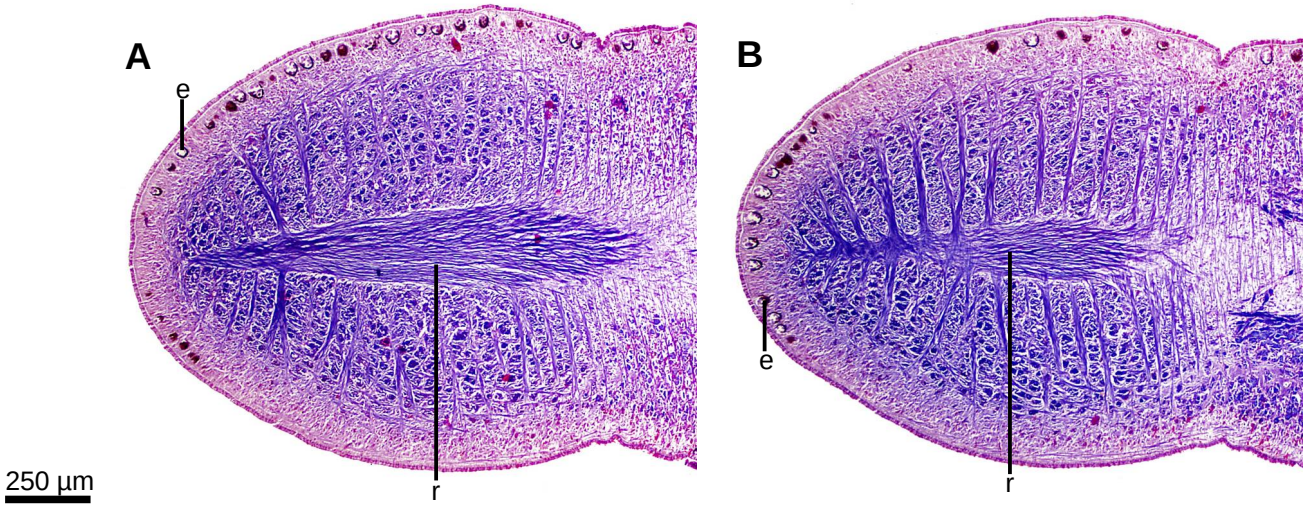

Fig. 29. *Supramontana 2* sp. n. Photomicrographs of horizontal sections of the cephalic region of holotype F2766 from a dorsal section (A) towards the ventral side of the body (B).

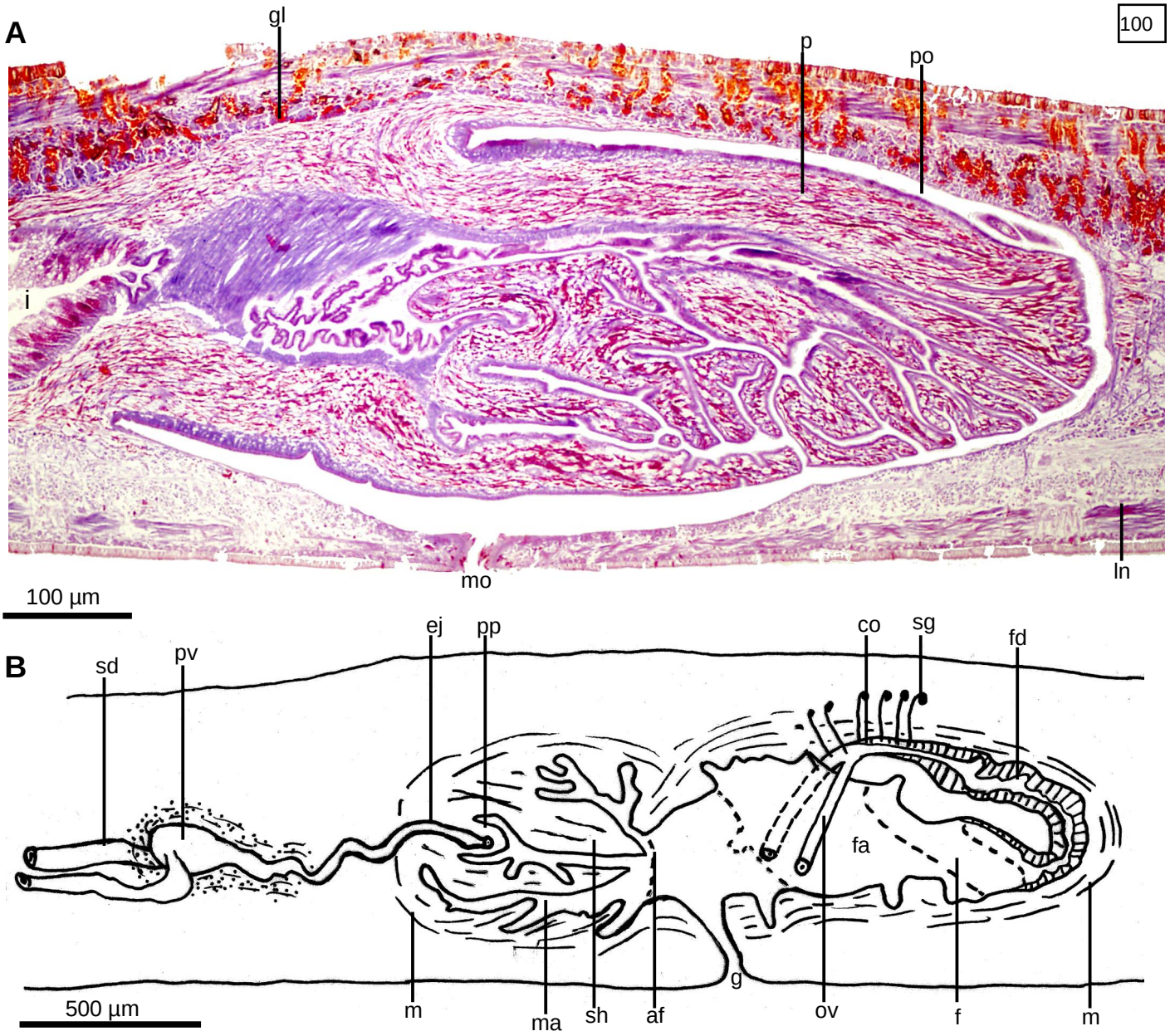

Fig. 30. *Supramontana 2* sp. n. (A): Photomicrographs of a sagittal section of the pharynx of holotype F2766. (B) diagrammatic reconstruction of the copulatory apparatus of the holotype.

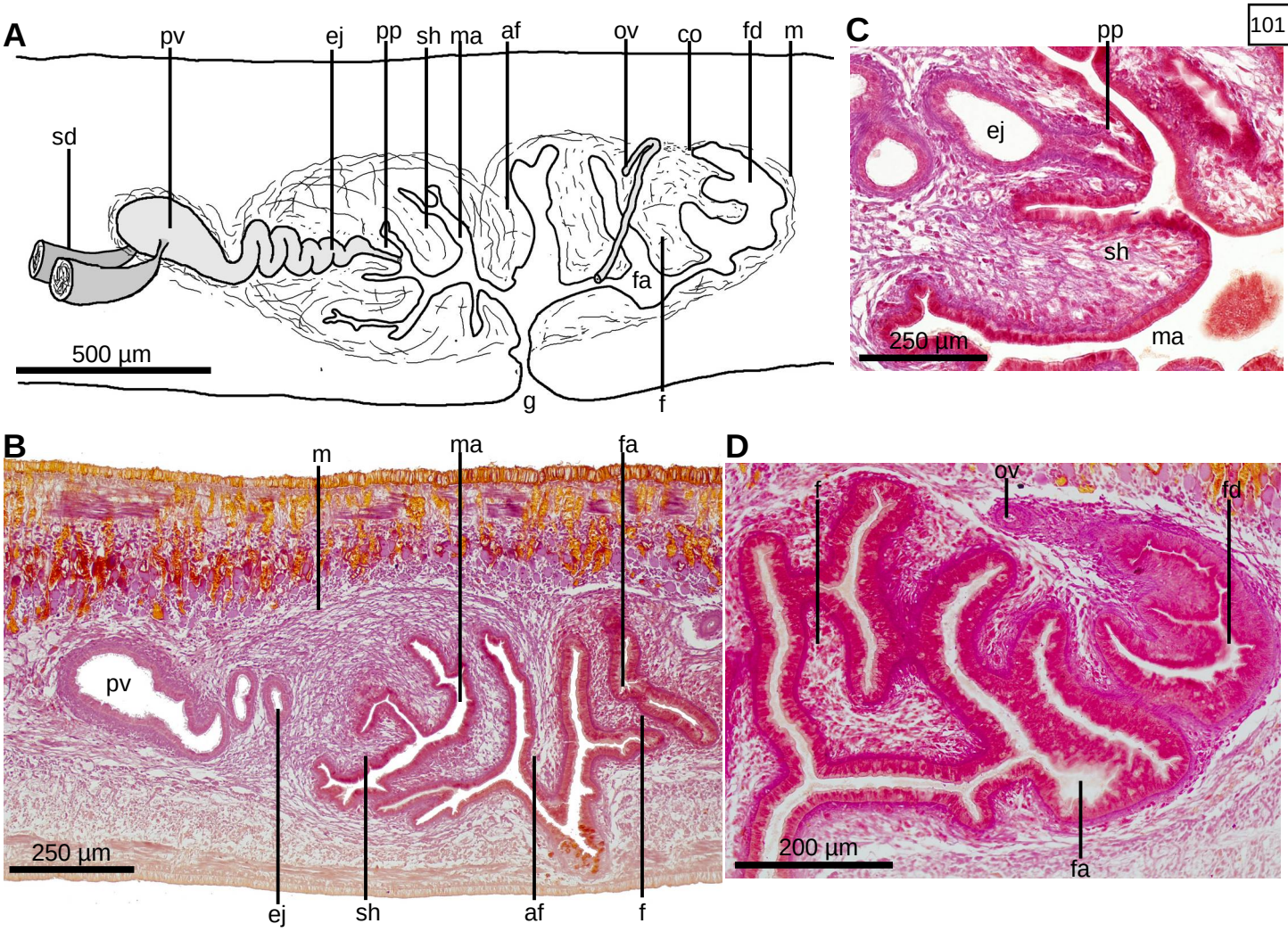

Fig. 31. *Supramontana 2* sp. n. Paratype. (A) diagrammatic reconstruction of the copulatory apparatus. (B): photomicrograph of a sagittal section of the copulatory apparatus. (C): photomicrograph of a sagittal section of penis papila. (D): photomicrograph of a sagittal section of the female atrium.

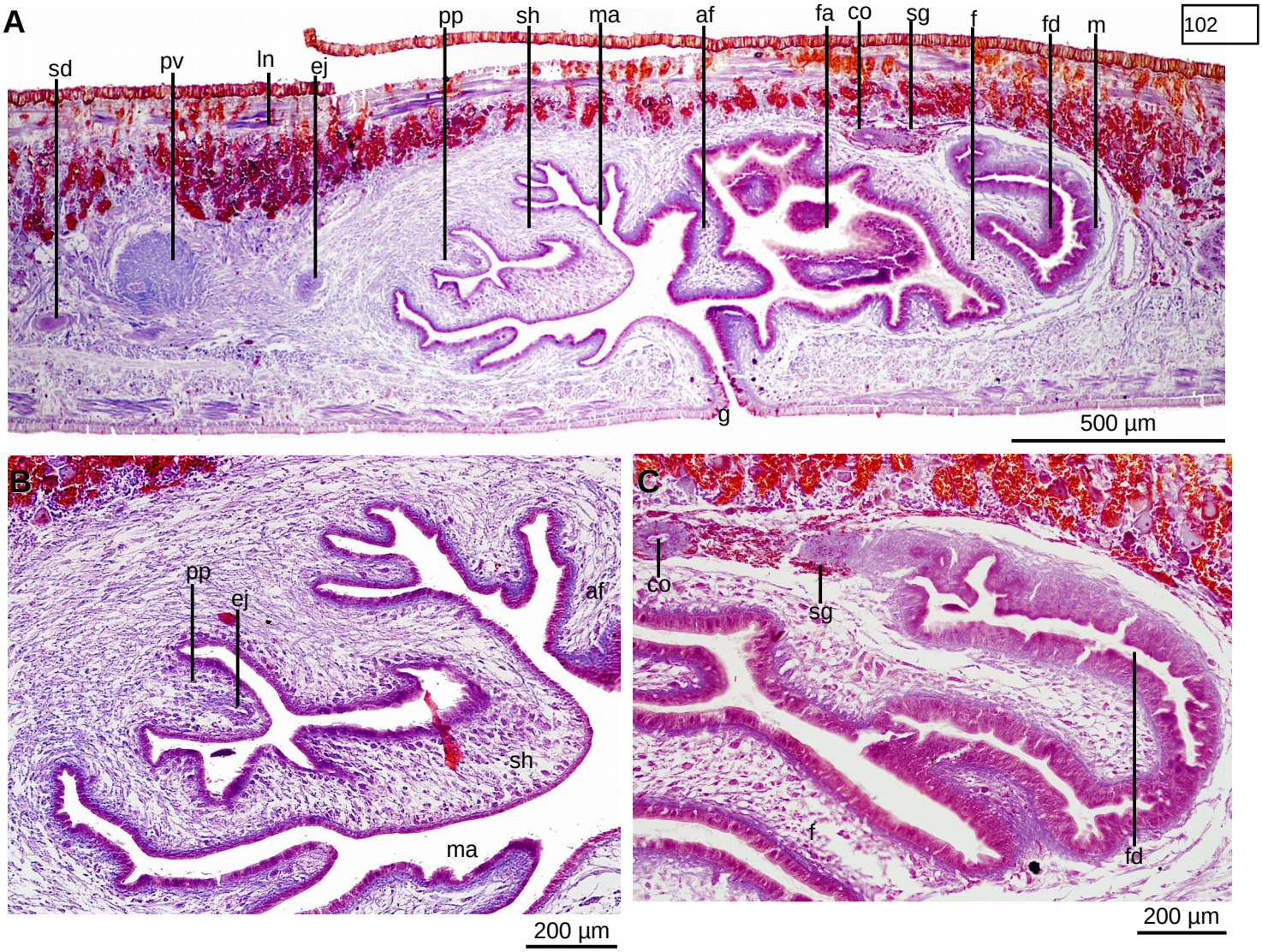

Fig. 32. *Supramontana 2* sp. n. Photomicrograph of a sagittal sections of the holotype. (A) copulatory apparatus. (B): male atrium. (C): female atrium.

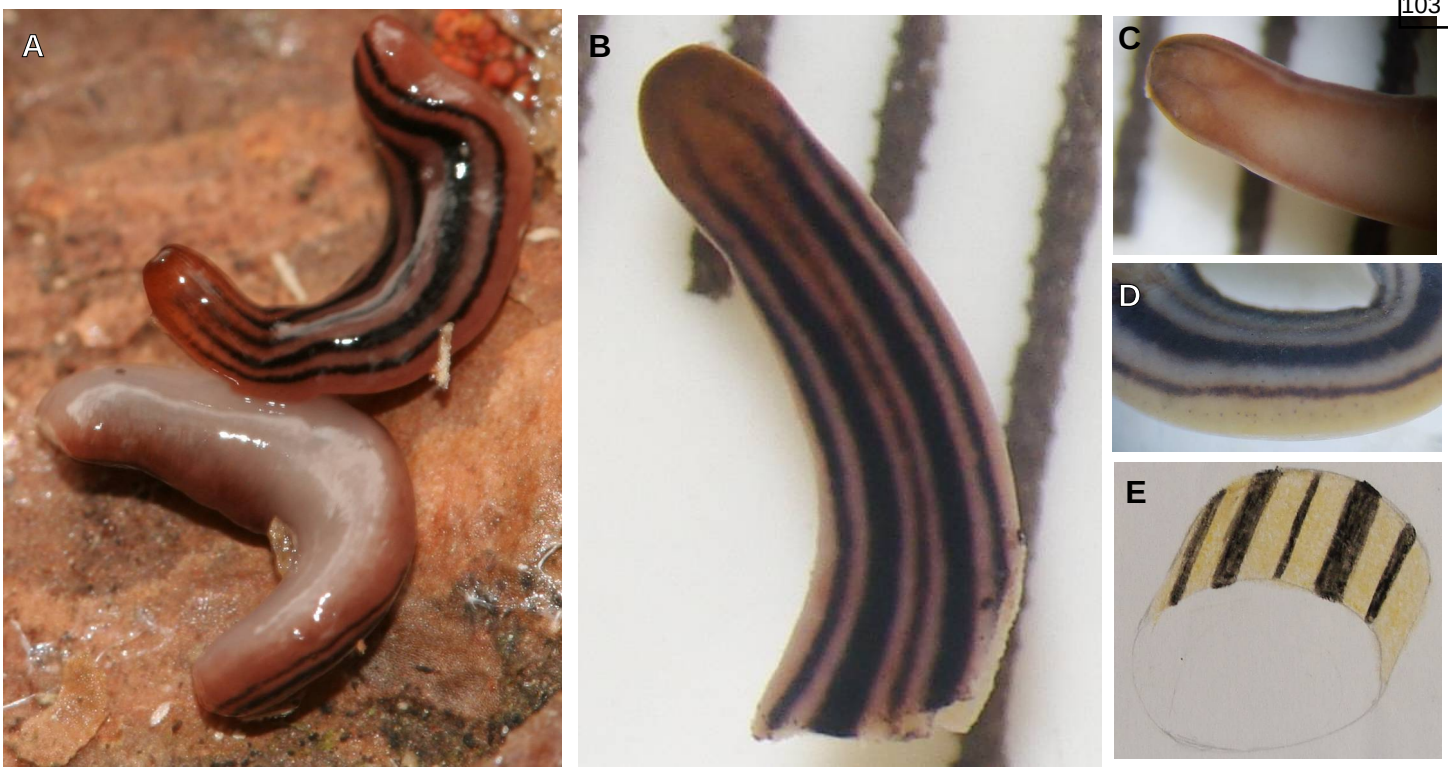

Fig. 33. *Supramontana 3* sp. n. (A): live paratype F2815 when collected. Dorsal (B), ventral (C), and lateral (D) views of the preserved holotype. (E): diagramatic representation of the dorsal color pattern.

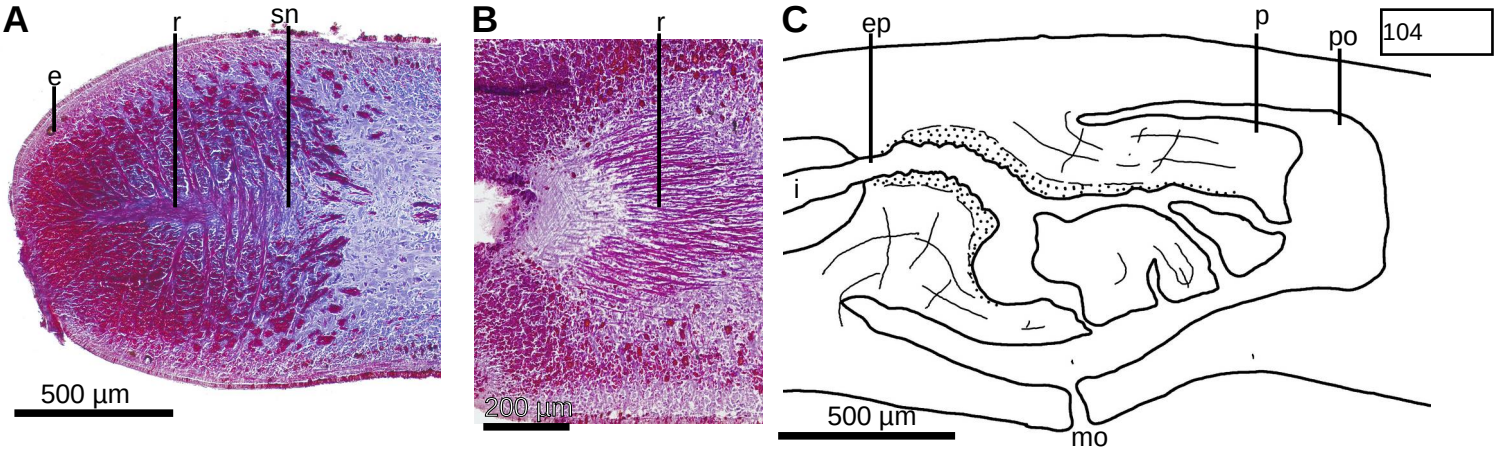

Fig. 34. *Supramontana 3* sp. n. Holotype. (A-B): Photomicrographs of horizontal sections of the cephalic region of the holotype. (C): diagramatic representation of the pharynx of the paratype F2043.

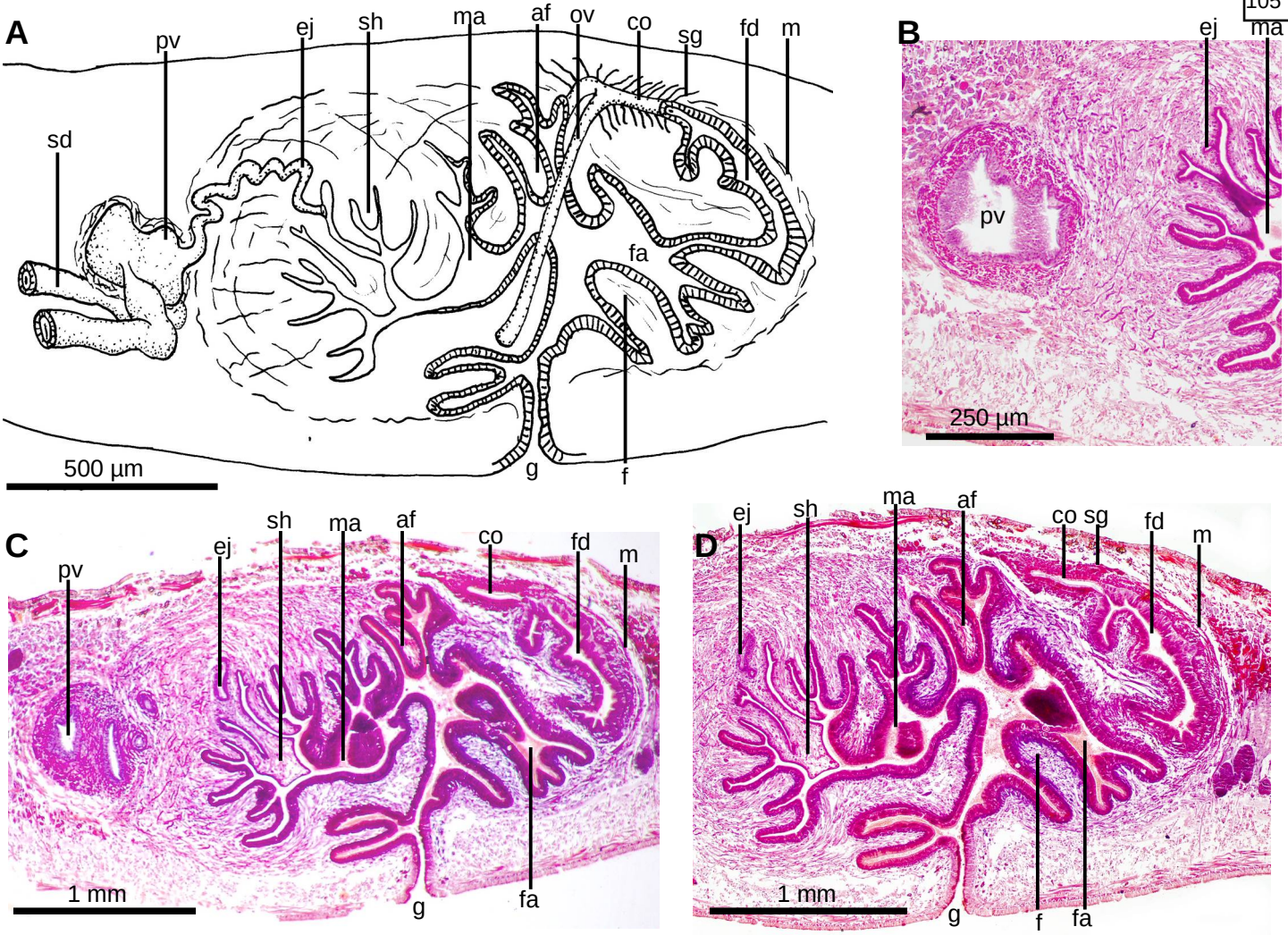

Fig. 35. *Supramontana 3* sp. n. Holotype. (A): diagrammatic reconstruction of the copulatory apparatus. (B): photomicrograph of a sagittal sections of the prostatic vesicle. (C-D): photomicrographs of the copulatory apparatus.

Fig. 36. *Supramontana 4* sp. n. Holotype. (A): live specimen. (B-C): cephalic region of the preserved specimen. (D): diagramatic representation of the dorsal color pattern.

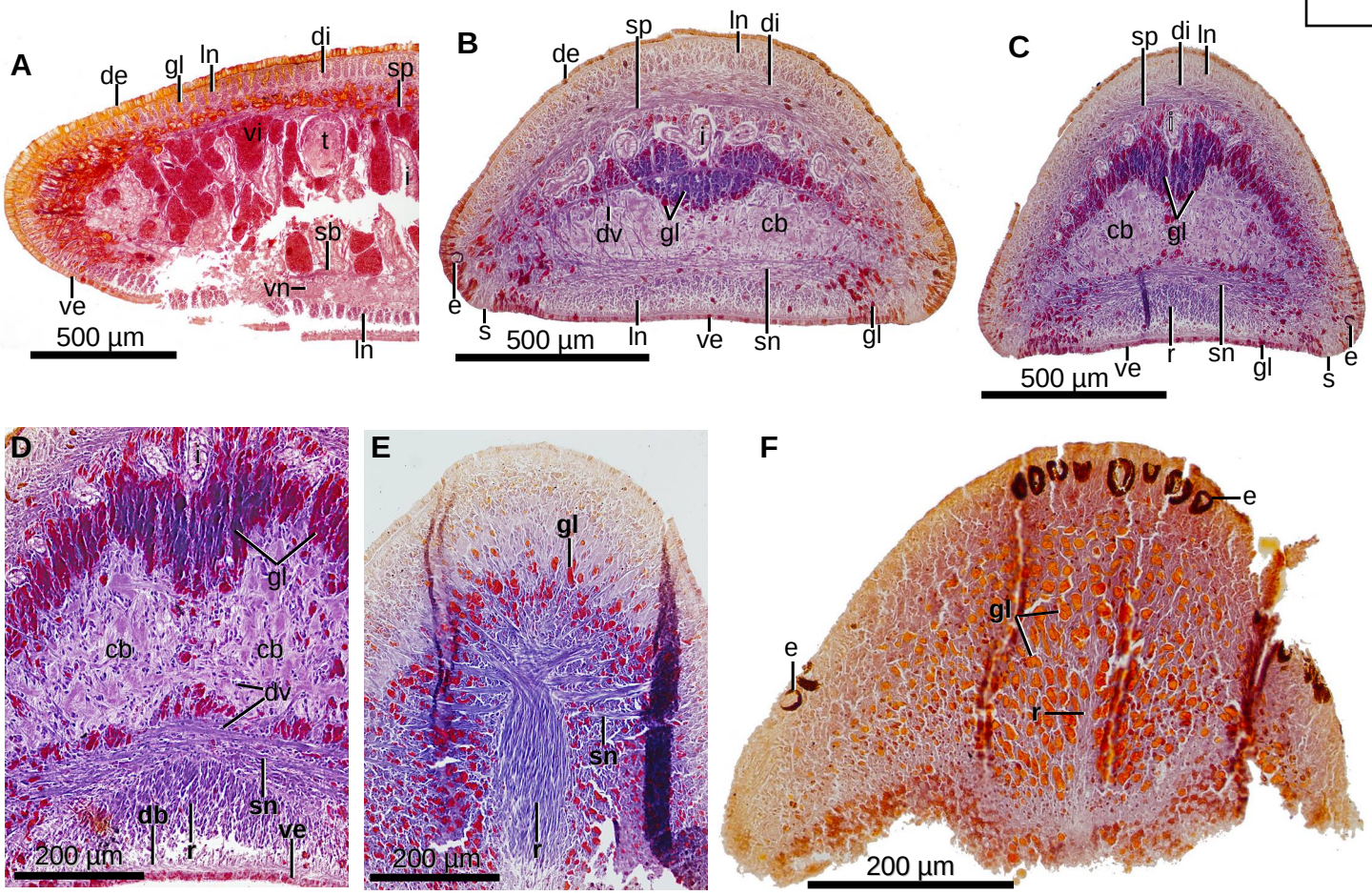

Fig. 37. *Supramontana 4* sp. n. Photomicrographs of sagittal sections of the holotype. (A): transverse section of the pre-pharyngeal region. (B-D): transverse sections of the cephalic region. (E-F): horizontal sections of the cephalic region.

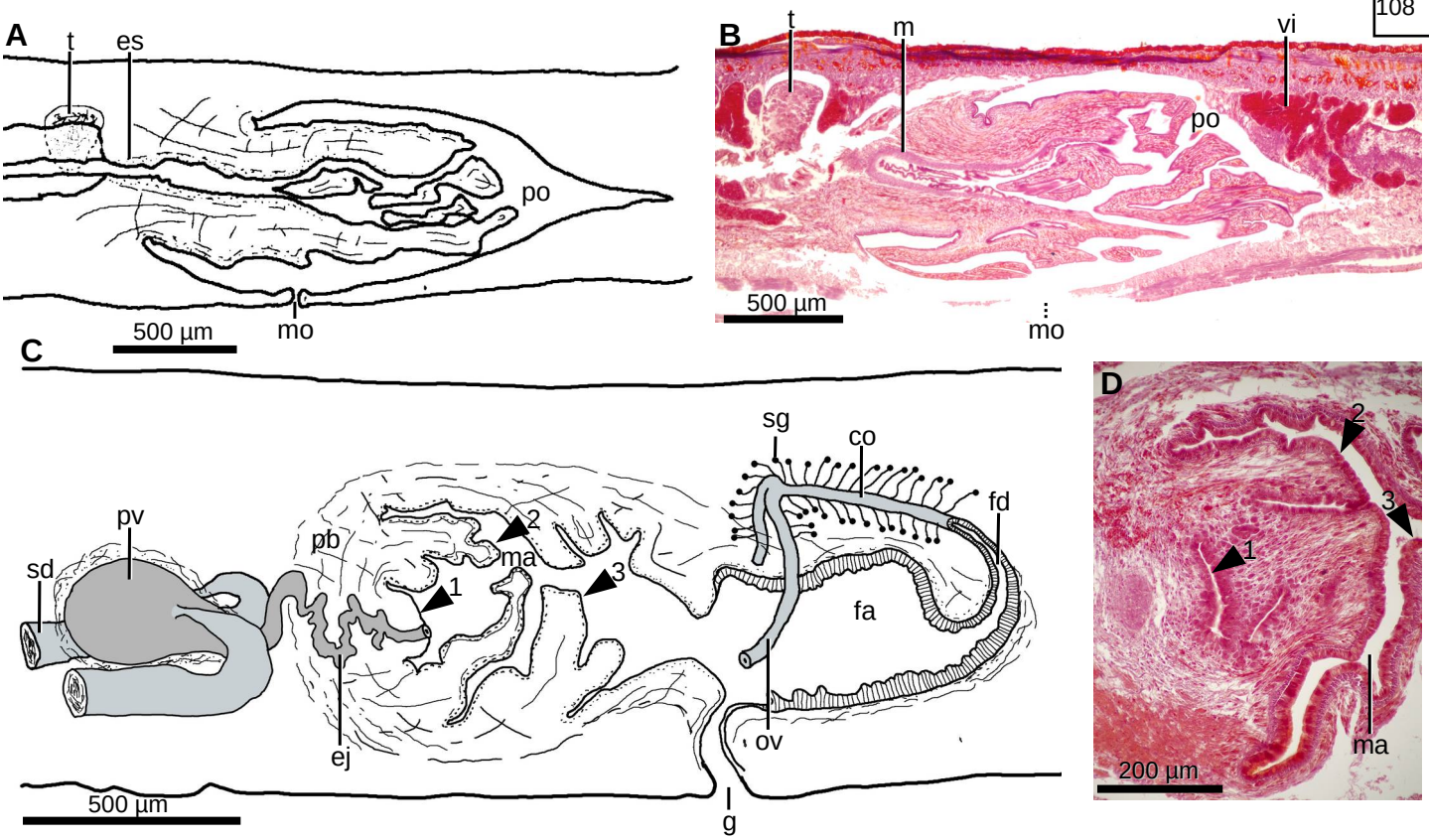

Fig. 38. *Supramontana 4* sp. n. Holotype. (A): diagrammatic reconstruction of the pharynx. (B): photomicrograph of a sagittal section of the pharynx. (C): diagrammatic reconstruction of the copulatory apparatus. (D): photomicrograph of a sagittal section of the anterior folds of the male atrium.

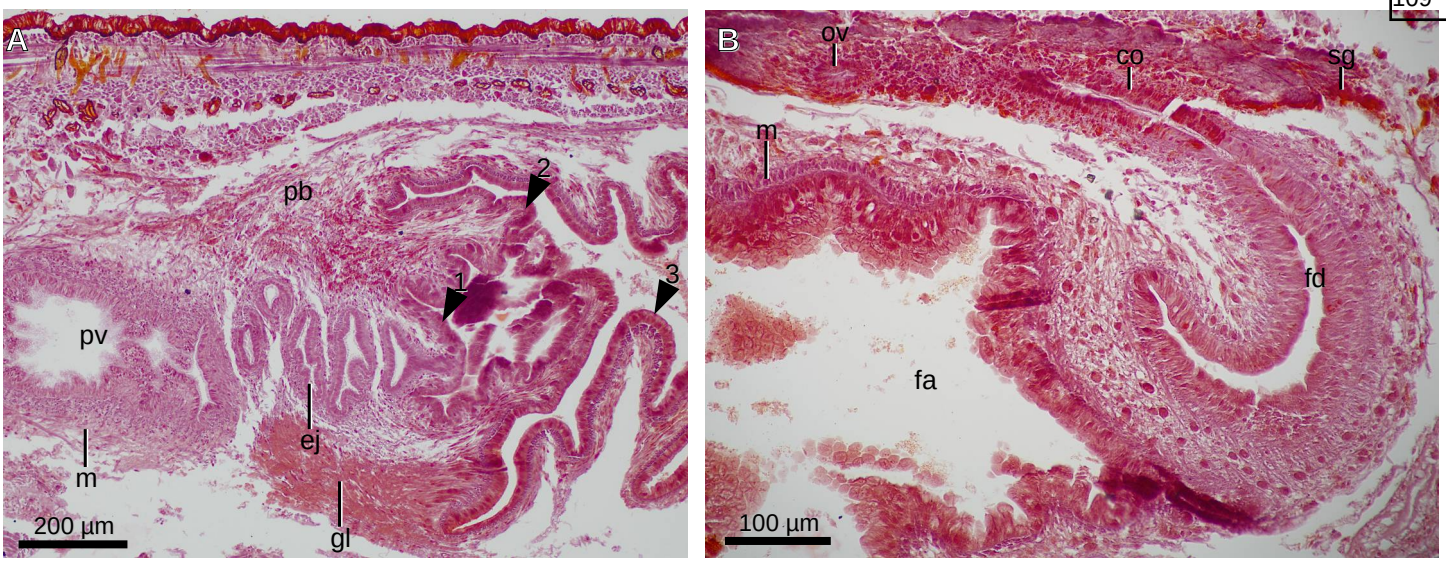

Fig. 39. *Supramontana 4* sp. n. Holotype. Photomicrographs of sagittal sections of the male atrium (A) and female atrium (B).

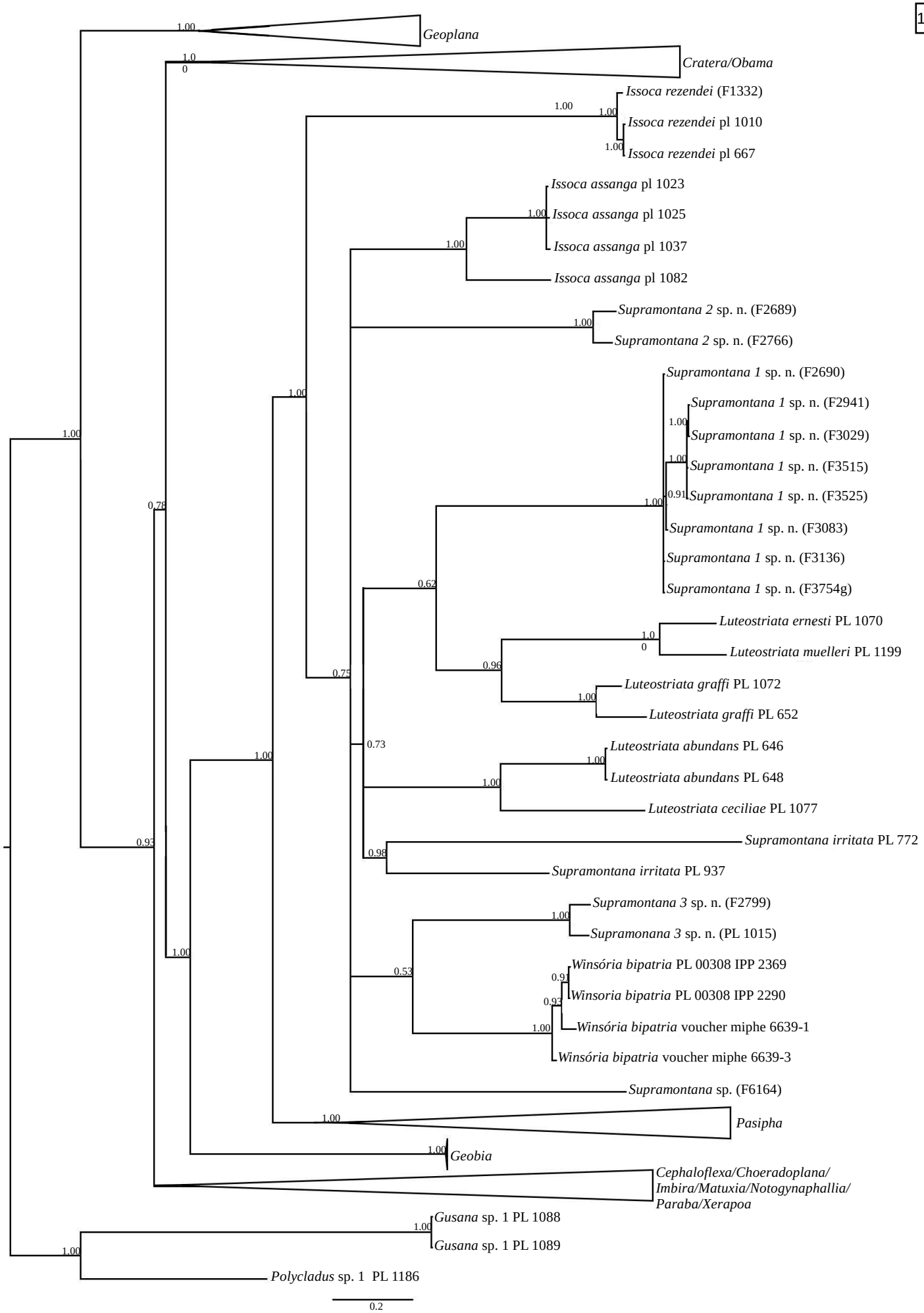

Fig. S1. Phylogenetic tree showing the topology inferred by Bayesian Inference from the the concatenated genes COI + 28S rDNA. Numbers at the nodes correspond posterior probability. Scale bar represents substitutions per site. Some clades are collapsed.

Tab. 1. Individuals used in the study and GenBank accession numbers for the sequences. Sequences generated for this study are indicated with an asterisk *.

Species	Field number	Accession number	COI - Accession number	28S rDNA - Accession number
Cratera pseudovaginuloides (Riester, 1938)	F1244	MZUSP PL 670	KC608251	KC608366
Cratera pseudovaginuloides (Riester, 1938)	F1245	MZUSP PL 671	KC608252	KC608367
Cratera tamoia (Froehlich, 1955)	F1139	MZUSP PL 665	KC608246	KC608361
Cratera tamoia (Froehlich, 1955)	F1336	MZUSP PL 672	KC608254	KC608369
Cephaloflexa araucariana Carbayo & Leal-Zanchet, 2003	F3381	MZUSP PL 1072	KC608319	KC608436
Cephaloflexa araucariana Carbayo & Leal-Zanchet, 2003	F3387	MZUSP PL 1073	KC608316	KC608433
Cephaloflexa bergi (Graff, 1899)	F1034	MZUSP PL 303	KC608238	KC608353
Cephaloflexa bergi (Graff, 1899)	F1038	MZUSP PL 305	KC608240	KC608355
Choeradoplana albonigra (Riester, 1938)	F4081	MZUSP PL 1083	KC608327	KC608444
Choeradoplana gladismariae Carbayo & Froehlich, 2012	F3092	MZUSP PL 1003	KC608306	KC608423
Choeradoplana gladismariae Carbayo & Froehlich, 2012	F3802	MZUSP PL 1004	KC608326	KC608443
Geobia subterrânea (Schultze & Müller, 1857)	F0358	MZUSP PL 650	KC608225	KC608340
Geobia subterrânea (Schultze & Müller, 1857)	F1355	MZUSP PL 673	KC608255	KC608370
Geoplana boraceia Almeida & Carbayo, 2018	F3389	MZUSP PL 1073	KC608330	KC608447
Geoplana boraceia Almeida & Carbayo, 2018	F4358	MZUSP PL 1086	KC608329	KC608446
Geoplana cambara Almeida & Carbayo, 2018	F1614	MZUSP PL 1009	KC608262	KC608377
Geoplana pulchella Schultze & Müller, 1857	F3249	MZUSP PL 1068	KC608310	KC608427
Gusana sp. 1	F4421	MZUSP PL 1088	KC608331	KC608448
Gusana sp. 1	F4428	MZUSP	KC608332	KC608449

Species	Field number	Accession number	COI - Accession number	28S rDNA - Accession number
		PL 1089		
Imbira guaiana (Leal-Zanchet & Carbayo, 2001)	F3361	MZUSP PL 1071	KC608314	KC608431
Imbira guaiana (Leal-Zanchet & Carbayo, 2001)	F0432	MZUSP PL 653	KC608229	KC608344
Imbira marcusi Carbayo et al., 2013	F2833	MZUSP PL 404	KC608291	KC608406
Imbira marcusi Carbayo et al., 2013	F1041	MZUSP PL 1190	KC608241	KC608356
Issoca rezendei (Schirch, 1929)	F1679	MZUSP PL 1010	KC608263	KC608378
Issoca rezendei (Schirch, 1929)	F1182	MZUSP PL 667	KC608248	KC608363
Issoca rezendei (Schirch, 1929)	F1332	MZUSP PL XXX		
Matuxia matuta (Froehlich, 1954)	F2184	MZUSP PL 1021	KC608276	KC608391
Matuxia matuta (Froehlich, 1954)	F2187	MZUSP PL 1022	KC608277	KC608392
Matuxia tuxaua (Froehlich, 1954)	F3059	MZUSP PL 1058	KC608302	KC608419
Matuxia tuxaua (Froehlich, 1954)	F1275	MZUSP PL 1192	KC608253	KC608368
Notogynaphallia sexstriata (Graff, 1899)	F0792	MZUSP PL 656	KC608232	KC608347
Notogynaphallia sexstriata (Graff, 1899)	F1413	MZUSP PL 680	KC608257	KC608372
Obama carinata (Riester, 1938)	F3084	MZUSP PL 1062	KC608304	KC608421
Obama carinata (Riester, 1938)	F3093	MZUSP PL 1064	KC608307	KC608424
Obama josefi (Carbayo & Leal-Zanchet, 2001)	F3389	MZUSP PL 1074	KC608317	KC608434
Obama josefi (Carbayo & Leal-Zanchet, 2001)	F3402	MZUSP PL 1075	KC608318	KC608435
Paraba franciscana (Leal-Zanchet & Carbayo, 2001)	F5485	MZUSP PL 935 IPP 848	KC608335	KC608452
Paraba franciscana (Leal-Zanchet & Carbayo, 2001)	F3357	MZUSP PL 1069	KC608312	KC608429

Species	Field number	Accession number	COI - Accession number	28S rDNA - Accession number
Paraba multicolor (Graff, 1899)	F2101	MZUSP PL 1017	KC608271	KC608386
Paraba multicolor (Graff, 1899)	F2997	MZUSP PL 1055	KC608299	KC608415
Pasipha pasipha (Marcus, 1951)	F1841	MZUSP PL 1012	KC608266	KC608381
Pasipha pasipha (Marcus, 1951)	F2871	MZUSP PL 1053	KC608295	KC608410
Pasipha pinima (Froehlich, 1954)	F2585	MZUSP PL 717	KC608280	KC608395
Pasipha pinima (Froehlich, 1954)	F1714	MZUSP PL 1011	KC608264	KC608379
Pasipha tapetilla (Marcus, 1951)	F2878	MZUSP PL 732	KC608296	KC608411
Pasipha tapetilla (Marcus, 1951)	F5631	MZUSP PL 938	KC608336	KC608453
Polycladus sp. 1	F0397	MZUSP PL 1186	KC608228	KC608343
Supramontana abundans (Graff, 1899)	F0205	MZUSP PL 646	KC608223	KC608338
Supramontana abundans (Graff, 1899)	F0238	MZUSP PL 648	KC608224	KC608339
Supramontana assanga (Araujo & Carbayo, 2018)	F2250	MZUSP PL 1023		
Supramontana assanga (Araujo & Carbayo, 2018)	F2274	MZUSP PL 1025		
Supramontana assanga (Araujo & Carbayo, 2018)	F2394	MZUSP PL 1037		
Supramontana assanga (Araujo & Carbayo, 2018)	F4057	MZUSP PL 1082		
Supramontana 1 sp. n.	F2690	MZUSP PL XXX		
Supramontana 1 sp. n.	F2941	MZUSP PL XXX		
Supramontana 1 sp. n.	F3029	MZUSP PL XXX		
Supramontana 1 sp. n.	F3083	MZUSP PL XXX		
Supramontana 1 sp. n.	F3136	MZUSP PL XXX		

Species	Field number	Accession number	COI - Accession number	28S rDNA - Accession number
Supramontana 1 sp. n.	F3515	MZUSP PL XXX		
Supramontana 1 sp. n.	F3525	MZUSP PL XXX		
Supramontana 1 sp. n.	F3754g	MZUSP PL XXX		
Supramontana ceciliae (Froehlich & Leal-Zanchet, 2003)	F3451	MZUSP PL 1077	KC608321	KC608438
Supramontana ernesti (Leal-Zanchet & Froehlich, 2006)	F3358	MZUSP PL 1070	KC608313	KC608430
Supramontana graffi (Leal-Zanchet & Froehlich, 2006)	F0384	MZUSP PL 652	KC608227	KC608342
Supramontana graffi (Leal-Zanchet & Froehlich, 2006)	F3381	MZUSP PL 1072	KC608315	KC608432
Supramontana irritata Carbayo & Leal-Zanchet, 2003	F3452	MZUSP PL 772	KC608322	KC608439
Supramontana irritata Carbayo & Leal-Zanchet, 2003	F5483 IPP 860	MZUSP PL 937	KC608334	KC608451
Supramontana muelleri (Diesing, 1861)	F3268	MZUSP PL 1199	KC608428	KC608311
Supramontana 2 sp. n.	F2766	MZUSP PL XXX		
Supramontana 2 sp. n.	F2689	MZUSP PL XXX		
Supramontana 3 sp. n.	F2799	MZUSP PL XXX		
Supramontana 3 sp. n.	F2043	MZUSP PL 1015	KC608270	KC608385
Supramontana sp. n.	F6164	MZUSP PL XXX		
Xerapoa trina (Marcus, 1951)	F1239	MZUSP PL 669	KC608250	KC608365
Xerapoa trina (Marcus, 1951)	F1134	MZUSP PL 1191	KC608244	KC608359

Tab. 2. List of primers used to amplify and sequencing the DNA fragments.

Gene region	Primer name	Utilization	Sequence (5' to 3')	Reference	Annealing temperature
28S rDNA	LSU 5F (Forward)	Amplification and sequencing	TAGGTCGACCCGCTGAAYTTAAGCA	Littlewood *et al*. (1997)	56-58ºC
	Rob1 (Forward)	Sequencing	GTCCAATAGCAAACAAGTCCCG	Heneberg et al. (2013)	-
	LSU 330F (Forward)	Sequencing	CAAGTACCGTGAGGGAAAGTTG	Williams & Ozawa (2006)	-
	Rob2 (Reverse)	Sequencing	CACGYACTRTTTACCTC	Chisholm et al., (2001)	-
	ECD-2 (Reverse)	Sequencing	CCTTGGTCCGTGTTTCAAGACGGG	Littlewood *et al*. (1997)	-
	LSU 1500R (Reverse)	Amplification and sequencing	GCTATCCTGAGGGAAACTTCG	Tkach *et al*. (1999)	56-58ºC
COI	BarS (Forward)	Amplification and sequencing	GTTATGCCTGTAATGATTG	Álvarez-Presas *et al*. (2011)	45ºC
	FlatwormCOIF (Forward)	Sequencing	GAGCAACAACATAATAAGTATCATG	Sunnucks *et al*. (2006)	-
	COIR (Reverse)	Amplification and sequencing	CCWGTYARMCCHCCWAYAGTAAA	Lázaro *et al*. (2009)	45ºC

Appendix

Parameter for acquisition of mCT images of the copulatory apparatus of a syntype of *Issoca Rezendei* (Schirch, 1929)

```
[General]
Version=2.3.0.1032
Version-pca=2
Comment=
LoadDefault=1
SystemName=v|tome|x m

[AutoScO]
Active=1
ImgNr=8
ImageString=180:360:540:720:900:1080:1260:1440
Skip=10

[Geometry]
FDD=817.22215760
FOD=13.33250000
Magnification=61.29549279
VoxelSizeX=0.00326288
VoxelSizeY=0.00326288
CalibValue=-18.025
cx=949.50000000
cy=649.50000000
DetectorRot=0.00000000
Tilt=0.00000000
Old_CalibValue=-3.63200000

[CT]
Type=0
NumberImages=1440
StartImg=1441
RotationSector=360.00000000
NoRotation=0
EstimatedTime=0
RemainingTime=1440
ScanTimeCmpl=1440
NrImgDone=1441
NrImgCmplScan=1441
RefDriveEnabled=0
SkipForNewInterval=25
SkipAcc=1
FreeRayFactor=1.00010000
Wnd_L=0
Wnd_T=0
Wnd_R=10
Wnd_B=10
Level=1986.00000000

[VSensor]
EnableTiles=1
Start=0
NumTiles=1
Interval=60
Overlap=9
AdjustImg=1
SingleImgX=1910

[Trajectory]
Active=0

[CalibValue]
NumberImages=18
Averaging=2
Skip=3

[FastCT]
Active=0

[Image]
Top=362
Left=57
Bottom=1661
Right=1966
DimX=1900
DimY=1300
Rotation=0
MirrorX=0
MirrorY=0
BitPP=16
FreeRay=2147

[ImgProc]
SwBin=1
AddSwBin=0

[Warmup]
Enable=1
Counter=0
MaxTimes=10
TimeTrigOn=0
kV=205
Time=60

[Multiscan]
Active=0

[Multiline]
Installed=0

[CalibImages]
MGainMode=0
MGainPoints=3
Avg=50
Skip=10
EnableAutoAcq=1
MGainVoltage=50:50:50:
MGainCurrent=30:100:300:
GainImg=S:\CT_DATA\Mario de Pinna\Vandellia
sp_MUSM 20673\Vandellia sp_MUSM
20673__bright_50kV_300uA_1000ms_1Det.tif
MGainImg=S:\CT_DATA\Mario de Pinna\Vandellia
sp_MUSM 20673\Vandellia sp_MUSM
20673__bright_50kV_300uA_1000ms_1Det.tif
OffsetImg=S:\CT_DATA\Mario de Pinna\Vandellia
sp_MUSM 20673\Vandellia sp_MUSM
20673__Dark_1000.tif
DefPixelImg=C:\Program Files\phoenix x-ray\datosx 2
acq\CalibrationImages\pixmask_B1x1_x2024_y2024.tif

[SectorScan]
Active=0

[DetectorShift]
Enable=1
Mode=0
Amplitude=5
Interval=1
Step=1

[Detector]
InitTimeOut=60000
Name=dxr-250
PixelsizeX=0.20000000
PixelsizeY=0.20000000
NrPixelsX=2024
```

NrPixelsY=2024
Timing=5
TimingVal=1000.082
Avg=1
Skip=0
Binning=0
BitPP=14
CameraGain=2
SatValue=15563
SatPixNrLimit=4096

[Xray]
ComPort=0
Name=xs|300 d
ID=2303
InitTimeout=20000
Voltage=50
Current=300
Mode=0
Filter=Unknown
Collimation=0
WaitTime=1000
WaitForStable=30000
FocDistX=0.00000000
FocDistY=0.00000000
SpinStepkV=10
SpinStepuA=10
Macro=0
RestrictNumSpots=0
PreWarning=0
MinGainCurrent=10

[Cnc]
InitTimeout=8000
CollisionDetection=1
JoyDriveDoorOpen=0
SecPosSample=250.00000000
MinSampleDetPos=300.00000000
EnableKeyboardJoy=0
KeyJoyVelocityFactor=0.25000000

[Axis]
XSample=-0.011250
YSample=178.157250
ZSample=13.332500
RSample=2246.736900
XDetector=0.000000

[AcqSrvManager]
RecvPcIp=
ExePath=c:\Program Files\phoenix x-ray\datosx 2 acq\srv\dtxaSrv.exe

[Net]
Enable=1
IP=
[BHC_Values]
BHC_Param=2